Recruitment of Podosome Components Involved in the Remodelling of the Actin Cytoskeleton

Thesis

Recruitment of podosome components involved in the remodelling of the actin cytoskeleton

Luca Crimaldi

Discipline: Life sciences

Sponsoring establishment: Consorzio Mario Negri Sud

Thesis submitted in accordance with the requirements of the

Open University for the degree of Doctor of Philosophy

February 2009

Submission date: 27 Feb. 2009

Date of award: 22 June 2009

ProQuest LLC.
789 East Eisenhower Parkway
P.O. Box 1346
Ann Arbor, MI 48106 – 1346

Ai miei genitori,

per avermi sempre sostenuto con affetto.

To my parents,

for their loving support.

Abstract

Podosomes are dynamic, actin-rich structures that are involved in cell adhesion and extracellular matrix degradation; they are composed of a densely packed actin core surrounded by a ring structure made of components commonly found in focal adhesions. Podosome formation is characterized by the recruitment of AFAP-110, p190RhoGAP, and cortactin, which have specific roles in Src activation, local down-regulation of RhoA activity, and actin polymerization, respectively. However, the precise function of p190RhoGAP in podosome formation is not clear yet. By employing siRNA-mediated expression knockdown and expressing a catalytically inactive point mutant, I provide evidence that p190RhoGAP is required for podosome formation. It is well documented that Src-induced interaction of p190RhoGAP with p120RasGAP regulates p190RhoGAP activity and subcellular localization. In this thesis, I show that p190RhoGAP is constitutively associated in a complex with p120RasGAP in vascular smooth muscle cells, and that p120RasGAP translocates to podosomes upon PDBu stimulation. Nevertheless, siRNA-mediated knockdown of p120RasGAP expression does not impair p190RhoGAP recruitment or podosome formation, indicating that p120RasGAP is not essential for podosome formation. The molecular mechanism that underlies the specific recruitment of critical podosome components to sites of podosome formation remains unknown. The scaffold protein Tks5 is localized to podosomes in Src-transformed fibroblasts and in vascular smooth muscle cells, and may serve as a specific recruiting adapter for various components during podosome formation. I show here that induced mislocalization of Tks5 to the surface of mitochondria leads to a major subcellular

redistribution of AFAP-110, p190RhoGAP, and cortactin, and to inhibition of podosome formation in vascular smooth muscle cells. Analysis of a series of similarly mistargeted deletion mutants of Tks5 indicates that the fifth SH3 domain is essential for this recruitment. A Tks5-GFP mutant lacking the PX domain also inhibits podosome formation and induces the redistribution of AFAP-110, p190RhoGAP, and cortactin to the perinuclear area. Together these findings demonstrate that Tks5 plays a central role in the recruitment of AFAP-110, p190RhoGAP, and cortactin to drive podosome formation. Evidence from osteoclasts and tumour cells cultured on different substrates indicates that the physical parameters of the underlying substrate influence the ability of cells to form podosomes or the related structures invadopodia. However, it is unclear how vascular smooth muscle cells respond to contact with different types of substrates. Thus, the last part of this thesis is dedicated to determine how podosome-forming vascular smooth muscle cells respond to alterations in the properties of the underlying substrate. I show here that A7r5 cells cultured on cross-linked gelatin degrade matrix by forming invadopodia-like structures. This is the first time that a cell type is reported to be capable of forming both podosomes and invadopodia in different conditions.

Table of Contents

List of Figures

CHAPTER 1 – Introduction

CHAPTER 3 – Results

CHAPTER 4 – Discussion

List of Tables

CHAPTER 2 – Materials and Methods

Abbreviations

ACTH	adrenocorticotropic hormone
ADAM	a disintegrin and metalloproteinase
ADF	actin depolymerization factor
ADP	adenosine diphosphate
Arp	actin related protein
Arpc	actin related protein complex
ATP	adenosine triphosphate
BSA	bovine serum albumin
Cdc42	cell division cycle 42
CNF1	cytotoxic necrotizing factor 1
CSF-1	colony stimulating factor 1
DMEM	Dulbecco's Modified Eagles Medium
DNA	deoxyribonucleic acid
ECM	extracellular matrix
EGF	epidermal growth factor
F-actin	filament actin
FAK	focal adhesion kinase
G-actin	globular actin
GAP	GTPase-activating protein
GBD	GTPase-binding domain
GDI	guanine nucleotide dissociation inhibitors

GEF	guanine exchange factor
GFP	green fluorescent protein
GTP	guanosine triphosphate
GTPase	guanosine triphosphatase
HUVECs	human umbilical vein endothelial cells
IP	immunoprecipitation
kDa	kilo Dalton
LIMK	LIM kinase
mDia	mammalian diaphanous
MMPs	matrix metalloproteinases
MTOC	microtuble-organizing center
NTA	N-terminal acidic
N-WASp	neuronal WASp
p120RasGAP	Ras GTPase-Activating Protein of 120 kDa
p190RhoGAP	Rho GTPase-Activating Protein of 190 kDa
PAE	porcine aortic endothelial
PAK	p21 associated kinase
PBS	phosphate buffered saline
PCR	polymerase chain reaction
PDBu	phorbol-12,13-dibutyrate
PH	pleckstrin homology
PI3K	phosphatidylinositol 3-kinase
PIX	PAK-interacting exchange factor
PKC	protein kinase C

PMA	phorbol-12-myristate-13-acetate
PtdInsP	phosphatidylinositol-phosphate
PtdIns(4)P	phosphatidylinositol (4)-phosphate
PtdIns(3,4)P2	phosphatidylinositol (3,4)-bisphosphate
PtdIns(4,5)P2	phosphatidylinositol (4,5)-bisphosphate
Rac	ras-related C3 botulinum toxin substrate
Rho	Ras homology
RNA	ribonucleic acid
ROCK	Rho kinase
SDS	sodium dodecyl sulphate
SDS-PAGE	sodium dodecyl sulphate-polyacrylamide gel electrophoresis
SH3	Src homology domain 3
siRNA	small interfering RNA
TGF	transforming growth factor
TNF	tumor necrosis factor
TPA	12-O-tetradecanoylphorbol-13-acetate
ULF	unit length filament
VCA	verproline-cofilin-homology-acidic
VEGF	vascular endothelial growth factor
WAS	Wiskott-Aldrich syndrome
WASp	Wiskot-Aldrich-syndrome protein
WH	WASp homology
WIP	WASp-interacting protein

CHAPTER 1

Introduction

1.1 The cytoskeleton

The cytoskeleton is a complex dynamic three-dimensional network of filaments that extends throughout the cytoplasm and gives shape and mechanical support to cells. In fact, the cytoskeleton organizes the structures and the activities of the cell, and is important in a wide range of cellular functions such as adhesion, cell-cell contact, connection of cell-surface receptors with cytosolic proteins, cell polarity, cell motility, intracellular trafficking of organelles and vesicles, chromosome segregation and cytokinesis, cell contractility. The cytoskeleton is composed of three types of filaments: microfilaments, intermediate filaments, and microtubules.

Microfilaments, or actin filaments (F-actin), are about 8 nm in diameter and are polymers of globular actin (G-actin), which is the most abundant protein in eukaryotic cells amounting to 10% by weight of total cell protein content. Actin is a 43 kDa protein and is present in all eukaryotic cells. Each actin molecule can bind adenosine triphosphate (ATP), which is hydrolyzed to adenosine diphosphate (ADP) after incorporation of the actin molecule into the filament. Although energy is not required for actin polymerization in vitro, ATP-bound actin polymerizes faster

than the ADP-bound form (Engel et al., 1977). There are six genetic isoforms in higher mammals (Vandekerckhove and Weber, 1978): two smooth muscle isoforms (α-smooth muscle actin and γ-smooth muscle actin), two striated muscle isoforms (α-skeletal actin and α-cardiac actin) and two cytoplasmic isoforms (β-cytoplasmic actin and γ-cytoplasmic actin). These actin isoforms exhibit a high degree of amino acid sequence similarity, for example skeletal muscle α-actins of human, mouse, rat, rabbit and chicken are identical (Hennessey *et al.*, 1993). Most species have several actin genes, like the worm *Caenorhabditis elegans* that has four distinct actin genes (Krause *et al.*, 1989) and plants that have between five and eight different genes (McLean *et al.*, 1990). On the other hand, lower eukaryotes, like the yeast *Saccharomyces cerevisiae* carry only a single actin gene (Gallwitz and Sures, 1980). Prokaryotic cells have actin homologues, which exhibit high structural resemblance to eukaryotic actins, despite low amino acid sequence similarity, and assemble into dynamic filamentous structures like F-actin in eukaryotes (Carballido-Lopez, 2006). The subtle differences in the amino acid sequences of eukaryotic actin isoforms confer functional diversity and allow actin isoforms to segregate into different structures within cells (Otey *et al.*, 1988; DeNofrio *et al.*, 1989). Under conditions used to grow protein crystals actin monomers have the tendency to spontaneously self-assemble into filaments, hence the first actin monomer crystal structure was determined in the presence of the actin-monomer binding protein DNAse I, which blocks actin polymerization (Mannherz *et al.*, 1977). The crystal structure of actin in the absence of an actin-binding protein has been reported later (Otterbein *et al.*, 2001) (Figure 1.1), whereas no atomic structure has been solved for F-actin, although models have been proposed and low-resolution structural data have been presented (Popp *et al.*, 1987; Oda *et al.*, 2001). G-actin displays four prominent domains numbered 1-

4. Domains 1 and 2 are separated from 3 and 4 by a cleft that is occupied by an ATP or ADP molecule complexed with a Mg^{2+} ion (Kinosian *et al.*, 1993). F-actin is formed by two intertwined strands of actin subunits and displays a specific polarity: the end of the filament at which the ATP/ADP-binding cleft is exposed is designated the minus or pointed end (domains 2 and 4) while the opposite side, that is in contact with the neighbouring actin subunits, is the plus or barbed end (domains 1 and 3); each subunit of the filament is surrounded by four others. In a cell actin continuously undergo cycles of polymerization and depolymerization, leading to a dynamic assembly and disassembly of actin filaments, processes that are tightly regulated by a large number of actin-binding proteins, which act within a specific space and time frame. These proteins bind to monomers or filaments, and control actin dynamics in different ways, resulting in nucleation, capping, stabilization, severing, depolymerization, cross-linking, bundling, monomer sequestration or delivering, and monomer nucleotide exchange.

The intermediate filaments are rope-like fibres of 10 nm in diameter that are formed mainly by four different classes of proteins, each one comprising several members. The type I and type II intermediate filaments (comprising the basic and acidic keratins) are expressed in epithelial cells and specialized derivatives (such as hair and nails). The type III of intermediate filaments includes vimentin, which is expressed in many cells of mesenchymal origin, desmin, which is muscle-specific, glial fibrillary acidic protein, which is found in glial cells, and peripherin, which is present in neurons. Nuclear lamins (type IV) form a meshwork that stabilizes the inner membrane of the nuclear envelope in all cell types. Neurofilaments are typically expressed in neurons. The intermediate filaments have an important role in the maintenance of cell shape, in the anchorage of the nucleus and some other organelles, in the formation of the nuclear lamina, in the

mechanical support for the extensions of neurons, and in cell-cell contacts. Although the amino acid sequences of the subunits are not conserved, all the different types of intermediate filaments have similar structures. The subunit is constituted by a conserved central α-helical rod domain flanked by non-α-helical N-terminal (termed the head) and C-terminal (termed the tail) end domains (Goldman *et al.*, 2008). The central rod mediates the formation of a coiled-coil structure, whereas the head and the tail domains are variable in size and sequence and contribute to the functional diversity of the intermediate filaments, being also important sites of regulation and interaction with other cellular elements. The assembly of the intermediate filaments is a process that follows the following steps: two individual subunits self-assemble to form a parallel coiled-coil dimer, two dimers associate in an anti-parallel manner to form a staggered tetramer, two tetramers combine to form octamers, and four octamers join to form the ULF (unit length filament); finally, individual ULF join end-to-end to form short filaments and these then grow into longer filaments by the continued addition of ULF as well as the end-to-end fusion of existing filaments (Goldman *et al.*, 2008).

The microtubules are rigid hollow tubes with a diameter of 25 nm and a lumen of 15 nm; they are constituted by heterodimers of α-tubulin and β-tubulin, which polymerize forming 13 laterally associated protofilaments. α-tubulin and β-tubulin are 50% identical at the amino acid sequence level, and each subunit has a molecular weight of about 50 kDa. The polymerization of the α/β-heterodimers is catalyzed by the hydrolysis of guanosine triphosphate (GTP) by β-tubulin subunits (Desai and Mitchison, 1997). The two ends of the microtubule are designated as plus and minus, and have different rates of polymerization; β-tubulin points towards the plus end, where polymerisation occurs faster, whereas α-tubulin points towards

the minus end, where depolymerization occurs faster. Microtubules have a crucial role in the maintenance of cell shape, in cell motility (they are the structural components of cilia and flagella), in the trafficking of vesicles and organelles, and in chromosome segregation during cell division. Microtubules are attached at their minus ends at the microtubule-organizing centre (MTOC), which is a cytosolic structure that is involved in the assembly and orientation of microtubules. A third tubulin isoform, γ-tubulin, localizes at the MTOC and is essential for microtubule nucleation, helping the formation of ring structures that serve as templates for microtubule growth (Moritz *et al.*, 1995).

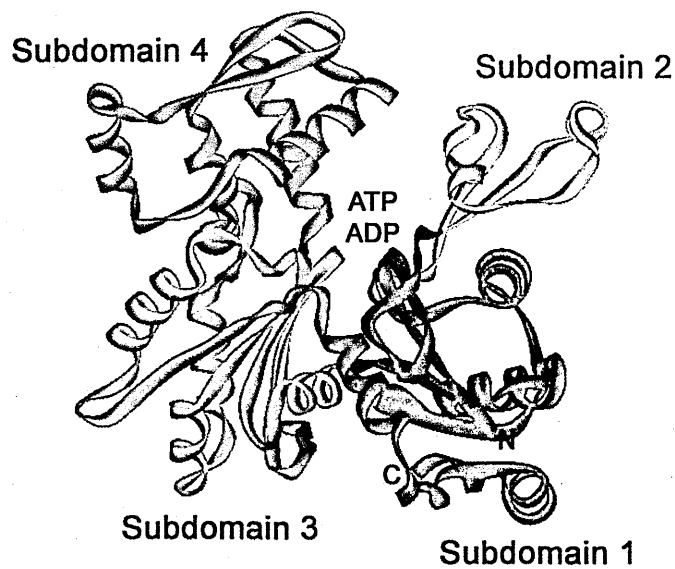

Figure 1.1 – Ribbon representation of the crystal structure of the actin monomer. The four domains are represented in different colours. ADP or ATP is bound at the centre of the molecule, inside the cleft (modified from Otterbein et al., 2001).

1.1.1 Assembly of actin filaments

Although association and dissociation of actin monomers from the filament can occur at both ends, association predominantly occurs at the barbed end, while dissociation at the pointed end (Wegner, 1976). *In vitro* under low ionic strength conditions actin is monomeric, while increasing the ionic strength to physiological levels (2 mM $MgCl_2$ or 100 mM KCl) induces monomeric actin to polymerize into synthetic F-actin (Kasai *et al.*, 1962b). Polymerization of actin occurs in three steps *in vitro* (Kasai *et al.*, 1962b, 1962a; Pollard, 2007). The first step is the nucleation phase, which is characterized by the energetically unfavourable process of aggregating three actin monomers to form a stable trimer, which can support the addition of further actin monomers for the formation of the filament. The second step is the elongation phase, which is a favourable process particularly at the fast-growing barbed end: ATP bound to each subunit is hydrolyzed to ADP with a half life of 2 seconds, and the γ-phosphate dissociates slowly over roughly 6 minutes; ADP bound to actin filaments has never been observed to exchange with ATP in the medium, so nucleotide exchange occurs only on actin monomers. The third step is the steady-state phase, which is reached when there is equilibrium between filaments and monomers; during this phase, exchange of actin monomers continues at the ends of the filament, but the total mass remains the same. This flux of actin subunits between the pointed end and the barbed end is known as treadmilling, whose rate is regulated by actin-binding proteins.

Different toxins promote depolymerization or stabilization of actin filaments. Cytochalasin is a fungal alkaloid that binds to the barbed ends of the actin filaments, thus inhibiting the association of actin subunits at that end, resulting in the depolymerization of the filament (Cooper, 1987). Latrunculin is another alkaloid

from the sponge *Latrunculia magnifica* that binds and sequesters actin monomers, thus inhibiting their incorporation into the filaments and resulting in their depolymerization (Coue *et al.*, 1987). Phalloidin is a bicyclic heptapeptide purified from the poisonous mushroom *Amanita phalloides*, that binds the actin filament, thus stabilizing it and protecting it from depolymerization (Lengsfeld *et al.*, 1974). These three toxins are widely used for actin cytoskeleton studies due to their specificities.

The dynamic assembly and disassembly of filaments and the formation of larger structures are key aspects of actin function, and are regulated by many actin-binding proteins. These proteins bind to filaments or monomers and control their structure and dynamics by: nucleating; capping; stabilizing; severing; depolymerizing; cross-linking; bundling; sequestering or delivering monomers; promoting monomer nucleotide exchange. The functional diversity of the actin-binding proteins and their coordinated actions at specific times and locations defines the various and distinct roles of actin filaments in the cell. Actin filaments at the leading edge of a migrating cell (lamellipodium) have different dynamics and composition compared to the filaments working in muscle contraction or constituting the microvilli at the apical surface of intestine's epithelial cells.

Cells use three different ways to trigger actin polymerization: 1) nucleation of filaments from monomeric actin; 2) severing of existing filaments to create uncapped barbed ends and; 3) uncapping of existing barbed ends (Higgs and Pollard, 1999).

Nucleation is initiated by three classes of actin-binding proteins identified so far: the formins, spire, and the actin-related protein-2/3 (ARP2/3) complex; each one activates nucleation by a distinct mechanism (Goley and Welch, 2006). The

formins promote the nucleation of unbranched filaments by stabilization of an actin dimer or trimer to facilitate the nucleation event; they remain associated with the growing barbed ends of filaments, and sequential binding and release interactions might allow formins to "walk" with the polymerizing barbed end. The spire proteins have four tandem G-actin-binding Wiskott–Aldrich syndrome protein (WASP)-homology-2 (WH2) domains, which mediate longitudinal association of four actin subunits and function as a scaffold for polymerization into an unbranched filament. Spire can cap pointed ends and prevent their depolymerization *in vitro*. The ARP2/3 complex was the first nucleator to be identified and it has a crucial role in the formation of branched-actin-filament networks during different processes ranging from cell motility to endocytosis. Arp2/3 is a multimeric protein complex that regulates actin dynamics in different ways: it binds to actin filaments, creates 70° branches and acts as a cross-linker. The Arp2/3 complex is made of seven polypeptides: Arp2 of 45 kDa, Arp3 of 47 kDa, actin-related protein complex (Arpc) 1 of 41 kDa, Arpc2 of 34 kDa, Arpc3 of 21 kDa, Arpc4 of 20 kDa and Arpc5 of 16 kDa (Welch *et al.*, 1997). Arp2/3 promotes actin filament formation by the generation of templates that nucleate actin polymerization and initiates actin filament branches by binding to the sides of existing filaments (Welch *et al.*, 1997). The nucleation activity of Arp2/3 is directly regulated mainly by members of the Wiskott-Aldrich syndrome (WASp)/Scar protein family (Machesky *et al.*, 1999).

The WASp/Scar family of proteins includes WASp of 53-kDa, neuronal WASp (N-WASp) of 55-kDa, and the 62-kDa WASP family Verprolin-homologous protein (WAVE, which is the vertebrate homologue of Scar). The proteins of this family interact with a variety of molecules known to influence the dynamics of the cytoskeleton, and integrate different cellular signals (e.g. growth factor receptor signals) through their functional domains with the actin cytoskeleton. The

WASp/Scar proteins share similar C-terminal regions, which are composed of the verprolin-homology domain (V; also known as WASP-homology-2 domain [WH2]), the cofilin-homology domain (also known as central domain [C]), and the acidic domain (A). Collectively, these three domains form the VCA region. The VCA region binds to an actin monomer and to the Arp2/3 complex, leading to the activation of its nucleation activity (Machesky *et al.*, 1999; Rohatgi *et al.*, 1999). The N-terminal regions of WASPs are different from those of WAVEs. WASP and N-WASP contain a WH1 domain (also known as the Ena-VASP-homology-1 [EVH1] domain), that is followed by a basic region and a GTPase-binding domain (GBD; also known as the Cdc42/Rac-interactive binding [CRIB] region). The WH1 domain binds to the WASP-interacting protein (WIP) family of proteins. It has been shown for N-WASp that the WH1 domain interacts with the C-terminal VCA region and inhibits the activation of the Arp2/3 complex; activated Cdc42 can bind to the GBD and block the intramolecular interaction between the C- and N- termini, resulting in the activation of the Arp2/3 complex (Symons *et al.*, 1996; Rohatgi *et al.*, 2000). On the other hand, WAVEs lack a GBD, although they are regulated by Rac (Miki *et al.*, 1998b). Furthermore, it was shown that the phosphatidylinositol (4,5)-bisphosphate [PtdIns(4,5)P2] binds to the basic region, resulting in WASp activation, which leads to the activation of Arp2/3 nucleation activity (Miki *et al.*, 1996).

A family of proline-rich proteins, called verprolins in yeast and WASp-interacting protein (WIP) family of proteins in animals, binds WASp and N-WASp. These proteins have N-terminal WH2 domains, a central proline-rich domain, and a C-terminal domain that binds WASp and N-WASp, resulting in the inhibition of their nucleation promoting activity. Cdc42, PtdIns(4,5)P2, and SH3 proteins release this

inhibition, allowing WASp to stimulate actin assembly by Arp2/3 complex; however there is evidence that WIP is required for WASp function (Pollard, 2007).

Cortactin is an actin-binding protein and one of the major Src substrate; it binds and activates the Arp2/3 complex, promoting branched actin polymerization. Cortactin is composed of four major domains: the N-terminal acidic (NTA), followed by 6.5 tandem repeats of 37 amino acids, a proline-rich region and the C-terminal SH3 domain (Cosen-Binker and Kapus, 2006; Weaver, 2008). Binding sites for the Arp2/3 complex and for actin filaments are found in the NTA and tandem repeat domains, respectively. These binding sites are both necessary and sufficient for direct regulation of Arp2/3-complex-mediated branched actin assembly (Uruno *et al.*, 2001; Weaver *et al.*, 2001). The C-terminus is the scaffold and regulatory part of the molecule, as the proline-rich domain contains phosphorylation sites for a number of kinases and the SH3 domain can bind many other signalling proteins. Clear evidence indicates that cortactin and N-WASp function synergistically, binding simultaneously to Arp2/3 complex (Figure 1.2) (Weaver *et al.*, 2003).

Actin polymerization can also start by severing of existing filaments to create uncapped barbed ends, and by the release of capping proteins from the tip of the filament. Gelsolin is an 80 kDa protein that breaks and caps actin filaments, thus producing short filaments that cannot elongate: upon a stimulus, the release of intracellular calcium activates gelsolin to sever actin filaments and cap their barbed ends (Sun *et al.*, 1999). In addition, membrane-bound PtdIns(4,5)P2 can remove the gelsolin cap and contribute to actin polymerization.

1.1.2 Actin-monomer-binding proteins

Non-muscle cells maintain a high concentration of unpolymerized actin (≤100 μM) and the vast majority is bound to ATP. Interestingly, 100 μM of actin monomers in physiological concentrations of salt polymerize rapidly in vitro, leaving only 0.1 μM of monomers (known as the critical concentration). Thus, a regulatory mechanism has been identified in cells, that maintains the high levels of actin monomers. This mechanism involves the action of the actin-monomer-binding proteins, which regulate actin polymerization and depolymerization by sequestering G-actin, exchanging the nucleotide ADP for ATP and delivering the monomer to the barbed end of the filament (Pollard *et al.*, 2000). The best-characterized actin-monomer-binding proteins are the actin depolymerization factor (ADF) /cofilin family of proteins, twinfilin, WASp/Scar family of proteins, thymosin and profilin.

ADFs and cofilins are both of 18.5 kDa, and increase actin filament turnover by binding ADP-actin monomers and increasing the dissociation rate of actin from the pointed ends of the filaments, but not from the barbed ends. In fact ADF/cofilins bind ADP-actin monomers with greater affinity than ATP-actin, and have greater affinity for ADP-actin filaments than ATP-actin filaments or ADP+Pi-actin filaments (Carlier *et al.*, 1997). Twinfilin is a 44 kDa protein that sequesters actin monomers with a stochiometry of 1:1 and binds ADP-actin preferentially, inhibiting the exchange of ADP for ATP, and thus affecting actin polymerization (Goode *et al.*, 1998). Thymosins are small proteins of 5 kDa that sequester G-actin through their WH2 domain (Paunola *et al.*, 2002) and prevent the delivery of actin monomers to the barbed end of the filaments. Profilins are proteins of 19 kDa, that, not only sequester G-actin, but can also bind the barbed end of the actin filament and promote filament polymerization (Tilney *et al.*, 1983); it has also been shown that

profilin can displace thymosin from actin monomers and transport actin to the barbed end of actin filaments (Pantaloni and Carlier, 1993). A similar mechanism has been observed between ADF/cofilins and twinfilin: ADF/cofilins deliver ADP-actin monomers to twinfilin, which keep the monomers in their ADP form close to the barbed ends (Goode *et al.*, 1998). Here, actin monomers can be released and undergo nucleotide exchange to assemble into the plus end of the filament either spontaneously or via interaction with profilin (Palmgren *et al.*, 2002). Thus, actin-monomer-binding proteins can be classified into monomer-sequestering proteins (thymosin and twinfilin), ATP-monomer-binding proteins (profilin and thymosin), ADP-monomer-binding proteins (ADF/cofilins, twinfilin), depolymerization promoters (ADF/cofilins), and ADP-actin nucleotide exchange inhibitors (twinfilin and ADF/cofilins).

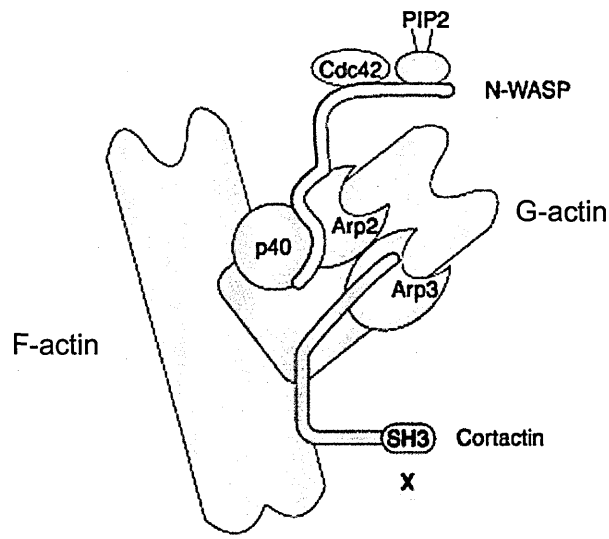

Figure 1.2 – Model of N-WASP and cortactin bound to the Arp2/3 complex at an actin filament branch point. Cortactin (dark blue) binds to Arp3, while N-WASP (red) binds to Arp2. Cortactin binds also actin filaments via its central repeats domain and a third molecule (X), such as dynamin, via its SH3 domain. Modified from Weaver *et al.*, 2003.

1.1.3 Actin stress fibres

Stress fibres are bundles of 10-30 actin filaments, which are held together by the actin crosslinking protein α-actinin (Pellegrin and Mellor, 2007); these actin filaments are associated with bipolar arrays of myosin II filaments, which alternate with α-actinin foci (Naumanen *et al.*, 2008). Myosin-mediated contractility is necessary for the integrity of actin stress fibres, as its inhibition leads to loss of stress fibres. Thus, actin stress fibres can generate contractile force, similarly to myofibrils of muscle cells. However, despite the periodic myosin α–actinin distribution resembling muscle sarcomers, stress fibres do not normally display repeatable contraction and relaxation cycles in relatively short timescale; instead, stress fibres appear to contract continuously with occasional relaxing or stretching. It has been also shown that stress fibres do not contract uniformly along their lengths and that the widths of myosin and α-actinin bands vary in different regions (Peterson *et al.*, 2004). Therefore, although actin stress fibres resemble myofibrils, they are less regularly organized. The continuous contraction of stress fibres is often in equilibrium with adhesion strength, especially in ventral stress fibres, which are connected to the substrate at both ends. This results in stable actin bundles that maintain a constant length under tension, which may be one of the major roles of actin stress fibres in cells. Based on their subcellular localization and interactions with focal adhesions, actin stress fibres of cultured mammalian cells can be divided into three classes (Naumanen *et al.*, 2008). Ventral stress fibres are contractile actin bundles, which display a periodic distribution of myosin and α-actinin, and they are typically associated with focal adhesions at their both ends. Ventral stress fibres are responsible for the tail retraction and other cell shape changes due to increased contractility, and work against membrane tension at cell borders. Transverse arcs are curved actin bundles, which also display a periodic

distribution of myosin and α-actinin. These structures are not directly attached to focal adhesions, but they are connected to the substrate via dorsal stress fibres. In migrating cells, they flow from the leading edge towards the cell center, and they contract continuously during this flow. The contractile force is transmitted to the substrate via dorsal stress fibres. These types of fibres are actin bundles that attach to focal adhesion at one end and rise towards the dorsal section of the cells at the other end. By contrast, to ventral stress fibres and transverse arcs, dorsal stress fibres do not typically display periodic α-actinin-myosin distribution.

1.1.4 Signalling pathways regulating actin cytoskeleton

Cells have complex mechanisms to adapt the actin cytoskeleton in order to perform different tasks in different environmental conditions. The binding to the membrane receptors by many molecules, such as growth factors, pro-inflammatory molecules or components of the extracellular matrix can activate specific signalling pathways, which lead to actin cytoskeleton remodelling. In many cases the activation of a specific signalling pathway results in Ca^{2+} release and generation of different types of phosphatidylinositols, which both regulate the assembly of actin filaments by controlling the activity of capping, monomer-binding and severing proteins. Binding of PtdIns(4,5)P2 to profilin inhibits its association with actin (Lassing and Lindberg, 1985, 1988). The severing activity of gelsolin can be regulated either by Ca^{2+} or by PtdIns(4,5)P2: binding of Ca^{2+} to gelsolin activates its severing activity, whereas binding of PtdIns(4,5)P2 inhibits gelsolin activity (Janmey *et al.*, 1987; Bearer, 1991). ADF and cofilin activities are inhibited by phosphatidylinositol (4)-phosphate [PtdIns(4)P] and PtdIns(4,5)P2 (Yonezawa *et al.*, 1990).

The Rho family of small GTPases are known to be key regulators of signalling pathways that link extracellular and intracellular stimuli to the organization of the cytoskeleton, resulting in the formation of lamellipodia, membrane ruffles, filopodia and stress fibres. Signalling pathways through Rho GTPases are initiated by the activation of many different types of plasma-membrane receptors. Rho GTPases cycle between an inactive GDP-bound form and an active GTP-bound form, which activates a plethora of downstream effectors. The cycle between the inactive and the active state is regulated by GDP/GTP exchange factors (GEFs), GTPase-activating proteins (GAPs), and guanine nucleotide dissociation inhibitors (GDIs) (Hall and Nobes, 2000; Buchsbaum, 2007). GEFs are responsible for the conversion of the inactive GDP-bound form to the active GTP-bound form, and consequently GEFs act as Rho GTPases activators. GAPs accelerate the low intrinsic GTPase activity of Rho GTPases, thus working as Rho GTPases inactivators. GDIs inhibit the dissociation of GDP from Rho GTPases, which results in Rho GTPases signalling inhibition.

The Rho family of small GTPases in mammalian cells includes Ras homology (Rho), ras-related C3 botulinum toxin substrate (Rac) and cell division cycle 42 (Cdc42). Their respective isoforms are RhoA, RhoB and RhoC for Rho; Rac1, Rac2 and Rac3 for Rac; G25K and Cdc42Hs for Cdc42 (Hall and Nobes, 2000). Rho proteins regulate the assembly of actin stress fibres (Ridley and Hall, 1992); Rac proteins regulate actin polymerization at the cell periphery, inducing the formation of lamellipodia and membrane ruffles (Ridley *et al.*, 1992); Cdc42 proteins trigger filopodia formation (Kozma *et al.*, 1995). In addition, all three types of GTPases regulate the formation of focal adhesions, which are closely associated with the actin structures (Hotchin and Hall, 1995; Nobes and Hall, 1995). However, locally restricted regulation of actin in specific cell areas is not the

result of the activation of a single signalling pathway by a single protein, but rather the outcome of several pathways that are activated in parallel. Indeed, Rho family GTPases coordinate cytoskeleton rearrangements in concert, and the activation of Cdc42 can lead to the activation of Rac, which in turn activates Rho (Nobes and Hall, 1995).

Rac and Cdc42 proteins can activate WAVE and N-WASp respectively, which in turn activate the nucleation activity of the Arp2/3 complex (Miki *et al.*, 1998a; Miki *et al.*, 1998b; Machesky *et al.*, 1999). Both GTPases can also activate LIM kinase 1 and 2 (LIMK1 and LIMK2) respectively, which in turn phosphorylate and inactivate cofilin, thus inhibiting actin filament disassembly (Arber *et al.*, 1998; Sumi *et al.*, 1999). Furthermore, Rac also triggers dissociation of gelsolin from actin filaments to promote actin polymerization (Arcaro, 1998).

Rho proteins induce the formation of actin stress fibres through several downstream effectors, including mammalian diaphanous (mDia) and Rho kinase (p160ROCK) (Narumiya *et al.*, 1997; Watanabe *et al.*, 1997). In addition Rho also induces the formation of focal adhesions through p160ROCK (Narumiya *et al.*, 1997). p160ROCK is able to active LIMK2, which in turns phosphorylates cofilin; phosphorylated cofilin dissociates from actin filaments, hence allowing actin polymerization (Maekawa *et al.*, 1999). mDia was shown to interact with profilin and to induce actin polymerization, probably by recruiting profilin to the sites of actin polymerization (Frazier and Field, 1997; Watanabe *et al.*, 1997).

Other effectors of Rho GTPases are PI kinases, which generate phosphatidylinositol phosphates. Rho and Rac physically interact with and regulate the PI(4)P 5-kinase, which is responsible for the major generation of PtdIns(4,5)P2 (Chong *et al.*, 1994; Tolias *et al.*, 1995).

1.2 Cell-Matrix adhesions

Cell adhesion to the extracellular matrix (ECM) is essential for normal embryonic development and tissue homeostasis. Structurally defined adhesion sites between cultured cells and the ECM were initially described about 30 years ago in studies using interference-reflection microscopy and electron microscopy. These studies revealed that matrix adhesion occurs at specialized, elongated small regions along the ventral plasma membrane, which are tightly connected with the substrate and leave a gap of only 10-15 nm. Early studies also identified the presence of different types of adhesions within a single cell at one time (Izzard and Lochner, 1980). So far, it has been found that different forms of cellular structures can mediate interactions with the ECM, depending upon the cell type and the tissue environment. Most of cell-ECM adhesions are mediated by integrins, which are a family of glycosylated, heterodimeric transmembrane adhesion receptors that consist of non-covalently bound α- and β-subunits. On two-dimensional substrate, adhesion sites are distributed asymmetrically across the ventral surface of the cell and are associated with morphologically distinct actin structures. Based on subsequent detailed analyses, these integrin-mediated adhesion sites have been classified into three main groups: focal complexes, focal adhesions and fibrillar adhesions (Geiger *et al.*, 2001). Focal complexes are small, transient structures, which usually form just behind the leading edge of spreading or migrating cells; they can support the growth of nascent filopodial and lamellipodial actin networks and are considered to be involved in the sampling of the ECM environment prior to formation of more stable contacts. Focal adhesions are larger, more stable and mature structures, that derive from the maturation of focal complexes, and are located across the base of an adherent cell. Focal adhesions contain multiple signalling and actin-binding proteins responsible for providing mechanical stability

and for allowing transmission of tractional forces from cell to ECM and vice versa. Fibrillar adhesions have been described in three-dimensional matrix systems or in cells plated on two-dimensional complex ECM and are thought to be derived from a subset of focal adhesions. Fibrillar adhesions are long, highly stable complexes that run parallel to bundles of fibronectin; as such they are highly enriched in tensin and active $\alpha5\beta1$ integrin and are sites of localized matrix deposition and fibronectin fibrillogenesis beneath the cell (Zamir *et al.*, 2000). Detailed analyses of the distribution of adhesion proteins have revealed differences in concentration and post-translational modifications of these proteins among different adhesion types. For example, the more transient focal complexes do not contain zyxin (Zaidel-Bar *et al.*, 2004), whereas highly stable fibrillar adhesions do not contain β3 integrin or phosphorylated active FAK (Zaidel-Bar *et al.*, 2004). Moreover, focal complexes are induced by Rac and Cdc42, whereas the maturation of focal complexes into focal adhesions is dependent on Rho activity and acto-myosin tension (Romer *et al.*, 2006). The functional relevance of these differences in molecular composition has still to be determined but it is likely that distinct populations of proteins will give distinct mechanical properties to each adhesion.

1.2.1 Focal adhesions

Focal adhesions were first identified by electron microscopy (Abercrombie *et al.*, 1971) as electron-dense regions of the plasma membrane that make intimate contact with the substratum in cultured cells. They constitute not only the site of anchorage of the actin cytoskeleton to the cytoplasmic side of the plasma membrane, but also a site of integration of diverse signalling pathways. At the molecular level, focal adhesions are formed around a core of an α/β integrin

heterodimer, which binds to a component of the ECM on its extracellular side. This early adhesive site matures through recruitment of additional integrins and cytoskeletal components. Different signalling pathways are activated, leading to the interaction and ordered aggregation of more than 150 different proteins (Zaidel-Bar *et al.*, 2007), which include adaptors, kinases, GTPases, GEFs, and GAPs. At different time points and cellular locations, focal adhesion assembly is regulated by diverse molecular switches, such as phosphorylation, conformational changes, proteolysis, ligand density, contractility, surface rigidity and topography (Geiger and Bershadsky, 2001; Geiger *et al.*, 2001).

1.3 Podosomes and invadopodia: invasive adhesions

Podosomes and invadopodia are two closely related adhesion structures, that are actively involved in focal degradation of the ECM, and can be considered members of a larger group of invasive adhesions (Figure 1.3) (Buccione *et al.*, 2004; Gimona and Buccione, 2006). In the literature the two terms (podosomes and invadopodia) have often been used interchangeably in different cell types, but recently efforts have been made to understand the relationship between these two structures. The term podosomes were initially used to describe the ring- and dot-like, actin-rich structures that are formed by Rous-sarcoma-virus-transformed baby hamster kidney fibroblasts (Tarone *et al.*, 1985; Marchisio *et al.*, 1988). At present podosomes are defined as highly dynamic, actin-rich structures that are involved in the adhesion process of cells to solid substrates, and are composed of a densely packed actin core surrounded by a ring structure made of components commonly found in focal adhesions (Figure 1.4) (Gimona and Buccione, 2006). Podosomes can assemble into clusters, ring-shaped superstructures (called rosettes), and

belts, depending on the cell type and stage of differentiation. There is strong evidence that they are organelles devoted to the remodelling of ECM and cell migration.

Invadopodia were initially defined as stable, actin-rich protrusions stemming from the ventral surface of invasive cancer cells cultured on appropriate substrates, and displaying focal proteolytic activity towards the ECM (Mueller and Chen, 1991). This definition was later refined by the identification of a number of proteins, including integrins, tyrosine kinases, soluble and membrane-bound proteases, and actin-associated proteins, such as cortactin (Figure 1.5) (Gimona and Buccione, 2006). Other features typical of invadopodia include their localization proximal to the Golgi complex (Baldassarre *et al.*, 2003), and their extended half-life of two hours or more (Yamaguchi *et al.*, 2005).

1.3.1 Differences between podosomes and invadopodia

Diverse parameters distinguish podosomes from invadopodia (Linder and Kopp, 2005; Gimona and Buccione, 2006): (i) Podosomes and invadopodia have different shape and size. Podosomes are dots with an approximate diameter of 0.5-1 μm and a depth of 0.2-0.4 μm, while invadopodia are finger-like protrusions with a diameter of about 8 μm and they can reach a depth of several micrometers. (ii) While a cell typically forms dozens of podosomes, only few invadopodia are formed by a single cell. (iii) Podosomes and invadopodia display different subcellular localizations. While podosomes form almost exclusively at the periphery of the cell, invadopodia usually develop close to the perinuclear region and the Golgi apparatus. (iv) Podosomes and invadopodia have different lifetimes. Podosomes turn over in a range of few minutes (2–10), whereas invadopodia have

been observed in their same subcellular position for several hours. (v) In the case of podosomes it is clear that the area surrounding the actin-rich core is in close contact to the substrate, whereas the adhesive portions of invadopodia still remain to be identified. Real-time imaging experiments suggest that invadopodia remain attached to the substrate as the cell moves forward, but this scenario still needs confirmation and detailed analysis.

At the moment it is unclear whether podosomes and invadopodia are distinct and independent structures or whether they are two sides of the same coin, that is two alternative expressions of the same cellular response, following contact with the substratum. It has also been proposed that podosomes could be precursors of invadopodia, but actual development of invadopodia from podosomes has not yet been observed.

1.3.2 Podosomes in various cell types

Podosomes have been identified and studied for the first time in Src-transformed fibroblasts (Tarone *et al.*, 1985; Marchisio *et al.*, 1988), and since then the list of cell types forming podosomes got progressively longer.

The first cell type forming podosomes in a physiological context to be identified was the bone-resorbing osteoclast (Oreffo *et al.*, 1988; Zambonin-Zallone *et al.*, 1988; Zambonin-Zallone *et al.*, 1989). In osteoclasts the actin cytoskeleton is organized in two different dynamic structures: a "belt" of podosomes at the cell periphery (Destaing *et al.*, 2003), and a "sealing zone" (Teti *et al.*, 1991). The sealing zone in stationary, actively resorbing osteoclasts is composed of a core of F-actin, which is surrounded by an adhesive double ring-like structure containing

adhesion proteins, like talin and vinculin. By contrast, the formation of the podosome belt is associated with the migratory phase of osteoclasts, which alternate with the stationary phase of bone resorption (Lakkakorpi and Vaananen, 1991; Teti *et al.*, 1991; Lakkakorpi *et al.*, 2003). The F-actin-rich core of podosomes contains the Arp2/3-complex-dependent actin polymerization machinery and regulatory elements (Calle *et al.*, 2004; Hurst *et al.*, 2004). The outer rim of podosomes is enriched in integrins and classical focal adhesion markers, such as α-actinin, talin, vinculin and paxillin (Zambonin-Zallone *et al.*, 1989; Helfrich *et al.*, 1996; Nakamura *et al.*, 1999; Luxenburg *et al.*, 2006a). Using primary osteoclasts expressing GFP-actin, it has been shown that podosome belts and sealing zones are both present in mature osteoclasts: podosome belts form only in spread osteoclasts adhering onto glass, whereas the sealing zone forms in apico-basal polarized osteoclasts, which adhere onto mineralized matrix (Saltel *et al.*, 2004). The same authors showed also that the sealing zone forms as an independent structure upon contact with the mineralized matrix and not by the fusion of podosomes. Recently, a novel approach based on high-resolution scanning electron microscopy revealed that the sealing zone consists of a dense array of podosomes linked via a network of actin filaments (Luxenburg *et al.*, 2007). Thus, the sealing zone is made of individual podosomes, which differ from podosome belts in their degree of density and interconnectivity.

Podosomes have a role also in the function of macrophages (Figure 1.6, a). Wiskott-Aldrich syndrome (WAS) is a genetic disorder characterized by severe immunodeficiency, which is caused by mutations in WASp. WAS neutrophils (Ochs *et al.*, 1980), dendritic cells (Binks *et al.*, 1998), and primary macrophages (Badolato *et al.*, 1998; Zicha *et al.*, 1998) have been shown to have defects in cell motility, due to dysfunction in chemotaxis. In macrophages from WAS patients, it

has been demonstrated that this dysfunction is linked to the dislocalization of the Arp2/3 complex, which causes a failure in the development of podosomes (Linder *et al.*, 1999; Linder *et al.*, 2000a). All these defects could be restored upon exogenous expression of WASp in cells from WAS patients (Jones *et al.*, 2002). Macrophages migrate in response to colony stimulating factor 1 (CSF-1), which is secreted by injured endothelial cells and fibroblasts; it has been shown that CSF-1 increases the rate of podosome formation via phosphatidylinositol 3-kinase (PI3K) signalling in polarized migrating bone-marrow-derived macrophages in vitro (Jones *et al.*, 2002; Wheeler *et al.*, 2006a).

Dendritic cells also form podosomes to migrate (Burns *et al.*, 2001; Burns *et al.*, 2004). As for macrophages, also dendritic cells from WAS patients display dislocalization of the Arp2/3 complex and failure in the formation of podosomes, which could be restored by exogenous expression of WASp (Burns *et al.*, 2001). Similarly a lentiviral vector encoding human WASP could restore podosome formation and immune function in mouse WASp $^{-/-}$ dendritic cells (Charrier *et al.*, 2005). Furthermore, down-regulation of WASP expression by RNA interference significantly reduces podosome formation in primary dendritic cells, recapitulating the phenotype of cells derived from patients or mouse with inactivating mutations of the WAS gene (Olivier *et al.*, 2006).

Podosomes have been identified not only in a number of transformed cells of epithelial origin, including the HeLa, T47D, MCF-7 and HEK293 cell lines (Seals *et al.*, 2005), but also in the rat 804G bladder carcinoma cell line and in human primary keratinocytes (Spinardi *et al.*, 2004). In the latter two types of epithelial cells, each podosome is surrounded by a rosette of hemidesmosomes, thus suggesting an organized unit of cytoskeletal structures related to the firm epithelial adhesion to the basement membrane. In response to adrenocorticotropic hormone

(ACTH)-induced phosphorylation of caveolin and activation of protein kinase A, Y1 adrenocortical epithelial cells also form podosomes by the rearrangement of existing focal adhesions (Colonna and Podesta, 2005). Lately, it has been found that the protein kinase C (PKC) activator phorbol-12,13-dibutyrate (PDBu) induces reorganization of the actin cytoskeleton and podosome formation in primary normal human bronchial epithelial cells and in normal human airway epithelial BEAS2B cells (Xiao *et al.*, 2009). The authors suggest that podosomes may have an important role in mediating airway epithelial cell migration and invasion during tissue repair, airway branching and lung development.

There is strong evidence that podosomes are involved also in the adhesion, migration and invasion of endothelial cells, processes that are required for angiogenesis and vascular remodelling (Figure 1.6, c). It was first reported that in a porcine aortic endothelial (PAE) cell line, podosomes can be induced by cytotoxic necrotizing factor 1 (CNF1), an activator of Rho GTPases (Moreau *et al.*, 2003); the same authors found podosomes also in endothelial cells isolated from human aortas, freshly explanted from patients undergoing cardiac surgery. Successively, it was reported that in subconfluent human umbilical vein endothelial cells (HUVECs), podosomes are formed spontaneously, but their formation rate is increased after stimulation with cytokines like vascular endothelial growth factor (VEGF) and tumour necrosis factor α (TNFα), during co-culture with monocytes, or after wounding of an endothelial monolayer (Osiak *et al.*, 2005). Furthermore, transforming growth factor β (TGFβ) has been shown to promote podosome formation in primary bovine aortic endothelial cells (Varon *et al.*, 2006). Also phorbol esters, such as phorbol-12-myristate-13-acetate (PMA), are able to induce podosome formation in porcine aortic endothelial cells and HUVECs, after initial disruption of stress fibres (Tatin *et al.*, 2006). In most of these cases, it has been

shown that matrix metalloproteinases (MMPs), such as MT1-MMP, MMP-2 or MMP-9, are recruited to podosomes, resulting in the degradation of the underlying matrix (Osiak *et al.*, 2005; Tatin *et al.*, 2006; Varon *et al.*, 2006).

In response to phorbol esters like PDBu, 12-O-tetradecanoylphorbol-13-acetate (TPA) and PMA, A7r5 vascular smooth muscle cells disassemble actin stress fibres and focal adhesions to form peripheral podosomes (Figure 1.6, b), which were initially described as α-actin-rich, dense, peripheral structures (Fultz *et al.*, 2000), and later identified as podosomes (Hai *et al.*, 2002). Podosomes have been found also in primary cultures of rat aortic smooth muscle explants (Webb *et al.*, 2006), and in a human intestinal smooth muscle cell line (Lener *et al.*, 2006). It has been shown that podosome formation in A7r5 cells results in ECM degradation and cell motility (Burgstaller and Gimona, 2005), and that these podosomes form preferentially in the leading lamella of the polarized cell, similar to macrophages and dendritic cells. Podosome formation in vascular smooth muscle cells could be the mechanism by which these cells can escape the boundaries of the surrounding ECM, and migrate from the vascular medial layer into the intima during the pathological process of atherogenesis (Burgstaller and Gimona, 2005). Recently, podosomes have been identified also in myoblasts (Thompson *et al.*, 2008).

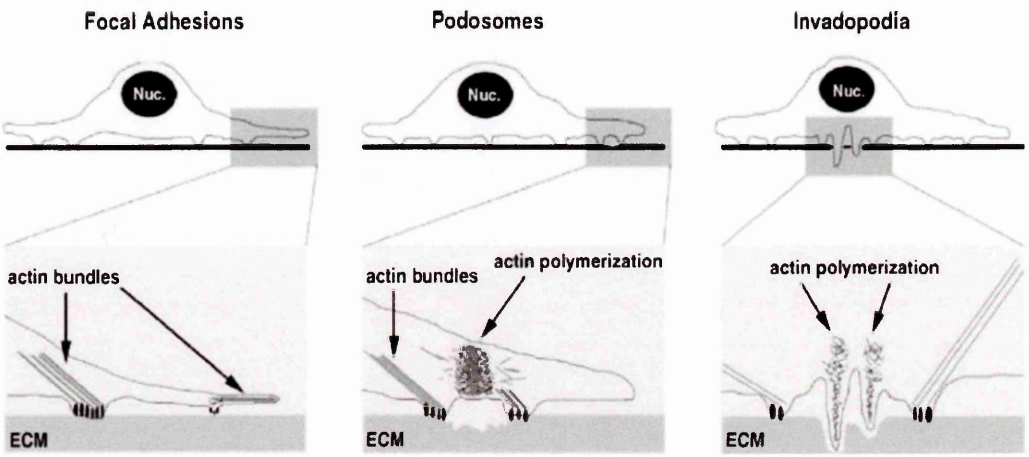

Figure 1.3 – Schematic representation of the organization of focal adhesions, podosomes and invadopodia. A hallmark of focal adhesions is the anchorage of bundled actin filaments to the sites of integrin clustering (black spheres). By contrast, podosomes and invadopodia are composed of de novo polymerized branched actin filaments meshworks, and lack prominent cytoskeleton-membrane linkages. From Gimona and Buccione, 2006.

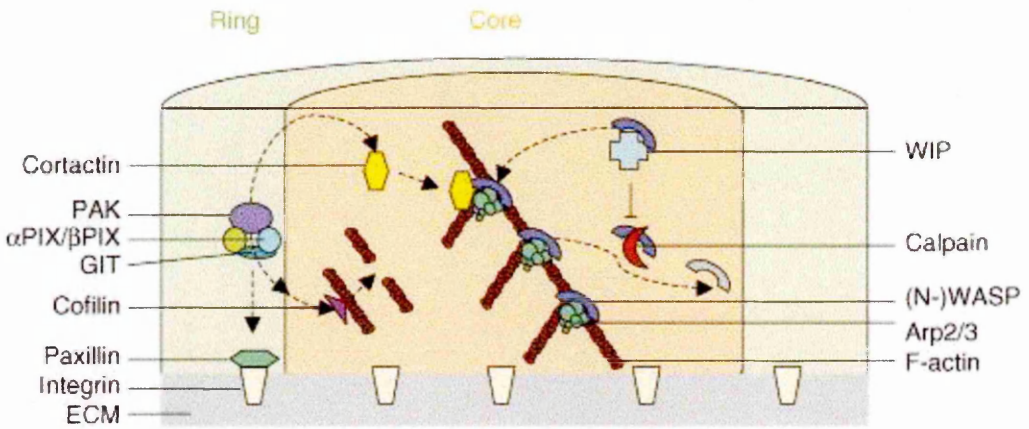

Figure 1.4 – Model of the structure of a podosome. This cartoon depicts a model of the podosome structure. In green is the ring structure, in pink is the actin-rich core, in gray is the extracellular matrix. The ring structure contains different signalling and cytoskeletal-associated proteins, while the actin-rich core contains actin filaments, Arp2/3-mediated actin polymerization machinery and diverse regulators of actin dynamics. From Linder, 2007.

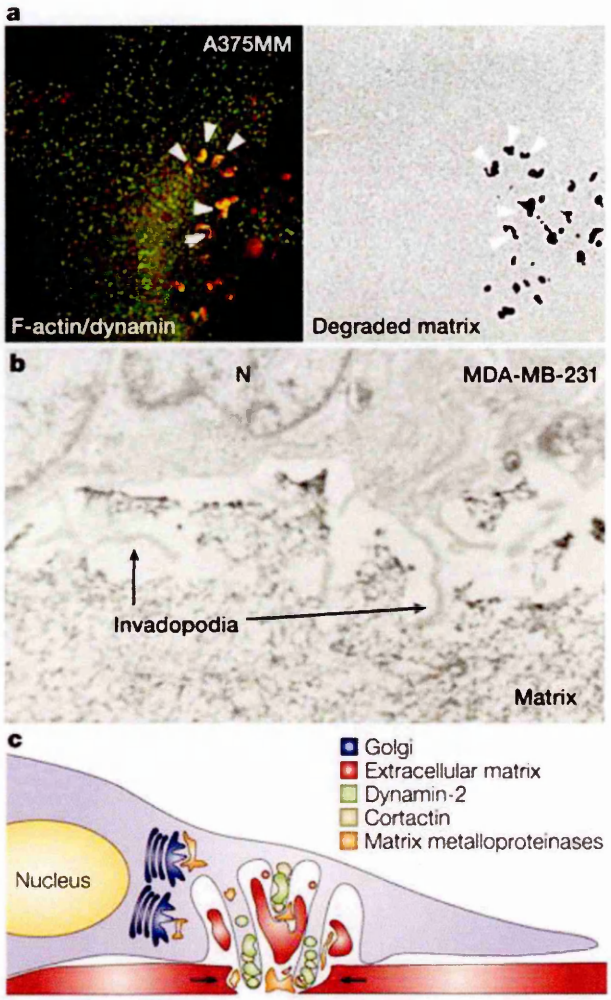

Figure 1.5 – Invadopodia structure and function. (a) The left panel shows the invasive and metastatic human A375MM melanoma cell line, stained for dynamin-2 (green) and F-actin (red). The arrowheads indicate the locations where the two proteins colocalize, which are the same where ECM has been degraded (black spots in the right panel). **(b)** Electron micrograph of an invasive MDA-MB-231 human breast tumour cell extending several long thin invadopodia (arrows) deep into the ECM at the cell base. **(c)** Schematic representation of invadopodia structure with some of the key components. The arrows show the sites of protrusion into the ECM. From Buccione *et al.*, 2004.

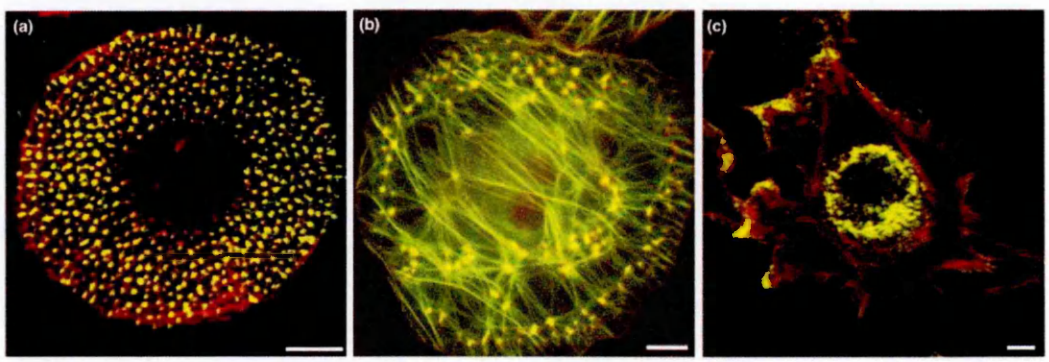

Figure 1.6 – Immunofluorescence micrographs of podosomes in various cell types. (a) Podosomes in a primary human macrophage. WASP (green) and F-actin (red) colocalize in the core structure of podosomes (yellow). **(b)** Podosomes in an A7r5 vascular smooth muscle cell. α-actinin-GFP (green) and F-actin (red) colocalize in the core structure of podosomes (yellow). **(c)** Podosomes in a human umbilical vein endothelial cell. α-actinin (green) and F-actin (red) colocalize (yellow) in a rosette formation of podosomes. From Linder, 2007.

1.3.3 The signalling pathways

The formation and function of invasive adhesions are regulated by a network of signal transduction pathways, triggered by extracellular signals. These signals include cytokines and growth factors, such as VEGF and TNFα (Osiak *et al.*, 2005), TGFβ (Varon *et al.*, 2006; Mandal *et al.*, 2008), CSF-1 (Wheeler *et al.*, 2006a), and epidermal growth factor (EGF) (Yamaguchi *et al.*, 2005). However, beside these signals, the attachment to the substratum is crucial, since podosomes and invadopodia are formed only in adherent cells, upon activation of integrins (Nakahara *et al.*, 1998; Pfaff and Jurdic, 2001; Redondo-Munoz *et al.*, 2006). All these extracellular signals trigger cascades, which involve activation of PKC (Colucci *et al.*, 1990; Bowden *et al.*, 1999; Hai *et al.*, 2002; Tatin *et al.*, 2006), activation of the tyrosine kinase Src (Nermut *et al.*, 1991; Lakkakorpi *et al.*, 2003; Gatesman *et al.*, 2004; Spinardi *et al.*, 2004; Luxenburg *et al.*, 2006b; Tatin *et al.*, 2006), as well as of other tyrosine kinases (Duong *et al.*, 1998; Nakahara *et al.*, 1998; Duong and Rodan, 2000), and regulation of Rho family GTPases. In all these cascades, Src is necessary and is the key mediator that phosphorylates most of the critical components and regulators of invasive adhesions.

The Rho GTPases RhoA, Rac and Cdc42 have all been shown to regulate invasive adhesion assembly and dynamics in various cell types; however, it seems that the specific mode of action of each one depends on the cell type. In osteoclasts RhoA activity is required for podosome formation and bone resorption (Chellaiah *et al.*, 2000). In Src-transformed fibroblasts, it has been shown that active RhoA localizes to podosomes and is necessary for Src-induced podosome assembly and function (Berdeaux *et al.*, 2004). In dendritic cells all three GTPases have a role in podosome formation or localization (Burns *et al.*, 2001). In

macrophages, expression of activated Cdc42 leads to podosome disassembly (Linder *et al.*, 1999), while knock-out experiments of Rac isoforms showed that Rac2 is essential for podosome formation (Wheeler *et al.*, 2006b). In endothelial cells the signaling system seems to be more complicated: in PAE cells activation of Cdc42 and down-regulation of RhoA activity induces podosome formation (Moreau *et al.*, 2003), while in HUVECs both activation or inactivation of either RhoA, Rac1 or Cdc42 reduced podosome formation, indicating a role in this process for all three GTPases, with RhoA acting as a downstream effector of cytokine signalling (Osiak *et al.*, 2005). Later on it was shown, by using RNA interference approach, that RhoA and Cdc42, but not Rac1, are required (downstream of PKC) for PMA-induced podosome formation in HUVECs (Tatin *et al.*, 2006). Thus, it seems that endothelial cells from different vascular beds use different signalling cascades, resulting in a different role of individual Rho GTPases on podosome formation. Collectively, these data suggest that podosomes are regulated by the integration of the activities of different Rho GTPases, and that local fine-tuning of the activity of individual Rho GTPases is crucial for podosome and invadopodia formation and dynamics. This has been confirmed by the finding that proteins regulating the GTPase cycle of Rho family members regulate invasive adhesion formation (Linder, 2007).

PAK (p21 associated kinase), a key downstream effector of activated Rac and Cdc42, and members of the PAK-interacting exchange factor (PIX) family have been shown to regulate podosomes and invadopodia. In smooth muscle cells, expression of active PAK1 induces podosome formation, and the interaction between PAK1 and βPIX is necessary for podosome formation (Webb *et al.*, 2005). Similarly in macrophages, PAK4 localizes to podosomes and PAK4 kinase activity regulates podosome size and number, together with αPIX (Gringel *et al.*, 2006).

1.3.3.1 p190RhoGAP

p190RhoGAP (named also p190A) is a Rho GTPase-Activating Protein of 190 kDa that, upon phosphorylation by Src, forms a complex with p120RasGAP (Ras GTPase-Activating Protein of 120 kDa), and down-regulates RhoA activity, resulting in the inhibition of actin stress fibre and focal adhesion formation (Settleman *et al.*, 1992; McGlade *et al.*, 1993; Hu and Settleman, 1997; Fincham *et al.*, 1999). It has also been reported that p190RhoGAP colocalizes with p120RasGAP at membrane ruffles in macrophages (Pixley *et al.*, 2005), and at arc-like actin structures following EGF stimulation in stably overexpressing Src fibroblasts (Chang *et al.*, 1995). Recent data suggest that p190RhoGAP has a role in triggering the formation of invadopodia and podosomes. It has been shown that F-actin and p190RhoGAP co-distribute in invadopodia, and microinjection of antibodies directed against p190RhoGAP inhibits localized matrix degradation (Nakahara *et al.*, 1998). In response to phorbol esters and subsequent PKC activation, p190RhoGAP is tyrosine-phosphorylated and recruited to the sites of podosome formation, where it may down-regulate RhoA activity (Brandt *et al.*, 2002; Burgstaller and Gimona, 2004).

p190B is another RhoGAP related to p190RhoGAP, but encoded by a different gene. Both proteins share 51% identity and display similar domain organisation, which include an N-terminal GTP-binding motif followed by four FF domains (protein-protein interacting domains harbouring two strictly conserved phenylalanine residues), a central domain and the C-terminal RhoGAP domain. Recently it has been shown that knockdown of p190B in HUVECs results in a decrease in MT1-MMP cell-surface presentation and MMP2 activation, and in a consequent reduction of podosome-mediated ECM degradation (Guegan *et al.*, 2008).

1.3.4 The actin machinery

Podosome and invadopodia formation requires *de novo* actin polymerization mediated by the Arp2/3 complex and its activators WASp, N-WASp, and cortactin. All these proteins have been found in the podosome core and in invadopodia, and have been shown to be necessary for their formation (Linder *et al.*, 1999; Linder *et al.*, 2000a; Burns *et al.*, 2001; Jones *et al.*, 2002; Mizutani *et al.*, 2002; Calle *et al.*, 2004; Osiak *et al.*, 2005; Yamaguchi *et al.*, 2005; Artym *et al.*, 2006; Bowden *et al.*, 2006; Olivier *et al.*, 2006; Tehrani *et al.*, 2006; Zhou *et al.*, 2006).

WASp stability and N-WASp recruitment to nascent invasive adhesions are probably facilitated by WIP, which has been localized to podosomes of endothelial cells (Moreau *et al.*, 2003) and dendritic cells (Chou *et al.*, 2006) and to invadopodia of carcinoma cells (Yamaguchi *et al.*, 2005). WIP seems to be critical for podosome and invadopodia formation, as interference with N-WASp interaction by a competitive peptide reduces invadopodia formation (Yamaguchi *et al.*, 2005), and $WIP^{-/-}$ dendritic cells do not form podosomes (Chou *et al.*, 2006).

1.3.5 The adhesion machinery

A number of different integrins are present in podosomes and invadopodia of different cell types (Gimona *et al.*, 2008). In epithelial cells, podosomes assemble mostly $\alpha6\beta4$, while in osteoclasts they recruit $\alpha v\beta1$, $\alpha2\beta1$ and $\alpha v\beta3$. The integrins $\alpha6\beta1$, $\alpha3\beta1$ and $\alpha5\beta1$ are enriched in the membrane fraction of invadopodia from melanoma cells, whereas $\alpha v\beta3$ is part of the MMP-2/MT1-MMP docking and activation complex in MCF7 breast carcinoma cells. It has been

shown that the non-integrin receptor for hyaluronic acid, CD44, clusters at podosomes to regulate their stability and adhesion via N-WASp, Src and cortactin (Chabadel *et al.*, 2007).

1.3.6 The matrix degradation machinery

Invadopodia of carcinoma cells (Baldassarre *et al.*, 2003; Yamaguchi *et al.*, 2005; Bowden *et al.*, 2006), osteoclasts (Teti *et al.*, 1991) and podosomes of transformed fibroblasts (Chen, 1989; Monsky *et al.*, 1993) have been initially recognized as structures that degrade ECM proteins, such as fibronectin, collagen and laminin (Kelly *et al.*, 1994). Only recently it has been shown that also podosomes of endothelial cells (Osiak *et al.*, 2005; Tatin *et al.*, 2006; Varon *et al.*, 2006), macrophages (Yamaguchi *et al.*, 2006), and smooth muscle cells (Burgstaller and Gimona, 2005; Furmaniak-Kazmierczak *et al.*, 2007) are capable of degrading ECM. Thus far, members of three classes of matrix-degrading enzymes have been identified in invasive adhesions: zinc-regulated metalloproteinases, serine proteases, and cathepsin cysteine proteases.

Major metalloproteinases constitute the families of "matrix metalloproteinases" (MMPs) and of "a disintegrin and metalloproteinase" (Kureishy *et al.*). A number of MMPs are secreted, while others are localized to the cell surface through membrane anchors or trans-membrane stretches (MT-MMPs). MMPs are synthesized as inactive pro-enzymes and become activated following proteolytic removal of a prodomain. MT1-MMP, MMP-2 and MMP-9 are metalloproteinases that have been identified in podosomes and invadopodia. MT1-MMP has been detected at invadopodia of melanoma cells (Nakahara *et al.*, 1997) and at podosomes in osteoclasts (Sato *et al.*, 1997), MMP-2 has been found in the

invasive adhesions of Src-transformed fibroblasts (Monsky *et al.*, 1993), MT1-MMP and MMP-2 have been localized to podosomes in endothelial cells (Osiak *et al.*, 2005; Tatin *et al.*, 2006), MMP-9 has been located at invasive adhesions of leukemia cells (Redondo-Munoz *et al.*, 2006).

ADAMs act as sheddases (enzymes that cleave proteins at the cell surface, resulting in the release of ectodomains) by cleaving growth factor and cytokine precursors into their active forms. Moreover, the disintegrin domain of ADAMs interacts with integrins, especially the β1 isoforms (Seals and Courtneidge, 2003). ADAM 12 associates with the adaptor protein Tks5 in Src-transformed fibroblasts, and both localize to podosomes (Abram *et al.*, 2003). In eosinophils, ADAM 8 and ADAM 10 are also localized to podosomes (Johansson *et al.*, 2004). However, a clear function of ADAMs in the regulation of invasive adhesions has not yet been demonstrated.

Among the serine proteinases, seprase and its homolog DPP4 have been shown to form a complex that localizes to invadopodia of migratory fibroblasts (Ghersi *et al.*, 2002), and migratory endothelial cells (Ghersi *et al.*, 2006), where they are involved in ECM degradation and cell invasion.

Recently, it has been shown that lysosomal cysteine protease cathepsin B has a role in the podosome-mediated ECM degradation and invasion in Src–transformed fibroblasts (Tu *et al.*, 2008). The same authors also observed that the lysosomal marker LAMP-1 localizes at the center of podosome rosettes, and that lysosomes fuse with podosomes, suggesting a role for lysosomes in the ECM degradation activity of podosomes.

1.3.7 Adaptor proteins

Adaptor proteins are composed of different combinations of protein/lipid and protein/protein interaction domains, and generally work to localize and coordinate the activity of different structural and enzymatic proteins involved in a specific cell process or signalling pathway. Some of them have been shown to be involved in the formation and function of invasive adhesions. Cortactin and the WASp/Scar family of proteins can be considered as adaptor proteins, since they can interact and coordinate the activity of many other proteins (see previous sections). The LIM domains in paxillin mediate its subcellular localization, and Src-dependent paxillin phosphorylation is required for podosome and invadopodia ring expansion (Badowski *et al.*, 2008). Other two adaptors have been demonstrated to be essential for invasive adhesions formation: AFAP-110 and Tks5.

1.3.7.1 AFAP-110

AFAP-110 is an actin-binding protein that contains two pleckstrin homology (PH) domains and a binding site for Src (Flynn *et al.*, 1993; Qian *et al.*, 1998). Strong evidence indicates that AFAP-110 acts to relay activation signals from activated PKC to Src. Expression of a constitutively active form of PKCα or treatment with PMA induces AFAP-110 to bind to activated PKCα and to colocalize with Src, resulting in Src activation and podosome formation (Gatesman *et al.*, 2004). The ability of AFAP-110 to colocalize with Src depends on the integrity of the amino-terminal PH domain, which binds to activated PKCα, while the ability of AFAP-110 to activate Src depends on the integrity of the proline-rich motif, which binds the SH3 domain of Src. Furthermore, PMA treatment could not activate Src or induce podosome formation in a cell line with no detectable AFAP-110, whereas ectopic expression of AFAP-110 in these cells could rescue PKCα-mediated

activation of Src and subsequent podosome formation; the rescue was not possible when expressing mutant forms of AFAP-110 that are unable to bind to, or colocalize with, Src (Gatesman *et al.*, 2004). It has also been shown that activation of PKCα by PMA directs activation of PI3K, resulting in i) translocation of AFAP-110 to sites where inactive Src resides, ii) colocalization of AFAP-110 with inactive Src and subsequent activation of Src, and iii) podosome formation (Walker *et al.*, 2007). Finally, AFAP-110 has been found to translocate from stress fibres to sites of podosome formation in PDBu-stimulated vascular smooth muscle cells (Burgstaller and Gimona, 2004).

1.3.7.2 Tks5

Tks5 was originally identified as a Src substrate, and was shown to be tyrosine-phosphorylated in Src-transformed fibroblasts and in normal cells following treatment with several growth factors (Lock *et al.*, 1998). Tks5 contains one N-terminal Phox homology (PX) domain, which can associate with PtdInsP and PtdIns(3,4)P2, five SH3 domains, three canonical polyproline motifs, and two Src-phosphorylation sites (Lock *et al.*, 1998; Abram *et al.*, 2003). Tks5 localizes to podosomes in Src-transformed fibroblasts in a PX domain-dependent manner (Abram *et al.*, 2003). It has been demonstrated that Tks5 is required for podosome formation, ECM degradation, and tissue invasion, both in cell culture and in vivo (Seals *et al.*, 2005; Blouw *et al.*, 2008). Tks5 interacts with several members of the ADAMs family, including ADAMs 12, 15, and 19; in addition, ADAM 12 was also shown to colocalize with Tks5 in podosomes (Abram *et al.*, 2003). Furthermore, elevated levels of expression of Tks5 have been detected in Src-transformed cells, in cultured invasive human cancer cells, and in melanoma samples, suggesting a key role in regulating invasive behaviour (Seals *et al.*, 2005). Lately, it has been

shown that Src-induced interaction between Tks5 and β-dystroglycan is involved in podosome formation in myoblast cells (Thompson *et al.*, 2008). All together, these data suggest that Tks5 is a multifunctional scaffold protein that recruits many different critical podosome components to the subcellular sites where podosomes are formed.

1.3.8 The initiation process

Assembly and turnover of invasive adhesions require an integration of adhesion and cytoskeleton reorganization, local regulation of signalling cascades, and intracellular trafficking. At the moment it is unclear how the initial clustering of components at the sites of invasive adhesion formation is driven, and what molecular players are involved. One hypothesis is that a specific initiation complex is involved, which should contain the basal components of actin polymerization machinery, and that is close to the plasma membrane; upon activation, this complex should trigger further recruitment and/or activation of the molecular components that are necessary to build the structure of the invasive adhesion. In macrophages and osteoclasts, podosomes form amidst a cloud of monomeric and filamentous actin (Linder *et al.*, 2000b; Akisaka *et al.*, 2001; Destaing *et al.*, 2003). By contrast, in phorbol ester-stimulated smooth muscle and endothelial cells, podosomes assemble specifically at the interface area between actin stress fibres and focal adhesions, following local remodelling of the actin cytoskeleton (Kaverina *et al.*, 2003; Burgstaller and Gimona, 2004; Tatin *et al.*, 2006). It is currently unclear what triggers the initiation of the process that leads to the formation of invasive adhesions, and which components need to be recruited first. Irrespective of the type of stimulus inducing podosomes in non-monocyte-derived cells, their

mode of formation looks similar: initially small clusters of cortactin grow in size (Burgstaller and Gimona, 2004; Zhou *et al.*, 2006), then Arp2/3-mediated actin polymerization machinery is recruited, and actin polymerization starts (Kaverina *et al.*, 2003). This first step proceeds in parallel with the recruitment of Rho GTPase-regulating factors, like p190RhoGAP (Burgstaller and Gimona, 2004), and of the Src-activator AFAP-110 (Burgstaller and Gimona, 2004; Gatesman *et al.*, 2004). Progression of this early phase of formation is accompanied by the dispersion of actin-cytoskeleton regulators (e.g., myosin II and tropomyosin), and the disassembly of existing actin stress fibres and focal adhesions.

Notably, the main initial trigger of invadopodia formation is the engagement of surface integrins (Nakahara *et al.*, 1996; Nakahara *et al.*, 1998; Mueller *et al.*, 1999), and activation of Src and cortactin clustering follow this initial step of integrin activation (Bowden *et al.*, 1999; Bowden *et al.*, 2006).

1.4 Aim of this thesis

In this thesis, I investigated the recruitment of podosome components that are involved in the remodelling of the actin cytoskeleton during the initial phase of podosome formation in PDBu-treated A7r5 vascular smooth muscle cells. A particular focus was placed on the roles played by Tks5, AFAP-110, p190RhoGAP, and cortactin in this process. The A7r5 cell line was specifically chosen for this project, because it was already a well-established model for podosome formation, which is induced by stimulating the cells with phorbol esters; this makes easy to study the initial phase of podosome formation without altering Src expression. Phorbol esters-induced podosome formation in A7r5 cells is triggered by activation of conventional PKCs and Src, which results in partial disassembly of actin stress

fibres and de novo actin polymerization at the interface area between actin stress fibres and focal adhesions. At the beginning of this project, the following proteins were known to be localized in the podosomes of A7r5 cells: F-actin, α-actinin, vinculin, PKC-α, SM22, cortactin, Arp2/3, zyxin, p190RhoGAP, AFAP-110.

At the beginning of this study, it was well established that in response to phorbol esters p190RhoGAP is activated by Src and is recruited to the sites of podosome formation, where it may down-regulate RhoA activity. It was thus examined if p190RhoGAP is necessary for podosome formation by knocking down its expression by siRNA, and testing for the ability of interfered cells to form podosomes. In addition, the requirement for the catalytical activity of p190RhoGAP for podosome formation was tested by expressing a GAP-defective dominant point mutant of p190RhoGAP. Since the Src-induced interaction of p190RhoGAP with p120RasGAP regulates p190RhoGAP activity and subcellular localization, the role of p120RasGAP in p190RhoGAP recruitment and podosome formation was also explored. AFAP-110 is required and sufficient for podosome formation in Src-over-expressing fibroblasts and epithelial cells, but data on its requirement for podosome formation in other cell contexts were missing. Hence, the requirement of AFAP-110 in PDBu-induced podosome formation in A7r5 cells was probed for by exogenously expressing a dominant negative form of AFAP-110, which cannot bind active PKCα.

While it is known that AFAP-110, p190RhoGAP, and cortactin are specifically recruited to sites of podosome formation, the molecular mechanism that underlies their recruitment remains largely unknown. Spatio-temporally regulated recruitment and regulation of signalling components is largely driven by a variety of modular scaffolding proteins. The adaptor protein Tks5 is a likely

candidate for acting as a key scaffolding molecule in invasive adhesions-forming cells. This study addressed the hypothesis that Tks5 acts to specifically recruit AFAP-110, p190RhoGAP, and cortactin to sites of podosome formation. For this purpose, subcellular mistargeting of Tks5 to the surface of mitochondria was induced by fusing the membrane anchor of the *Listeria monocytogenes* surface protein ActA to the C-terminus of a GFP-tagged Tks5 construct.

Finally, the expression of a membrane anchorage-defective Tks5 mutant, lacking the PX domain was analyzed, and the effects on the subcellular localization of AFAP-110, p190RhoGAP, and cortactin were monitored.

To this point the investigations were confined to A7r5 cells plated on rigid, non-degradable cell culture support (glass or plastic). However, it is well established that tumour cells and osteoclasts form their matrix degrading invadopodia and podosomes, respectively, only on suitable substrates. For example, melanoma cells fail to generate invadopodia, when plated on glass or plastic, but they spontaneously form ECM-degrading invadopodia when cultured on cross-linked gelatin. These data indicate that the physical parameters of the underlying substrate can potentially influence the ability of cells to form invasive adhesions. It was thus important to determine how podosome-forming A7r5 cells respond to alterations in the mechanical properties of the underlying substrate. It had been shown that primary aortic smooth muscle cells expressing active Src form ECM-degrading invadopodia (Furmaniak-Kazmierczak *et al.*, 2007), and that PDBu-treated A7r5 cells form podosomes, which degrade fibronectin (Burgstaller and Gimona, 2005). A potential scenario that emerged from these studies is that aortic smooth muscle cells degrade ECM only when they express active Src, or Cdc42 or Rac1 (Furmaniak-Kazmierczak *et al.*, 2007), or when they are stimulated with phorbol esters (Burgstaller and Gimona, 2005). In the last section of this thesis I

present data on the behaviour of A7r5 cells on cross-linked gelatin, which suggest an alternative scenario.

CHAPTER 2

Materials and Methods

2.1 Antibodies and reagents

Monoclonal antibodies to AFAP-110 and p190RhoGAP were from BD Biosciences, monoclonal anti-cortactin was from Upstate Biotechnologies Inc., monoclonal anti-p120RasGAP was from Santa Cruz Biotechnologies, polyclonal anti-actin was from Sigma-Aldrich. The polyclonal antibody to Tks5 was previously reported (Lock *et al.*, 1998) and kindly provided by Dr. Sara Courtneidge (Burnham Institute for Medical Research, La Jolla, CA, USA). Alexa 488- or Alexa 568-conjugated goat anti-mouse or goat anti-rabbit secondary antibodies, Alexa 568-conjugated phalloidin, and MitoTracker Red CMXRos were from Molecular Probes. Secondary horseradish peroxidase-coupled antibody was from Amersham. PDBu was from Calbiochem. Rhodamine B isothiocyanate and porcine type A gelatin were from Sigma-Aldrich.

2.2 cDNA constructs

The GFP-Tks5-mito construct was generated following standard cloning protocols, resulting in the EGFP moiety fused to the N-terminus, and the

mitochondrial targeting sequence of ActA fused to the C-terminus of Tks5. The cDNA of human Tks5 (Seals *et al.*, 2005) was amplified by PCR using the following forward (5'-ATG CTC GAG AAT GCT CGC CTA CTG CGT GCA-3') and reverse (5'-AGG AAG CTT CCG TTC TTT TTC TCA AGG TAG TTG-3') primers, and cloned into the GFP-mito vector via XhoI and HindIII restriction sites. The GFP-mito vector was generated by cloning the cDNA of the mitochondrial targeting sequence of ActA (Pistor *et al.*, 1994) into pEGFP-C2 (Clontech), as previously described (Grubinger and Gimona, 2004).

The deletion mutants of GFP-Tks5-mito were generated by mutagenesis, using the QuikChange Site-Directed Mutagenesis Kit from Stratagene, according to the manufacturer's instructions. The list of pairs of mutagenic primers used to generate each mutant is shown in Table 1.

The cDNA for GFP-p190RhoGAP was a kind gift from Dr. Ian G. Macara (University of Virginia School of Medicine, Charlottesville VA, USA). The mutant GFP-p190RhoGAP(R1283A) was obtained by the same approach as above using the following pair of mutagenic primers: forward (5'-CAG AAG GCA TCT ACG CGG TCA GCG GAA ACA AG-3') and reverse (5'-CTT GTT TCC GCT GAC CGC GTA GAT GCC TTC TG-3').

The cDNAs for GFP-AFAP-110 and GFP-AFAP-110(Δ180-226) were a kind gift from Dr. Daniel C. Flynn (West Virginia University, Department of Microbiology, Immunology and Cell Biology, Morgantown, WV, USA).

Tks5ΔPX-GFP was generated by amplifying the cDNA of human Tks5 by PCR using forward (5'-ATG CTC GAG AGA GGC TCG ACC CGA GGA TGT C-3') and reverse (5'-ATT AAG CTT GTT CTT CTT CTC AAG GTA G-3') primers, and cloning into the pEGFP-N1 vector via XhoI and HindIII restriction sites.

Table 1. List of primers used to generate GFP-Tks5-mito deletion mutants

GFP-Tks5-mito deletion mutant	Aminoacids deleted	5'-3' sequence of the pair of mutagenic primers *
GFP-Tks5(ΔPX)-mito	6-121	ATGCTCGCCTACTGCGAGGCTCGACCCGAG
		CTCGGGTCGAGCCTCGCAGTAGGCGAGCAT
GFP-Tks5(ΔSH3#1)-mito	154-209	GAGCCCATGATCCTGGGTACTCGGGATGAC
		GTCATCCCGAGTACCCAGGATCATGGGCTC
GFP-Tks5(ΔSH3#2)-mito	254-309	CAGCACAGCCGAGAGGATGACCTGCCAACC
		GGTTGGCAGGTCATCCTCTCGGCTGTGCTG
GFP-Tks5(ΔSH3#3)-mito	436-491	CCCCCTTCTGTTGAGAAGCCCAACCTGAGC
		GCTCAGGTTGGGCTTCTCAACAGAAGGGGG
GFP-Tks5(ΔSH3#4)-mito	828-883	TGGGAAGGGCCAGCCAACGAGCAACCTGAC
		GTCAGGTTGCTCGTTGGCTGGCCCTTCCCA
GFP-Tks5(ΔSH3#5)-mito	1060-1118	CACAATAACCTCAAAGGAAGCTTCGAATTC
		GAATTCGAAGCTTCCTTTGAGGTTATTGTG
GFP-Tks5(ΔPP1)-mito	426-433	CTGGGGTTCCAACTGGTTGAGGTGGAGTAC
		GTACTCCACCTCAACCAGTTGGAACCCCAG
GFP-Tks5(ΔPP2)-mito	505-516	AGCACGCTGACCCGGAAGGAGGCCGAGGAG
		CTCCTCGGCCTCCTTCCGGGTCAGCGTGCT
GFP-Tks5(ΔPP3)-mito	932-939	AGCAAGAAGGCCACGGGGGGCTTCGGCAAG
		CTTGCCGAAGCCCCCCGTGGCCTTCTTGCT

* Top row: forward primer Bottom row: reverse primer

2.3 Cell Culture, Induction of Podosomes and Transfection

A7r5 rat smooth muscle cells (ATCC) were grown in low glucose (1000 mg/l) DMEM without phenol red, supplemented with 10% FBS (PAA), penicillin/streptomycin (Gibco) at 37°C and 5% CO2. Formation of podosomes was induced by changing the culture medium to 1 µM PDBu in complete growth medium as described previously (Hai *et al.*, 2002). In ECM degradation experiments metalloproteinases were inhibited by culturing cells in complete

growth medium supplemented with 5 μM BB94 (Ayala *et al.*, 2008).

For transient expression, cells were grown in 60 mm plastic culture dishes and transfected using GeneJuice (Novagen), according to the manufacturer's instructions. Cells were replated onto 15 mm glass coverslips 12-18 hours post-transfection and prepared for immunofluorescence microscopy after 30-48 hours.

2.4 p190RhoGAP knockdown experiment

One duplex siRNA from Sigma directed against rat p190RhoGAP (sense strand: AAGGCAACCUGGGAGAGUAAC) was used to knockdown its expression. A pool of four non-targeting duplex siRNAs (Dharmacon) was used as control experiment. Cells were transfected with 100 nM siRNAs using Oligofectamine (Invitrogen) according to the manufacturer's instructions. After 18 hours transfected cells were replated either onto 15 mm glass coverslips or in 35 mm dishes, grown for 48 hours, then processed for immunofluorescence or SDS-PAGE.

2.5 p120RasGAP knockdown experiment

A pool of four siRNAs directed against p120RasGAP (Dharmacon) was used to knockdown its expression. A pool of four non-targeting duplex siRNAs (Dharmacon) was used in control experiments. Cells were transfected with 100 nM siRNAs using Oligofectamine (Invitrogen) according to the manufacturer's instructions. After 48 hours transfected cells were replated either onto 15 mm glass coverslips or in 35 mm dishes, grown for 48 hours, then processed for immunofluorescence or SDS-PAGE.

2.6 Immunofluorescence and microscopy

Cells on coverslips were washed twice in phosphate-buffered saline (PBS; 138 mM NaCl, 26 mM KCl, 84 mM Na_2HPO_4, 14 mM NaH_2PO_4, pH 7.4), fixed in 4% paraformaldehyde in PBS for 20 minutes, washed five times in PBS, and permeabilized with 0.2% Triton X-100 in PBS for 5 minutes. After blocking in 2% bovine serum albumin (BSA) for 1 hour, coverslips were incubated with primary and secondary antibodies, diluted in 2% BSA, and mounted in PROLONG GOLD mounting medium (Invitrogen). Staining with the MitoTracker Red probe was performed according to the manufacturer's instructions: briefly, cells were incubated in complete growth medium supplemented with 250 nM of dye for 30 minutes at 37°C, washed twice with complete growth medium, fixed in complete growth medium supplemented with 3.7 % formaldehyde for 15 minutes at 37°C, washed five times in PBS, and permeabilized with 0.2% Triton X-100 in PBS for 5 minutes.

Fluorescent images of p120RasGAP experiments were captured on a Zeiss Axiophot microscope equipped with an Axiocam driven by the manufacturer's software package (all Zeiss) using a Plan-Apochromat 63x (NA 1.4) oil immersion lens. Fluorescent images of all the other experiments were acquired on a Zeiss LSM 5 Pascal confocal microscope using a Plan-Apochromat 63x (NA 1.4) oil immersion lens (Zeiss).

2.7 Preparation of coverslips for ECM degradation assay

Rhodamine B-conjugated gelatin was prepared as follows: 180 mg of NaCl were dissolved in 50 ml of 50 mM $Na_2B_4O_7$ pH 9.3; 100 mg of porcine type A

gelatin were mixed with this solution, and incubated at 37°C for 1 hour. Following this incubation, 1.8 mg of Rhodamine B isothiocyanate were added and mixed at room temperature for a further 2 hours. Successively, the solution was dialysed in dialysis bags with a molecular weight cut-off of 1000 Da in 3 L of PBS at 37°C over-night. Finally, 1 g of saccharose was added to the solution.

Coverslips were prepared as follows: each coverslip was covered with a drop of Rhodamine B-conjugated gelatin for 5 minutes; after removing the excess of gelatin, the coverslips were incubated with 0.5% glutaraldehyde in PBS for 15 minutes on ice. Successively, the coverslips were washed with PBS three times, and incubated with an ice-cold solution of $NaBH_4$ (5 mg/ml in PBS) for 3 minutes. Coverslips were washed with PBS three times and sterilized in 70% ethanol. Finally, the coverslips were incubated with growth medium for 1 hour in the incubator and washed with growth medium once, before plating A7r5 cells.

2.8 Immunoprecipitation (IP)

A7r5 cells grown in 100mm dishes were washed three times with ice-cold PBS. Proteins were extracted subsequently in 0.5 ml of IP buffer [20 mM Imidazole, 150 mM NaCl, 40 mM KCl, 0.5 mM MgCl2, 5% (v/v) glycerol, 0.5% (v/v) Triton X-100, 0.1% (v/v) Nonidet P40, 4 mM Pefabloc (Roche), 1 mM Na3VO4] for 30 minutes on ice. The extract was collected and cellular residues were removed by centrifugation at 14,000 rpm for 10 minutes. The extracts were precleared for 60 minutes with Protein G-Sepharose (Amersham) in IP buffer and the supernatant was transferred to a fresh tube. 2.5 μg of anti-p120RasGAP antibody was added and the suspension was incubated on a rotating support at 4°C for 2 hours. After the addition of 50 μl of Protein G-Sepharose, the incubation was continued for a

further 2 hours. Beads were washed three times in IP buffer and resuspended in SDS sample buffer 2X (0.1 M Tris-HCl, pH 6.8, 4% SDS, 0.2% bromophenol blue, 30% glycerol, 5% β-Mercaptoethanol).

2.9 SDS-PAGE and Western Blotting

Samples were separated by SDS-PAGE on 10% polyacrylamide gels, using the Mini-PROTEAN II Cell (Bio-Rad), and blotted onto nitrocellulose (Protran, Perkin Elmer) with Mini Trans-Blot Cell (Bio-Rad). Blots were blocked in 10% non-fat, dry milk in TBS-T (20 mM Tris, pH 7.6, 0.8% NaCl, 0.1% Tween-20), and incubated with primary and secondary antibodies, which were diluted in 1% milk in TBS-T. Secondary antibodies were detected with the ECL chemiluminescence system (Amersham).

2.10 Statistics

Statistical analysis of the differences in the number of transfected cells with podosomes versus untransfected was assessed by using Student's t-test (a value of $p < 0.05$ was considered significant).

CHAPTER 3

Results

3.1 Role of p190RhoGAP in podosome formation

Despite some circumstantial evidence that suggests a role for p190RhoGAP in podosome formation by mediating the local inhibition of RhoA activity and the concomitant reduction in cellular contractility (Brandt *et al.*, 2002; Burgstaller and Gimona, 2004), there is no direct support for its involvement as a critical player in podosome formation. Considering the specific recruitment of both endogenous and ectopically expressed p190RhoGAP with key podosome components such as cortactin, the role of the RhoA inactivating GAP activity of p190RhoGAP in podosome formation was assessed. The involvement of one of p190RhoGAP main interactors, p120RasGAP, in its recruitment and podosome formation was also investigated.

3.1.1 The expression of p190RhoGAP is essential for podosome formation

The contribution of p190RhoGAP to podosome formation was tested using RNA interference approach. For this purpose, A7r5 cells were transiently

transfected with a siRNA specific for p190RhoGAP, which resulted in a strong knockdown of p190RhoGAP expression, whereas transfection with a pool of control non-targeting siRNAs did not alter p190RhoGAP expression compared to mock-transfected cells (Figure 3.1, A). The sequence of the siRNA duplex specific for p190RhoGAP was identical to that used in a previous study (Guegan *et al.*, 2008). In immunofluorescence microscopy, cells transfected with p190RhoGAP-specific siRNA showed a markedly reduced staining for endogenous p190RhoGAP, and were clearly distinguishable from neighbouring untransfected cells (Figure 3.2). After stimulation with PDBu, the number of p190RhoGAP siRNA-treated cells displaying podosomes was only one third compared to that of cells treated with the pool of control siRNAs (Figure 3.1, B). However, there was no obvious alteration in the actin core morphology in p190RhoGAP siRNA-treated cells, which were still able to form podosomes (Figure 3.2). These data indicate that p190RhoGAP expression is required for podosome formation.

3.1.2 The GAP activity of p190RhoGAP is essential for podosome formation

Next the role of the RhoA inactivating GAP activity of p190RhoGAP in podosome formation was assessed. For this purpose, I ectopically expressed the catalytically inactive point mutant p190RhoGAP(R1283A), which was shown to behave as a dominant-negative mutant (Tatsis *et al.*, 1998). In cells expressing GFP-p190RhoGAP(R1283A), PDBu stimulation did not induce actin stress fibres disassembly and the number of cells displaying podosomes was reduced by about 65% compared to cells expressing only GFP, or wild-type GFP-p190RhoGAP

(Figure 3.3). This result indicates that the catalytic activity of p190RhoGAP is essential for podosome formation.

3.1.3 p190RhoGAP and p120RasGAP are associated in a complex that localizes to podosomes

The potential interaction of p190RhoGAP with p120RasGAP was tested in A7r5 vascular smooth muscle cells, since an association between these two molecules had been described in other cell types. Endogenous p120RasGAP was immunoprecipitated and the samples were blotted for p190RhoGAP. Western blots showed that p120RasGAP and p190RhoGAP are indeed associated in a complex in both unstimulated and PDBu-stimulated A7r5 cells (Figure 3.4). The amount of p190RhoGAP that co-immunoprecipitated with p120RasGAP was only slightly increased in PDBu-stimulated versus unstimulated cells, indicating that formation of the p120RasGAP-p190RhoGAP complex in A7r5 cells is negligibly influenced by phorbol ester-stimulated activity of PKC.

These biochemical results were confirmed by immunofluorescence microscopy analysis. A7r5 cells were transfected with GFP-p190RhoGAP, fixed, and stained for p120RasGAP. In untreated cells, a partial colocalization of the two proteins at plasma membrane, in the perinuclear area and along actin stress fibres was detected, whereas in PDBu-treated cells p120RasGAP and p190RhoGAP colocalized to podosomes and membrane ruffles (Figure 3.5). From these results one may thus conclude that p190RhoGAP and p120RasGAP are associated in a complex, and that p120RasGAP translocates to podosomes after phorbol ester stimulation.

3.1.4 p120RasGAP is not required for podosome formation

To test the potential involvement of p120RasGAP in the recruitment of p190RhoGAP and in podosome formation, p120RasGAP expression was inhibited by RNA interference. A7r5 cells were transiently transfected with a pool of siRNAs targeting specifically p120RasGAP, which resulted in almost 90% of reduction of p120RasGAP protein levels, compared to mock-transfected cells (Figure 3.6, A). Following stimulation with PDBu, p120RasGAP siRNA-treated cells were fixed and stained for F-actin or p190RhoGAP. These cells formed podosomes normally (Figure 3.6, B), and the distribution of p190RhoGAP was unaffected. These data indicate that p120RasGAP is not required for p190RhoGAP recruitment or for podosome formation.

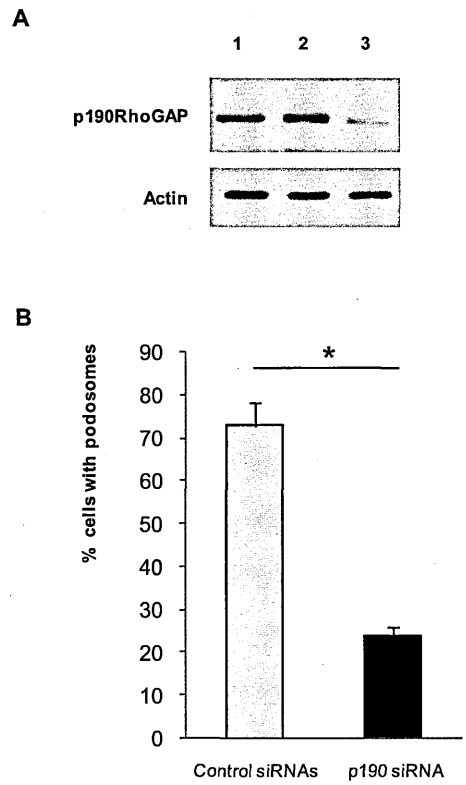

Figure 3.1 – Effect of p190RhoGAP expression knockdown on podosome formation. (A) A7r5 cells were mock-transfected (lane 1), or transfected with a pool of four non-targeting siRNAs (lane 2), or transfected with a siRNA duplex specific for p190RhoGAP (lane 3). After 66 hours, cells were lysed, and the protein extracts analyzed by Western blotting. The expression of p190RhoGAP did not change in non-targeting siRNAs-transfected cells, whereas transfection of the siRNA specific for p190RhoGAP induced a strong reduction of p190RhoGAP expression (top row); the level of actin expression remained unchanged (bottom row). **(B)** The percentage of cells transfected with control siRNAs or p190 siRNA, that displayed podosomes after stimulation with PDBu, was quantified. While 73% of control siRNAs-treated cells showed podosomes, only 24% of p190 siRNA-treated cells showed podosomes. The vertical axis represents the percentage of siRNA-transfected cells with podosomes; the percentage of mock-transfected cells with podosomes was set to 100%. Data from two independent experiments; n = at least 250 cells; * = $p < 0.03$.

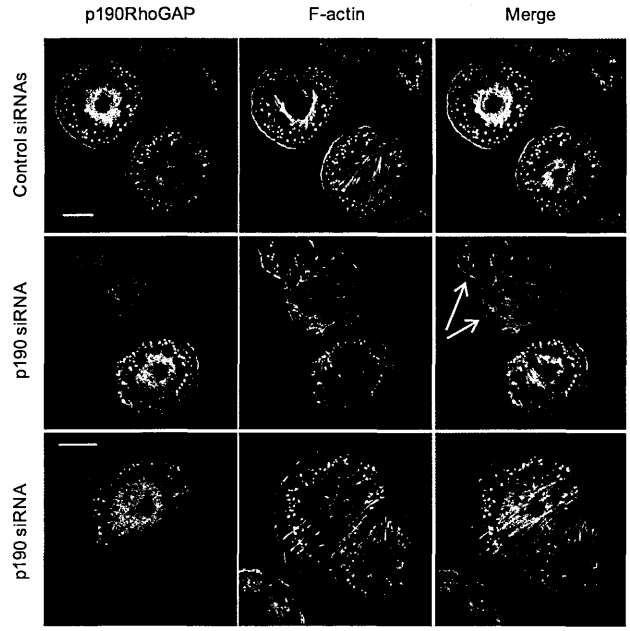

Figure 3.2 – Effect of p190RhoGAP knockdown on podosome formation. A7r5 cells transfected with a pool of four non-targeting siRNAs (top panels, control siRNAs), or transfected with the siRNA specific for p190RhoGAP (middle and bottom panels, p190 siRNA) were stimulated with PDBu for 30 minutes, fixed, and stained for p190RhoGAP (green) and F-actin (red). While control siRNA-transfected cells formed podosomes normally, most of the p190 siRNA-transfected cells did not form podosomes; arrows in the middle merge panel indicate two p190RhoGAP siRNA-transfected cells. p190RhoGAP siRNA-transfected cells, that retained the capability to form podosomes, displayed normal podosomal morphology (bottom panels). Bar, 30 μm.

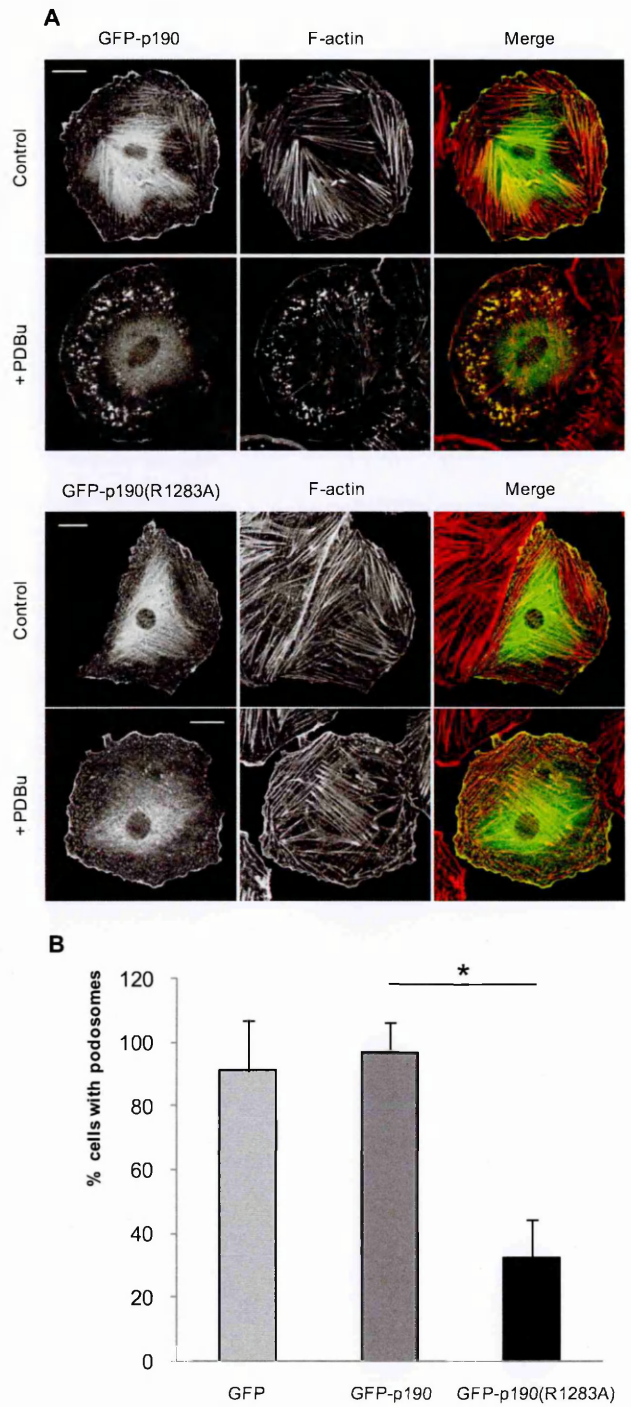

Figure 3.3 – The GAP activity of p190RhoGAP is required for podosome formation. (A) A7r5 cells were transfected with GFP-p190RhoGAP or the catalytically inactive mutant GFP-p190RhoGAP(R1283A), left unstimulated (control) or stimulated with PDBu for 30 minutes (+PDBu), fixed, and stained for F-

actin (red). While GFP-p190RhoGAP-transfected cells formed podosomes normally (top panels), most of the GFP-p190RhoGAP(R1283A) expressing cells did not display any podosome (bottom panels). Bar, 20 μm. **(B)** A7r5 cells were transfected with GFP, GFP-p190RhoGAP, or GFP-p190RhoGAP(R1283A), and the percentage of cells displaying podosomes after stimulation with PDBu was quantified. The GAP-defective mutant significantly reduces PDBu-induced podosome formation. The vertical axis represents the percentage of transfected cells with podosomes; the percentage of untransfected cells with podosomes was set to 100%. Data from three independent experiments; n = at least 30 cells; * = $p < 0.01$.

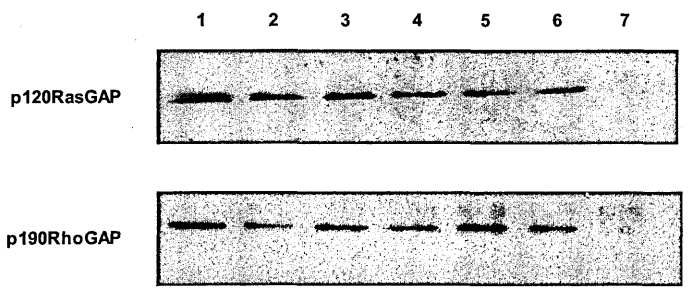

Figure 3.4 – p190RhoGAP co-immunoprecipitates with p120RasGAP. A7r5 cells were left untreated or treated with PDBu at different time points, lysed and subjected to p120RasGAP immunoprecipitation. Precipitated material was blotted and probed either for p120RasGAP (upper strip) or p190RhoGAP (lower strip). Immunoprecipitation with rabbit pre-immune serum was included as a negative control. The intensity of the bands indicates that similar amounts of p190RhoGAP co-immunoprecipitated with p120RasGAP in unstimulated and PDBu-stimulated cells. Lanes: 1 total lysate from untreated cells, 2 IP from untreated cells, 3 IP from cells treated with PDBu for 5 minutes, 4 IP from cells treated with PDBu for 10 minutes, 5 IP from cells treated with PDBu for 30 minutes, 6 IP from cells treated with PDBu for 60 minutes, 7 Negative control IP.

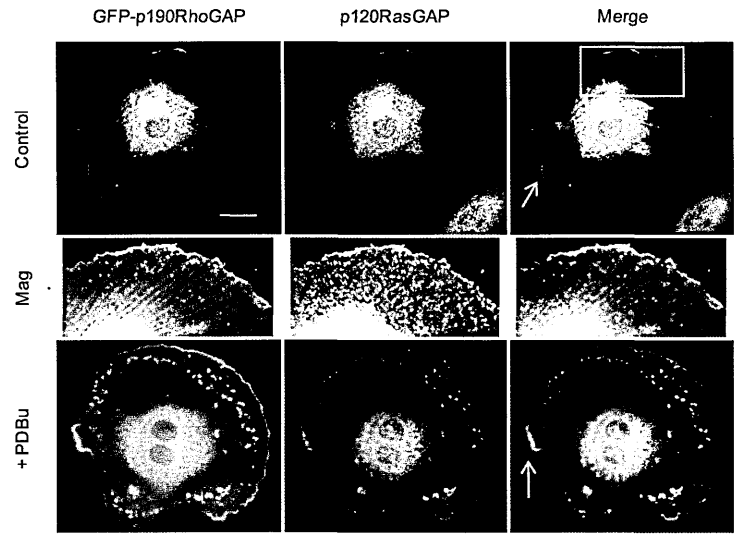

Figure 3.5 – p190RhoGAP colocalizes with p120RasGAP. A7r5 cells were transfected with GFP-p190RhoGAP and left unstimulated (control) or stimulated with PDBu for 30 minutes (+PDBu), fixed, and stained for p120RasGAP (red). In unstimulated cells, the two proteins colocalize at plasma membrane (white arrow), in the perinuclear area and along actin stress fibres. The middle panels (Mag) show a higher magnification of the boxed area in the merge panel above. In PDBu-stimulated cells, GFP-p190RhoGAP and p120RasGAP colocalize at membrane ruffles (Hennessey *et al.*) and podosomes. Bar, 20 μm.

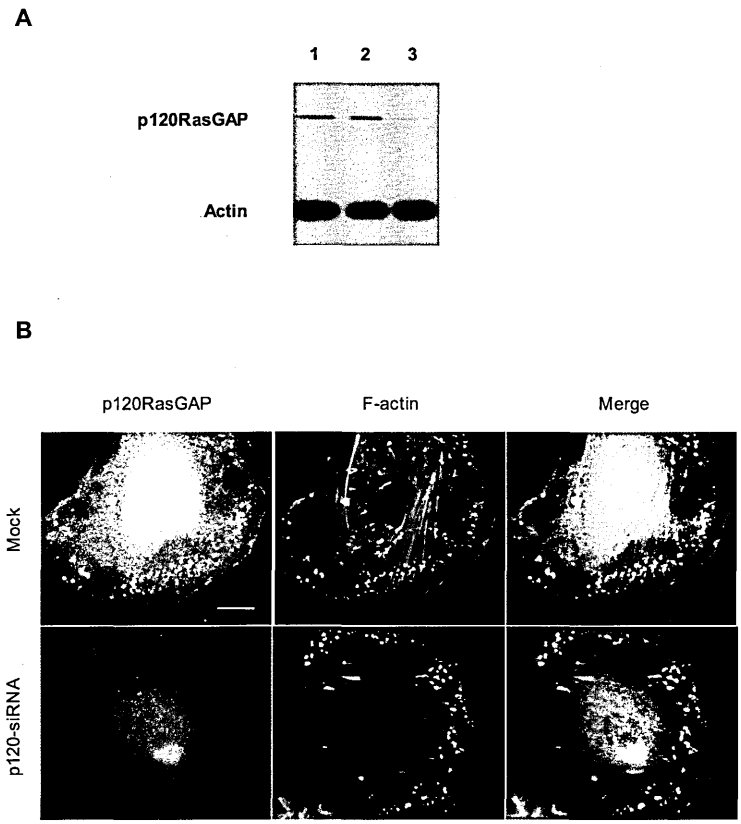

Figure 3.6 – Effect of p120RasGAP knockdown on podosome formation. (A) A7r5 cells were mock-transfected (lane 1), or transfected with a pool of four non-targeting siRNAs (lane 2), or transfected with a pool of four siRNAs specific for p120RasGAP (lane 3). After 96 hours, cells were lysed, and the protein extracts analyzed by Western blotting. The expression of p120RasGAP did not change in non-targeting siRNA-transfected cells, whereas transfection with the pool of p120RasGAP-specific siRNAs induced an almost 90% reduction in the p120RasGAP protein level (top lanes); the level of actin expression remained unchanged (bottom lanes). **(B)** A7r5 cells were either mock-transfected (top panels) or transfected with the pool of p120RasGAP-specific siRNAs (bottom panels) for 96 hours. Following stimulation with PDBu for 30 minutes, the cells were fixed, and stained for p120RasGAP (green) and F-actin (red). p120RasGAP-siRNA transfected cells formed podosomes normally, with no difference compared to mock-transfected cells. Bar, 20 μm.

3.2 Role of AFAP-110 in podosome formation

Clear evidence indicates that AFAP-110 is required for PKC- and Src-induced podosome formation in Src over-expressing fibroblasts and epithelial cells, but evidence for a requirement in other podosome forming cells is missing. Thus, I tested if AFAP-110 is essential also for PDBu-induced podosome formation in vascular smooth muscle cells, by over-expressing the dominant negative mutant AFAP-110(Δ180-226). This mutant harbors a deletion in the PH1 domain and, consequently, does not bind PKCα, resulting in the inhibition of Src activation and inhibition of podosome formation (Gatesman *et al.*, 2004).

PDBu stimulation of A7r5 cells transiently transfected with GFP-AFAP-110(Δ180-226) failed to induce noticeable actin remodelling: actin stress fibres were not disassembled and the number of cells displaying podosomes was reduced by about 65% compared to cells expressing only GFP or wild-type GFP-AFAP-110 (Figure 3.7). This finding is in good agreement with a previous report by Gatesman *et al.,* (2004), and confirms that AFAP-110 is also required for PKC-induced podosome formation in A7r5 cells.

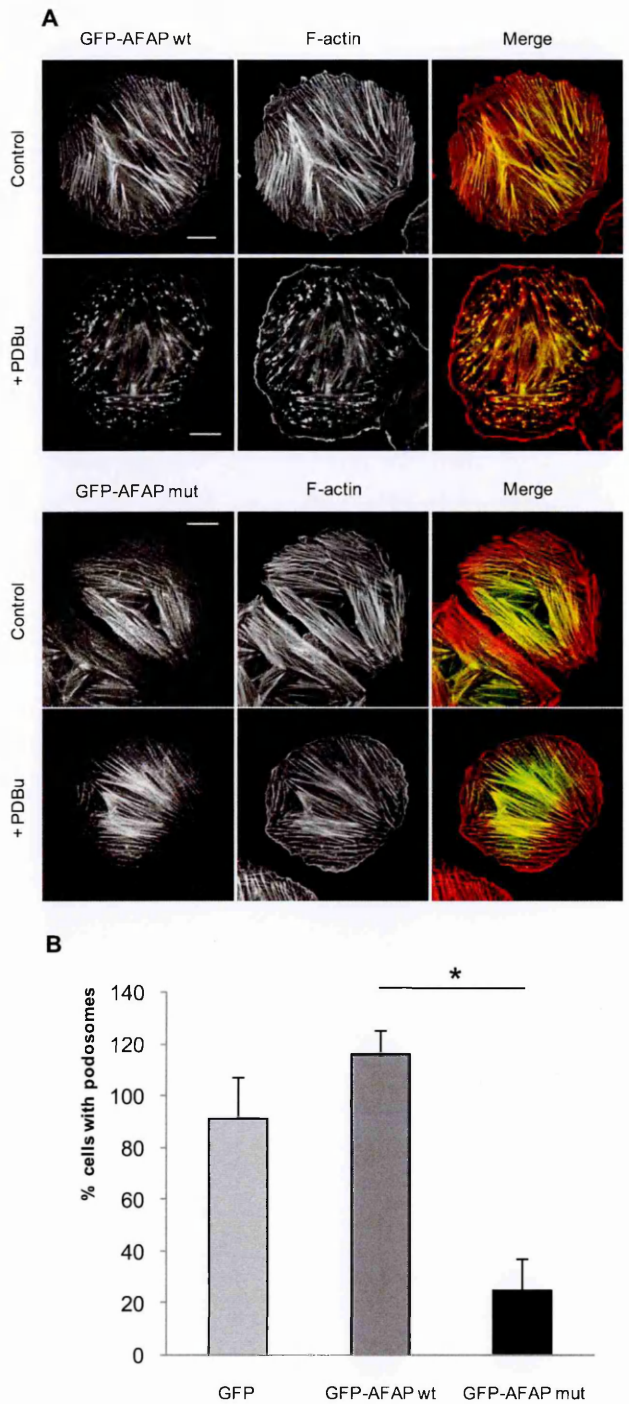

Figure 3.7 – AFAP-110 is required for podosome formation in vascular smooth muscle cells. (A) A7r5 cells were transfected with GFP-AFAP-110 or the PKC-binding mutant GFP-AFAP-110(Δ180-226), left unstimulated (control) or stimulated with PDBu for 30 minutes (+PDBu), fixed, and stained for F-actin (red).

While GFP-AFAP-110-transfected cells formed podosomes normally (top panels), most of the GFP-AFAP-110(Δ180-226) expressing cells did not display podosomes (bottom panels). Bar, 20 μm. **(B)** A7r5 cells were transfected with GFP, GFP-AFAP-110, or GFP-AFAP-110(Δ180-226), and the percentage of cells displaying podosomes after stimulation with PDBu was quantified. The over-expression of the mutant significantly reduces podosome formation. The vertical axis represents the percentage of transfected cells showing podosomes; the percentage of untransfected cells showing podosomes was set to 100%. Data from three independent experiments; n = at least 150 cells; * = $p < 0.01$.

3.3 Tks5 recruits AFAP-110, p190RhoGAP, and cortactin for podosome formation

Recruitment of podosome components and coordination of their activities in a defined spatio-temporal manner is required for the formation of active, matrix-degrading podosomes. The adaptor molecule Tks5 may function as a major recruitment factor for AFAP-110, p190RhoGAP, and cortactin to sites of podosome formation. To test this hypothesis, subcellular mistargeting of Tks5 to the surface of mitochondria was induced by fusing the membrane anchor of the *Listeria monocytogenes* surface protein ActA to the C-terminus of a GFP-tagged Tks5 construct (GFP-Tks5-mito). When expressed in eukaryotic cells, the membrane anchor of ActA displays a selective affinity for the mitochondrial membrane (Pistor *et al.*, 1994). This approach has already been used successfully to mistarget vinculin (Bubeck *et al.*, 1997), zyxin (Drees *et al.*, 2000; Fradelizi *et al.*, 2001), and the actin-binding protein CRP-2 (Grubinger and Gimona, 2004) to the surface of mitochondria. Since AFAP-110, p190RhoGAP, and cortactin do not show mitochondrial localization under normal conditions, this approach is suitable to determine the recruitment potential of Tks5. Thus, GFP-Tks5-mito was ectopically expressed, and the localization of AFAP-110, p190RhoGAP, and cortactin was analyzed. Additional data were obtained by the ectopic expression of a PX domain deleted mutant of Tks5 (Tks5ΔPX-GFP), which induced aberrant subcellular distribution of AFAP-110, p190RhoGAP, and cortactin.

3.3.1 Endogenous Tks5 localizes to podosomes in A7r5 cells

To analyze the distribution of endogenous Tks5, A7r5 cells were either left unstimulated or stimulated with PDBu for 30 minutes, and subsequently fixed and double stained for Tks5 and F-actin, or Tks5 and cortactin. In unstimulated cells, the majority of Tks5 is diffusely distributed in the cytoplasm and accumulates preferentially in the central region of the cell, in addition to an apparent association with the plasma membrane and actin stress fibres (Figure 3.8, top row). In PDBu-stimulated cells, Tks5 accumulates strongly in the core of podosomes together with F-actin and cortactin (Figure 3.8, middle and bottom rows). In agreement with previously published data, Tks5 rapidly accumulates in the areas of podosome formation in phorbol ester-stimulated vascular smooth muscle cells, and colocalizes with key components of podosome formation.

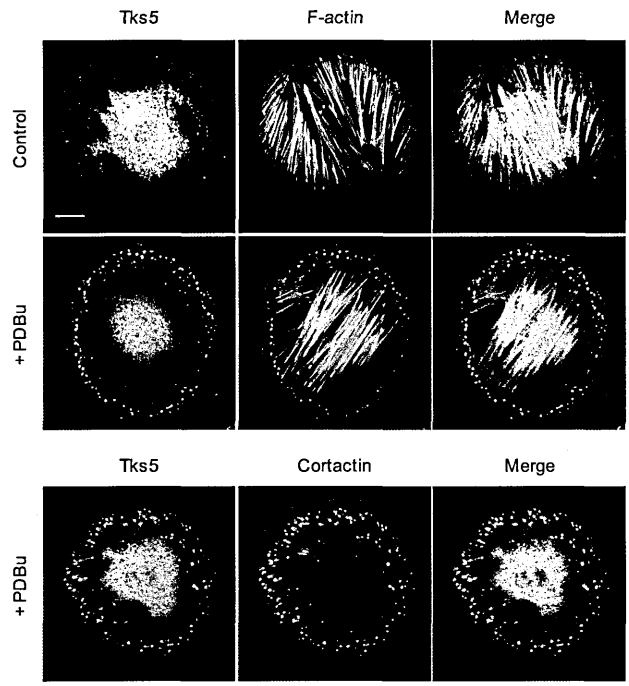

Figure 3.8 – Tks5 localizes to podosomes in PDBu-stimulated A7r5 cells. Cells were left unstimulated (control) or stimulated with PDBu for 30 minutes (+PDBu), fixed, and double stained for Tks5 (green) and F-actin (red), or Tks5 (green) and cortactin (red). In control cells, Tks5 is found diffusely around the central area of the cell, as well as at the plasma membrane and along actin stress fibres. In PDBu-stimulated cells, Tks5 localizes preferentially to the actin-rich cores of podosomes, together with cortactin. Bar, 20 μm.

3.3.2 Mistargeting of Tks5 to mitochondria

To induce mistargeting of Tks5 to mitochondria, A7r5 cells were transiently transfected with the construct GFP-Tks5-mito. Confocal imaging of transfected cells stained with the MitoTracker Red probe to visualize mitochondria, showed colocalization of GFP-Tks5-mito with MitoTracker staining, confirming that the construct was properly addressed to the surface of mitochondria (Figure 3.9). Notably, expression of GFP-Tks5-mito induced a pronounced alteration in the distribution of mitochondria, which appeared collapsed in the central area of the cell, while untransfected cells displayed a normal arrangement of mitochondria.

Colocalization of actin filaments with GFP-Tks5-mito at mitochondria aggregates could also be observed, markedly in unstimulated and to a lesser extent in PDBu-stimulated cells, suggesting that de novo polymerization or stabilization of existing actin filaments is increased at Tks5-enriched mitochondria (Figure 3.10, A). Expression of GFP-Tks5-mito strongly inhibited podosome formation following PDBu stimulation: the percentage of cells forming podosomes in response to phorbol ester was reduced six fold from 40.4% to 6.8% (Figure 3.10, B), and instead a significant increase in peripheral membrane ruffling activity was detected (arrow in Figure 3.10, A).

3.3.3 The mistargeted form of Tks5 recruits AFAP-110, p190RhoGAP, and cortactin to mitochondria

When GFP-Tks5-mito expressing cells were probed for the distribution of endogenous AFAP-110, p190RhoGAP, and cortactin, all three proteins were seen to colocalize with GFP-Tks5-mito in the mitochondria-containing aggregates

(Figure 3.11), indicating their recruitment by Tks5. This recruitment was specifically induced by the expression of the mistargeted form of Tks5, since the expression of mitochondria-targeted GFP alone did not induce the bundling of mitochondria and did not alter the distribution of AFAP-110, p190RhoGAP, and cortactin (Figure 3.12). Furthermore, the distribution of AFAP-110, p190RhoGAP, and cortactin in GFP-Tks5-mito expressing cells did not change after stimulation with PDBu (Figure 3.13), suggesting that recruitment by Tks5 is the overriding signal in the engagement of these podosome components.

3.3.4 The fifth SH3 domain of Tks5 is required for the recruitment of AFAP-110, p190RhoGAP, and cortactin

The multidomain adapter Tks5 contains one PX domain, three canonical polyproline motifs and five polyproline-recognizing SH3 domains. In order to understand which domain(s) of Tks5 are involved in the specific recruitment of AFAP-110, p190RhoGAP, and cortactin, a total of nine deletion mutants of GFP-Tks5-mito were generated, each individual mutant lacking one of the functional domains and motifs of Tks5 (Figure 3.14). Surprisingly, only the mutant lacking the fifth SH3 domain [GFP-Tks5(ΔSH3#5)-mito] was defective in recruiting AFAP-110, p190RhoGAP, and cortactin to mitochondria (Figure 3.15). Moreover, mitochondria enriched with this mutant were devoid of actin filaments (Figure 3.16). This finding points to a critical involvement of this domain in the recruitment of podosome components by Tks5. Notably, in cells expressing the GFP-Tks5(ΔSH3#5)-mito mutant the collapse and aggregation of mitochondria was less pronounced. However, podosome formation after stimulation with PDBu was as strongly impaired as in cells expressing the full length GFP-Tks5-mito construct, suggesting

that other critical podosome components can be recruited by Tks5, potentially via one of the other functional protein-protein interaction domains. Also when expressing any of the other deletion mutants of GFP-Tks5-mito, podosome formation was still strongly impaired.

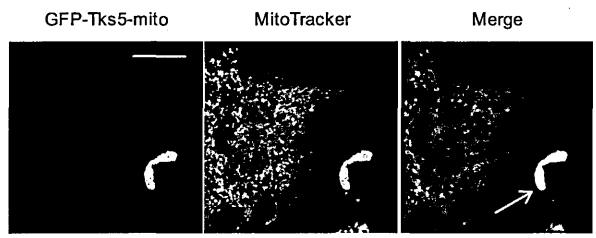

Figure 3.9 – GFP-Tks5-mito localizes to mitochondria. A7r5 cells transfected with GFP-Tks5-mito and stained with the MitoTracker Red probe show that GFP-Tks5-mito properly localizes to mitochondria. Mitochondria are collapsed around the perinuclear area in the cell expressing the Tks5 construct, compared to an untransfected cell (left). Arrow indicates the transfected cell. Bar, 20 μm.

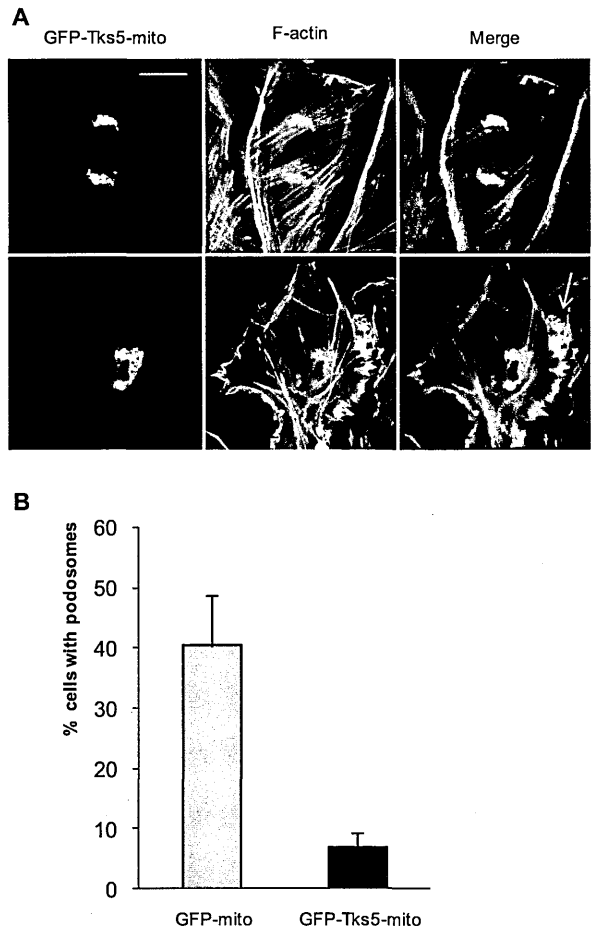

Figure 3.10 – GFP-Tks5-mito expression inhibits podosome formation. **(A)** A7r5 cells transfected with GFP-Tks5-mito were either left unstimulated (top panels) or stimulated with PDBu for 30 minutes (bottom panels), fixed, and stained for F-actin (red). A cloud of F-actin colocalizes with GFP-Tks5-mito in unstimulated and, to a lesser extent, in PDBu-stimulated cells. Podosome formation is inhibited while peripheral membrane ruffling activity is stimulated in PDBu-stimulated cells (Hennessey *et al.*). Bar, 20 μm. **(B)** A7r5 cells were transfected with GFP-Tks5-mito or GFP-mito, and the percentage of cells displaying podosomes after stimulation with PDBu was quantified. The vertical axis represents the percentage of transfected cells with podosomes; the percentage of untransfected cells with podosomes was set to 100%. Data from three independent experiments; n = at least 45 cells; $p < 0.01$.

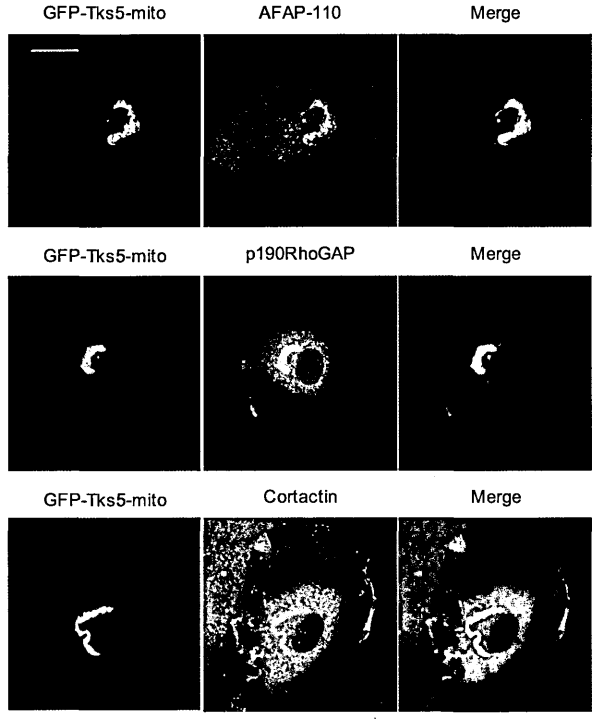

Figure 3.11 – GFP-Tks5-mito recruits AFAP-110, p190RhoGAP, and cortactin. A7r5 cells transfected with GFP-Tks5-mito were stained for AFAP-110, p190RhoGAP, or cortactin (red). All three proteins colocalize with GFP-Tks5-mito, indicating recruitment of these proteins to mitochondria by Tks5. Bar, 20 μm.

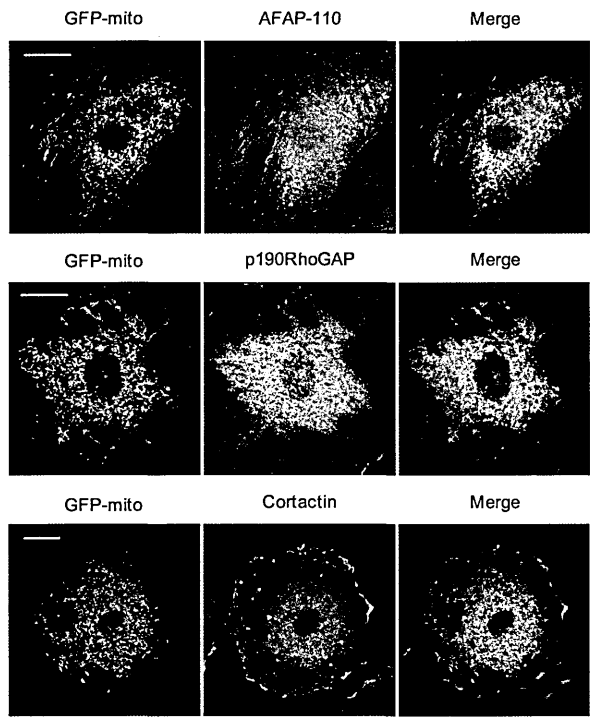

Figure 3.12 – GFP-mito does not recruit AFAP-110, p190RhoGAP, and cortactin. A7r5 cells transfected with GFP-mito were stained for AFAP-110, p190RhoGAP, or cortactin (red). None of the three proteins colocalize with GFP-mito, indicating that they are not recruited to mitochondria by the GFP moiety. Bar, 20 μm.

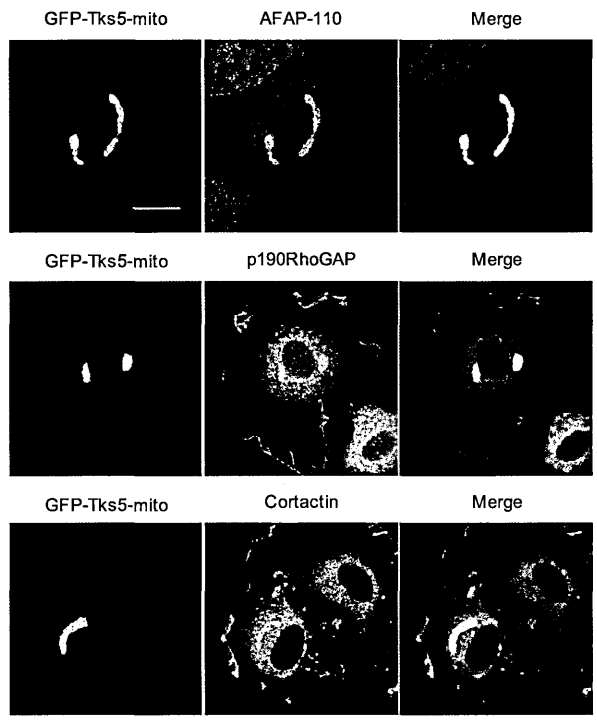

Figure 3.13 – PDBu stimulation does not change the ability of GFP-Tks5-mito to recruit AFAP-110, p190RhoGAP, and cortactin. A7r5 cells transfected with GFP-Tks5-mito were stimulated with PDBu for 30 minutes, fixed and stained for AFAP-110, p190RhoGAP, or cortactin (red). All three proteins colocalize with GFP-Tks5-mito as in unstimulated cells. Bar, 20 μm.

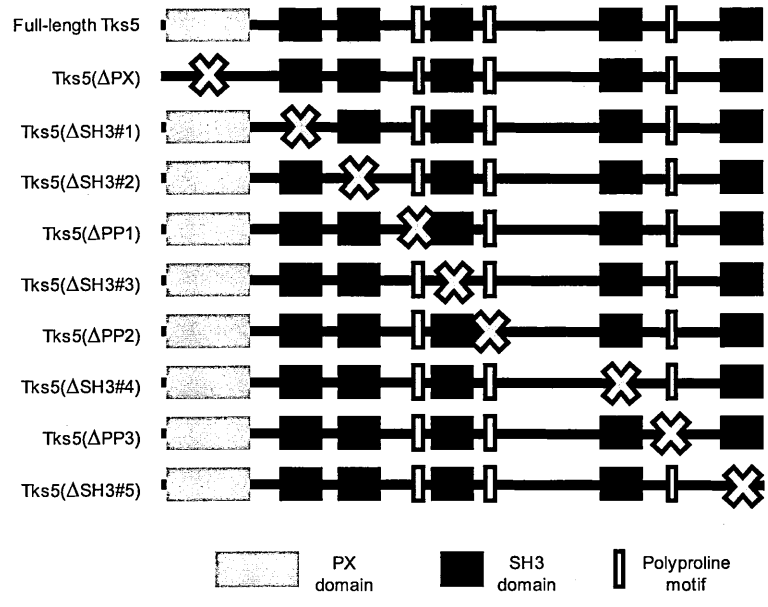

Figure 3.14 – Schematic representation of the deletion mutants of GFP-Tks5-mito used in this study. The domain structures of the full-length Tks5 and its deletion mutants are depicted. Boxes represent domains and motifs as indicated, and X indicates the deleted region.

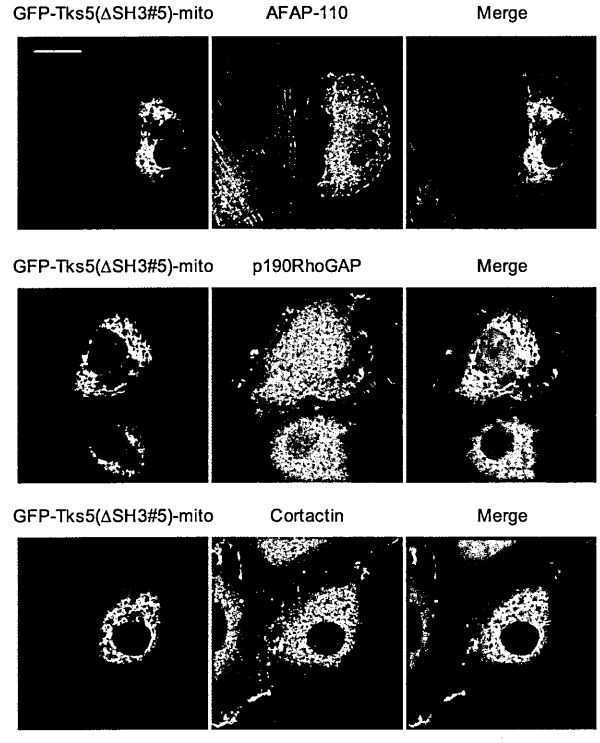

Figure 3.15 – The mutant GFP-Tks5(ΔSH3#5)-mito does not recruit AFAP-110, p190RhoGAP, or cortactin. A7r5 cells were transfected with GFP-Tks5(ΔSH3#5)-mito and stained for AFAP-110, or p190RhoGAP, or cortactin (red). No significant colocalization with the mutant Tks5 is observed. Bar, 20 μm.

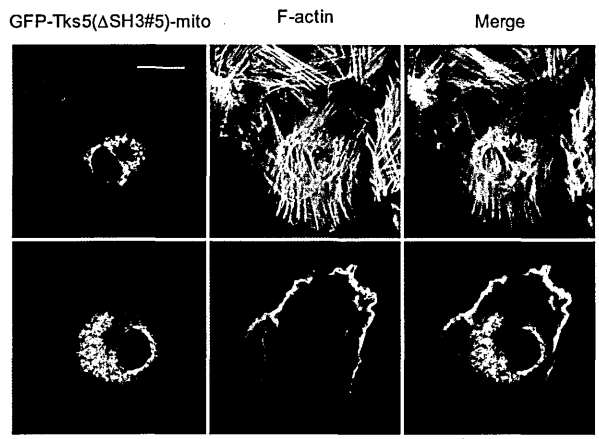

Figure 3.16 – GFP-Tks5(ΔSH3#5)-mito does not colocalize with F-actin. A7r5 cells transfected with GFP-Tks5(ΔSH3#5)-mito were either left unstimulated (top panels) or stimulated with PDBu for 30 minutes (bottom panels), fixed, and stained for F-actin (red). No cloud of F-actin colocalizing with the construct are observed in either condition, but PDBu-treated cells were still unable to form podosomes, and integrity of actin filaments was strongly impaired. Bar, 20 μm.

3.3.5. The PX domain of Tks5 is necessary for podosome formation

To test the role of the PX domain of Tks5 in the formation of podosomes, A7r5 cells were transiently transfected with a Tks5 mutant that lacks the PX domain (Tks5ΔPX-GFP). Unstimulated cells expressing this mutant protein were smaller and displayed an altered and disorganized actin cytoskeleton, with fewer bundles of stress fibres compared to normal cells, while a significant accumulation of Tks5ΔPX-GFP was observed in the perinuclear region, partially colocalizing with a diffuse array of F-actin (Figure 3.17, A). Treatment with PDBu failed to elicit podosome formation in these cells, but increased membrane ruffling activity at the cell periphery (Figure 3.17, A and B). Ectopically expressed full-length Tks5-GFP (containing the PX domain) displayed the same distribution and clustering dynamics in response to PDBu as endogenous Tks5. In agreement with previous studies (Seals *et al.*, 2005), Tks5-GFP facilitated podosome formation in PDBu-stimulated A7r5 cells by more than 50% compared to GFP alone.

Since the perinuclear accumulation of Tks5ΔPX-GFP was similar to what was observed with GFP-Tks5-mito accumulation, cells expressing Tks5ΔPX-GFP were also stained with the MitoTracker Red probe. As can be seen in Figure 3.18 the construct does not colocalize with mitochondria, which display normal morphology.

3.3.6 The Tks5(ΔPX) mutant recruits AFAP-110, p190RhoGAP, and cortactin

In A7r5 cells transfected with Tks5ΔPX-GFP and stained with antibodies to AFAP-110, p190RhoGAP, and cortactin, all three proteins were seen to partially colocalize with the accumulation of Tks5ΔPX-GFP construct (Figure 3.19). These results are similar to those obtained with the mistargeting of Tks5 to mitochondria, and confirm the general ability of Tks5 to recruit these proteins independently of a membrane-proximal subcellular localization.

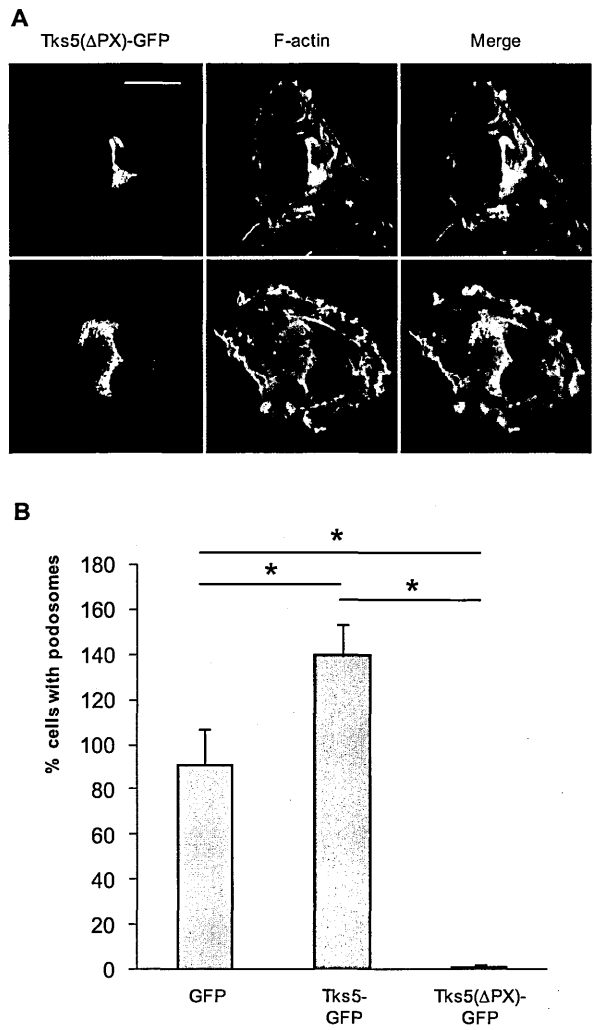

Figure 3.17 – Tks5ΔPX-GFP inhibits podosome formation. (A) A7r5 cells transfected with Tks5ΔPX-GFP were either left unstimulated (top panels) or stimulated with PDBu for 30 minutes (bottom panels), fixed, and stained for F-actin (red). Cells show a significant accumulation of Tks5ΔPX-GFP in the perinuclear region and a partial colocalization with F-actin. No podosomes are formed in PDBu-stimulated cells, and ruffling activity at the cell periphery is enhanced. **(B)** A7r5 cells were transfected with GFP, Tks5-GFP, or Tks5ΔPX-GFP, and the percentage of cells displaying podosomes after stimulation with PDBu was quantified. The vertical axis represents the percentage of transfected cells with podosomes; the percentage of untransfected cells with podosomes was set to 100%. Data from three independent experiments; n = at least 45 cells; * = $p < 0.01$.

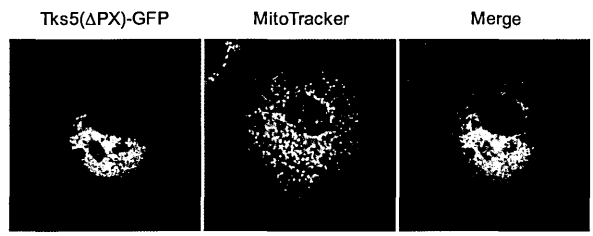

Figure 3.18 – Tks5ΔPX-GFP-containing aggregates are not mitochondria. A7r5 cells transfected with Tks5ΔPX-GFP and stained with the MitoTracker Red probe show that the aggregates formed by Tks5ΔPX-GFP do not contain mitochondria. Bar, 20 μm.

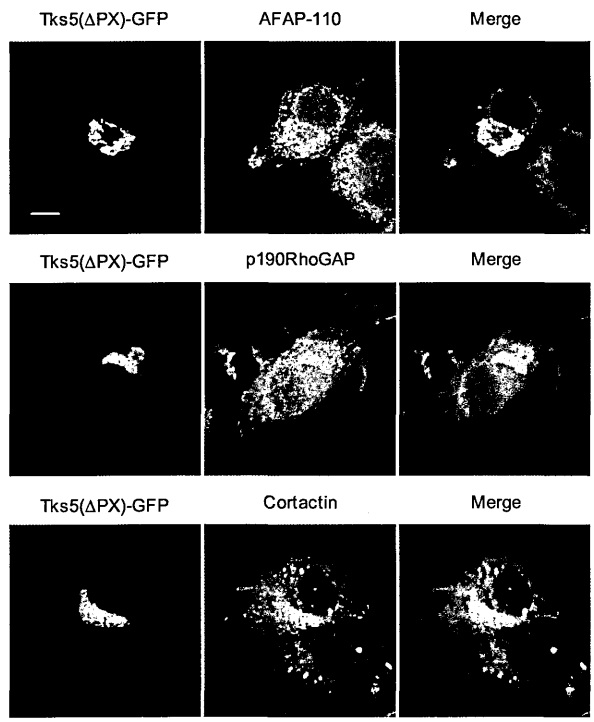

Figure 3.19 – Tks5ΔPX-GFP recruits AFAP-110, p190RhoGAP, and cortactin to the perinuclear area. A7r5 cells transfected with Tks5ΔPX-GFP were stained for AFAP-110, p190RhoGAP, or cortactin (red). All three proteins partially colocalize with the accumulation of Tks5ΔPX-GFP at the perinuclear area, indicating the specific recruitment of these proteins by Tks5. Bar, 10 μm.

3.4 A7r5 cells can form invadopodia-like structures

A7r5 cells cultured on cross-linked gelatin, spontaneously formed active ECM-degrading structures, enriched in F-actin and resembling invadopodia (Figure 3.20, A), without stimulation by PDBu. In these structures, F-actin was present either as clusters or as stress fibres passing through the area of gelatin degradation. An orthogonal view obtained by Z-sectioning of a single degradation area shows the columnar structure of the actin clusters (Figure 3.20, B). Since it is well established that the degradation activity of invadopodia depends on the action of metalloproteinases, A7r5 cells were cultured on cross-linked gelatin in the presence of BB94, which is a reversible broad-range inhibitor of metalloproteinases; as a consequence, the focalized degradation of gelatin was completely inhibited (Figure 3.21, A). Washing out BB94 from growth medium resulted in the rescue of cells' capability to degrade ECM, forming invadopodia-like structures (Figure 3.21, B). These invadopodia-like structures were enriched in clusters of F-actin (Figure 3.21, B and C) and cortactin (Figure 3.22), which were localized mainly at the border of the degradation area. Orthogonal views obtained by Z-sectioning of single degradation areas show that actin and cortactin clusters are arranged in columns that cross the entire width of the matrix layer.

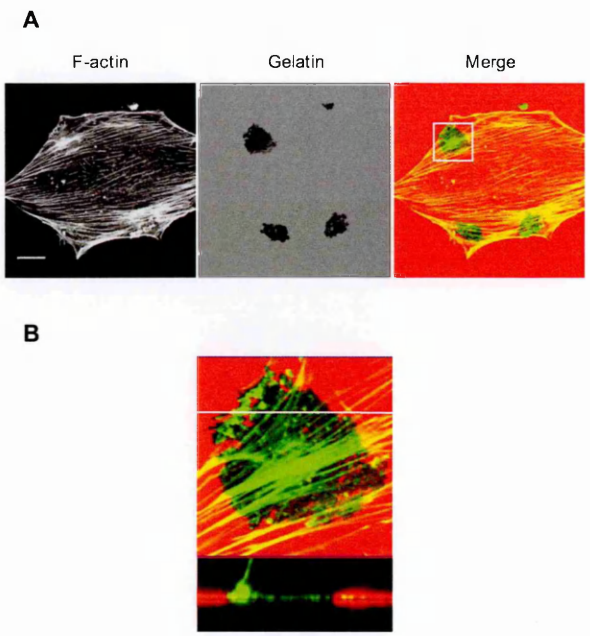

Figure 3.20 – A7r5 cells form invadopodia-like structures that degrade the ECM. (A) A7r5 cells were cultured for 18 hours on a matrix made of Rhodamine B-conjugated cross-linked gelatin, fixed and stained for F-actin (green). Degradation of gelatin results in the appearance of black, non-fluorescent regions. Three major degradation areas are visible at the periphery of the cell, that contain clusters of actin and stress fibres. Bar, 20 μm. **(B)** The boxed degradation area in the merged panel in (A) has been magnified and scanned along the vertical Z-axis; the image depicts one middle section. The lower panel of the picture shows an X–Z profile through the white line shown in the upper panel. At the border of the area where gelatin has been degraded, a large columnar cluster of actin with an incoming stress fibre can be identified. The Z distance between the optical sections was 0.25 μm.

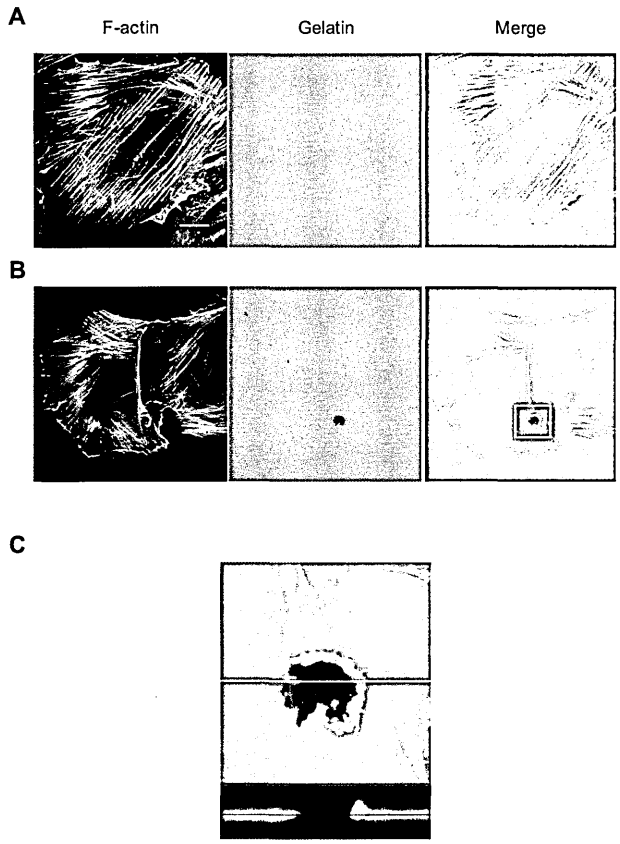

Figure 3.21 – Degradation of gelatin depends on the activity of metalloproteinases. (A) A7r5 cells were cultured for 16 hours on a matrix made of Rhodamine B-conjugated cross-linked gelatin in the presence of the metalloproteinase inhibitor BB94, fixed and stained for F-actin (green). Black, non-fluorescent regions are absent, indicating that degradation of gelatin was inhibited by the inactivation of metalloproteinases. Bar, 20 μm. **(B)** After culturing A7r5 cells as above, BB94 was washed out, and cells were cultured for further 3 hours, fixed and stained for F-actin (green). Small black, non-fluorescent regions became visible, indicating that degradation of gelatin started soon after washing out BB94. Clusters of F-actin were present both along the border of degradation areas and in the central area. **(C)** The boxed degradation area in the merged panel in (B) has been magnified and scanned along the vertical Z-axis. The lower panel of the picture shows an X–Z profile through the white line shown in the upper panel. At the borders of the area where gelatin has been degraded, two columnar clusters of actin can be identified. The Z distance between the optical sections was 0.25 μm.

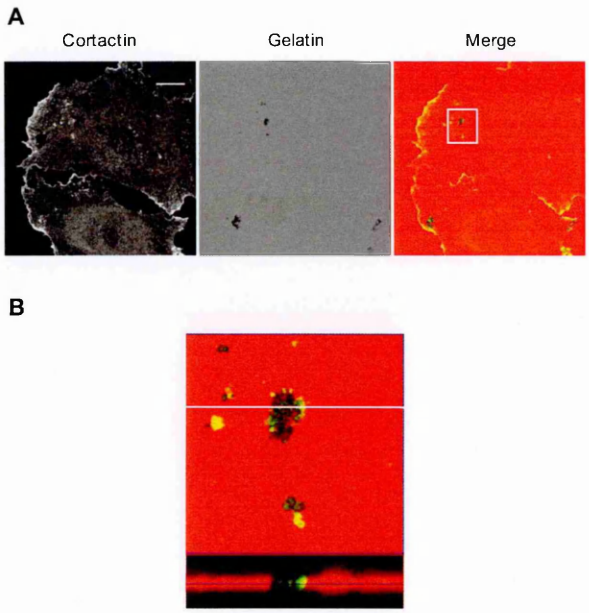

Figure 3.22 – Degradation areas contain clusters of cortactin. (A) A7r5 cells were cultured for 16 hours on a matrix made of Rhodamine B-conjugated cross-linked gelatin in the presence of BB94. After washing out BB94, cells were cultured for further 3 hours, fixed and stained for cortactin (green). Clusters of cortactin are present both along the border of degradation areas and in the central region. Bar, 20 μm. **(B)** The boxed degradation area in the merge panel in (A) has been magnified and scanned along the vertical Z-axis. The lower panel of the picture shows an X–Z profile through the white line shown in the upper panel. At the border of the area where gelatin has been degraded, a columnar cluster of cortactin can be identified. The Z distance between the optical sections was 0.25 μm.

CHAPTER 4

Discussion

4.1 Role of p190RhoGAP in podosome formation

Evidence from different cell systems indicates that RhoA activity must be locally down-regulated in a specific time-frame in order to start the formation of podosomes. It is known that p190RhoGAP inactivates RhoA and promotes the turnover of actin stress fibres and focal adhesion. Previously, it was also shown that PDBu stimulation induces Src-mediated p190RhoGAP tyrosine-phosphorylation and RhoA inactivation in A7r5 cells (Brandt *et al.*, 2002). In this thesis, I provide direct evidence for a requirement of p190RhoGAP in podosome formation, using essentially two approaches. As a first approach, the expression of p190RhoGAP was suppressed by RNA interference, employing a siRNA sequence specific for p190RhoGAP, which had been used successfully by others (Barberis *et al.*, 2005). This suppression resulted in the inhibition of podosome formation. As a second approach, the requirement for the GAP activity of p190RhoGAP in podosome formation was assessed by over-expression of the GAP-dead point mutant p190RhoGAP(R1283A), which also resulted in inhibition of podosome formation after PDBu stimulation. Both approaches gave similar results also in terms of the degree of inhibition of podosome formation, and in both cases the

number of treated cells displaying podosomes was reduced by two thirds compared to control cells.

These findings contrast a recent study on human umbilical vein endothelial cells (Guegan *et al.*, 2008), where the authors showed that siRNA-mediated knockdown of p190RhoGAP (p190A) increased both the number of cells showing podosomes as well as the podosome-associated ECM degradation activity. By contrast, knockdown of the related protein p190B resulted in a decrease in MT1-MMP cell-surface presentation and MMP2 activation, and in a reduction of podosome-associated ECM degradation activity. In this study the authors used two different siRNAs to target p190RhoGAP, one of which had the same sequence used in this thesis. Notably, transfection of A7r5 cells with the second siRNA sequence used by Guegan and colleagues did not result in satisfactory levels of silencing, even though the corresponding human and rat nucleotide sequences are identical. The discrepancy between the two studies might be due to differences in the cell systems used. Such a scenario is indeed supported by the finding that silencing of both p190 isoforms did not alter RhoA activity in endothelial cells (Guegan *et al.*, 2008), suggesting that compensatory effects due to the activity of other RhoGAPs may indeed account for these differences. Thus, a possible explanation for the apparent discrepancy is that in endothelial cells other RhoGAPs may be expressed, that perfom overlapping or redundant functions. In further support for this explanation, it has been reported lately that another RhoGAP (RhoGAP7) is required for the down-regulation of Rho activity and subsequent podosome formation in Src-transformed fibroblasts (Schramp *et al.*, 2008).

p120RasGAP is a well-documented binding partner of p190RhoGAP, and it had been suggested that activity and subcellular localization of p190RhoGAP is regulated by the association with p120RasGAP (see chapter 1.3.3.1). In fibroblasts

stably over-expressing Src, both p190RhoGAP and p120RasGAP localize to the perinuclear area in quiescent cells, whereas they redistribute together to arc-like actin structures following EGF stimulation (Chang *et al.*, 1995). Other studies suggested that p190RhoGAP translocation to the plasma membrane is mediated by p120RasGAP. In neutrophils, p190RhoGAP and p120RasGAP are constitutively associated and translocate to the plasma membrane during integrin-mediated spreading, followed by a slow activation of p190RhoGAP and subsequent down-regulation of RhoA activity (Dib *et al.*, 2001). Similarly, in fibroblasts, integrin-mediated adhesion induces p190RhoGAP activation by promoting its association with p120RasGAP, which results in the recruitment of p120RasGAP-associated p190RhoGAP to the cell periphery, where it inhibits RhoA; disruption of this complex prevents recruitment of p190RhoGAP to the cell periphery and its subsequent activation, leading to a blockage of adhesion-dependent Rho inhibition (Bradley *et al.*, 2006). In bone-marrow-derived macrophages deficient for the transcriptional repressor BCL6, reduced access of p190RhoGAP to RhoA at the plasma membrane is correlated with reduced translocation of p120RasGAP to the plasma membrane, and reduced co-immunoprecipitation of p190RhoGAP by p120RasGAP; these cells display abnormal high levels of RhoA activation, which leads to altered cell adhesion and motility (Pixley *et al.*, 2005). Additionally, it has been shown that the calcium-dependent lipid binding (CaLB) motif of p120RasGAP mediates its membrane association in response to elevated intracellular Ca^{2+} (Gawler *et al.*, 1995a; Gawler *et al.*, 1995b). Collectively, all these data point to a role for p120RasGAP in targeting p190RhoGAP to specific locations at the plasma membrane, where p190RhoGAP can exert its function in down regulating Rho activity, in response to a specific extracellular stimulus. Thus, it was hypothesized that p120RasGAP may have a role in podosome formation, by addressing

p190RhoGAP from the cytosol to the sites of podosome formation at the plasma membrane, specifically in response to PDBu-induced Src activation. To test this hypothesis, the association of p190RhoGAP and p120RasGAP in unstimulated or PDBu-stimulated A7r5 vascular smooth muscle cells was examined in the course of this thesis. However, p190RhoGAP and p120RasGAP co-immunoprecipitated in either condition, indicating that in A7r5 cells the formation of the p120RasGAP/p190RhoGAP complex is constitutive and is only slightly enhanced by stimulation with PDBu. This biochemical result was confirmed by immunofluorescence microscopy: p120RasGAP and GFP-p190RhoGAP partially colocalized in the perinuclear region, at the plasma membrane, and on actin stress fibres. Interestingly, they also colocalized at podosomes in PDBu-stimulated cells, indicating that probably p190RhoGAP is already complexed with p120RasGAP, prior to its recruitment to the sites of podosome formation. I also assessed the role of p120RasGAP in the formation of podosomes by knocking down its expression through transfection of a pool of specific siRNAs: neither the distribution of p190RhoGAP nor podosome formation was affected. This latter result suggests that p120RasGAP is not required for the recruitment of p190RhoGAP to the sites of podosome formation.

4.2 Role of AFAP-110 in podosome formation

In the last years, the role of AFAP-110 in podosome formation has been elucitated in Src over-expressing fibroblasts and epithelial cells. Ectopically expressing a dominant negative mutant of AFAP-110, which cannot bind active PKCα, I confirmed that AFAP-110 is required for PKC-induced podosome formation also in vascular smooth muscle cells. This points to a general role for

AFAP-110 in mediating PKC-induced Src activation and subsequent podosome formation also in other cell types. This also implies that AFAP-110 must be recruited to specific sites at the plasma membrane in order to relay the signal from PKC to Src.

4.3 Role of Tks5 in podosome formation

PKC and Src are upstream activators of the signalling cascades that lead to actin remodelling and podosome formation, and AFAP-110 mediates the PKC-dependent activation of Src, which in turn phosphorylates multiple targets to trigger the formation of podosomes (Gatesman *et al.*, 2004). Podosome formation in cultured vascular smooth muscle cells requires a spatially and temporally restricted regulation of actin cytoskeleton stability and dynamics, which involves local down-regulation of RhoA activity, in order to disassemble pre-existing actin filaments and focal adhesions, followed by local induction of polymerization of new actin filaments. These processes are mediated by a series of Src substrates such as p190RhoGAP and cortactin, via inactivation of RhoA and activation of Arp2/3-dependent actin polymerization, respectively. Thus, coordination of the activities of AFAP-110, Src, p190RhoGAP and cortactin in a defined spatio-temporal manner is required for the generation of active, matrix-degrading podosomes. I hypothesized that a specific scaffolding protein that recruits and assembles AFAP-110, p190RhoGAP and cortactin into a multi-protein complex is responsible for this coordination. In this thesis, I ectopically expressed a form of Tks5, which was mistargeted to the surface of mitochondria, to assess the role of Tks5 in the specific recruitment of AFAP-110, p190RhoGAP, and cortactin to sites of podosome formation. The mistargeted-form of Tks5 (GFP-Tks5-mito) was indeed

able to recruit AFAP-110, p190RhoGAP, and cortactin via its C-terminal SH3 domain, and its expression significantly impaired podosome formation. The induction of actin polymerization away from the plasma membrane (as seen by the accumulation of F-actin around mitochondrial aggregates) may in part explain the observed alterations in cell size and actin cytoskeleton morphology displayed by GFP-Tks5-mito expressing cells, as well as the alteration in the distribution of mitochondria, which move along both actin cables and microtubules (Anesti and Scorrano, 2006; Boldogh and Pon, 2007; Frederick and Shaw, 2007). These data suggest that the proper subcellular localization and specific accumulation of AFAP-110, p190RhoGAP, and cortactin is essential to propagate podosome formation; they also suggest that recruitment and sequestration of these components away from the normal sites of podosome formation at the ventral side of the plasma membrane depletes the cell of the available molecular components, leading to a block in podosome formation. The construct GFP-Tks5-mito can recruit AFAP-110, p190RhoGAP, and cortactin even in the absence of PDBu, further indicating that a fraction of these proteins may form a constitutive complex in the cell. This complex may be directed to sites of podosome formation after stimulation with PDBu, probably through the targeting of the PX domain of Tks5 to sites of the plasma membrane that are enriched in specific phosphoinositides. Such a scenario is indeed supported by recent work in Src-transformed cells (Oikawa *et al.*, 2008), in which the authors showed that accumulation of PtdIns(3,4)P2 at focal adhesions triggers Tks5 translocation to these sites, with a subsequent Tks5-mediated accumulation of the Arp2/3 activator N-WASp, the induction of actin polymerization, and consequently, podosome formation. The PX domain of Tks5 is able to bind PtdInsP and PtdIns(3,4)P2, which are the products of PI3K (Abram *et al.*, 2003), and activation of PKCα by PMA directs activation of PI3K, resulting in *i)*

translocation of AFAP-110 to sites where inactive Src resides, *ii)* colocalization of AFAP-110 with inactive Src and subsequent activation of Src, and *iii)* podosome formation (Walker *et al.*, 2007). It has also been demonstrated that inactivation of the catalytic subunit p110δ of PI3K leads to reduced Src-mediated p190RhoGAP tyrosine-phosphorylation and activity, and increased RhoA-GTP levels, further suggesting that PI3K activity results in Src-mediated p190RhoGAP activation and subsequent down-regulation of RhoA activity (Papakonstanti *et al.*, 2007). In addition, it has been shown that keratinocyte growth factor (KGF) and fibroblast growth factor 10 (FGF10) stimulate cortactin translocation to the leading edge of human keratinocytes in a Src- and PI3K-dependent manner (Ceccarelli *et al.*, 2007). All together, these data lend strong support to a model in which activation of PI3K drives formation of a complex that includes Tks5, AFAP-110, p190RhoGAP, and cortactin to the specific sites of podosome formation at the plasma membrane. The role of Tks5 as a critical recruiter of podosome components during the process of podosome formation is supported by a recent study, which shows that Src-induced interaction between Tks5 and β-dystroglycan is important for podosome formation and results in the translocation of both proteins to podosomes in PDBu-stimulated myoblast cells (Thompson *et al.*, 2008). The authors also show that Src can be co-immunoprecipitated with Tks5 and dystroglycan, suggesting the existence of a ternary complex composed of these three proteins.

The analysis of the deletion mutants of GFP-Tks5-mito revealed that only the fifth SH3 domain of Tks5 is required for the recruitment of AFAP-110, p190RhoGAP, and cortactin. It is currently uncertain if this domain interacts directly with the poly proline-rich regions from one or all three of these proteins; since I failed to co-immunoprecipitate Tks5 with either protein, an indirect interaction may be involved. This is supported by the observation that Src induces association of

Tks5 with another adaptor molecule, Grb2, which is required for the proper addressing of Tks5 to PtdIns(3,4)P2-enriched sites of podosome formation (Oikawa *et al.*, 2008). Moreover, the fifth SH3 domain of Tks5 was shown to bind ADAM 19 (Abram *et al.*, 2003). It is reasonable to consider that also other protein-protein interaction domains or motifs of Tks5 are involved in recruiting factors that are required for podosome formation, other than AFAP-110, p190RhoGAP, and cortactin. Cells expressing the mitochondria-localized mutant GFP-Tks5(ΔSH3#5)-mito were still unable to form podosomes after stimulation with PDBu, even though AFAP-110, p190RhoGAP, and cortactin were not recruited and sequestered by the construct. Indeed a recent study identified the first and fifth SH3 domain of Tks5 to be involved in the interaction with dynamin 2, the third and fifth SH3 domain to mediate the interaction with the WASp interactor WIP and the focal adhesion component zyxin, and all five SH3 domains to bind N-WASP (Oikawa *et al.*, 2008). All these proteins have been shown to be involved in podosome formation and function (Ochoa *et al.*, 2000; Mizutani *et al.*, 2002; Moreau *et al.*, 2003; Chou *et al.*, 2006). In addition, it has been found that Tks5 molecules mutated in any of the first SH3 domains inhibit podosomes in Src-transformed fibroblasts (Sara Courtneidge, personal communication), confirming that also these domains have a role in podosome formation.

PX domains target membranes via binding to phosphoinositides (Sato *et al.*, 2001), and the PX domain of Tks5 is required for the targeting of Tks5 to podosomes, as well as for the ability of Tks5 to induce podosome formation in cells that cannot form these transient adhesion structures spontaneously (Abram *et al.*, 2003; Seals *et al.*, 2005). To further analyze the role of the PX domain in Tks5 capability of recruiting critical podosome components, I over-expressed a Tks5 mutant that lacks the PX domain (Tks5ΔPX-GFP) in A7r5 cells, resulting in the blockage of

podosome formation. The accumulation of Tks5ΔPX-GFP observed in the perinuclear region, resembled the aggregates of GFP-Tks5-mito-enriched mitochondria; they both colocalized with a cloud of F-actin, indicating that Tks5 is capable of inducing local actin rearrangement. These data are in agreement with previous work (Seals *et al.*, 2005), which demonstrated that, while co-expression of active Src and full length Tks5 induced formation of podosomes in a cell line lacking the ability for spontaneous podosome formation, a PX domain-deleted Tks5 mutant was unable to promote podosome formation. In support of the results obtained with the mitochondrial-mistargeting approach, Tks5ΔPX-GFP accumulation was seen to colocalize with AFAP-110, p190RhoGAP, and cortactin, indicating that these proteins are recruited by Tks5, and that the presence of the PX domain inhibits this recruitment. This evidence corroborates a model, in which the PX domain is responsible for targeting Tks5 to the plasma membrane upon phorbol ester stimulation and subsequent PKC activation; thereafter engagement of the PX domain with PtdIns(3,4)P2 would result in recruitment of critical components of the podosome machinery, such as AFAP-110, p190RhoGAP, and cortactin, and in the coordination of their activities.

4.4 Invadopodia in vascular smooth muscle cells

The migration of vascular smooth muscle cells is a critical factor in the development and progression of cardiovascular diseases, such as atherosclerosis and post-angioplasty restenosis. In the medial layer of healthy arteries, vascular smooth muscle cells are in a quiescent and differentiated contractile state. In response to vessel wall damage, these cells switch to a synthetic state, which is characterized by a less differentiated and more proliferative phenotype, and by the

capability to degrade ECM and migrate (Owens *et al.*, 2004). This invasive ability allows synthetic vascular smooth muscle cells to migrate to the sub-endothelial intimal layer, where they participate in the formation of neo-intimal lesions and contribute to the development and progression of atherosclerosis and restenosis (Schwartz, 1997; Indolfi *et al.*, 2003).

It has been reported that the expression of activated forms of Src, Cdc42 and Rac1, induces primary rat aorta vascular smooth muscle cells to form actin-rich protrusions that degrade ECM and are morphologically similar to invadopodia (Furmaniak-Kazmierczak *et al.*, 2007). The authors also reported that invadopodia formation in these cells is only weakly supported by PBDu, in contrast to podosome formation in A7r5 cells, and further demonstrated that, when embedded in a three-dimensional collagen matrix, these primary vascular smooth muscle cells form actin- and cortactin-rich protrusions that penetrate through holes in the matrix. These protrusions are similar to invadopodia formed by active-Src expressing cells on a two-dimensional matrix, thus suggesting that the presence of a three-dimensional ECM around primary vascular smooth muscle cells is sufficient to induce these cells to form invadopodia that digest ECM and facilitate cell migration. Upon spreading on flexible polyacrylamide substrates coated with either fibronectin or type 1 collagen, A7r5 cells were shown to induce rearrangement of the matrix, because of contractile forces exerted by their acto-myosin system; nevertheless they degraded the matrix only through PDBu-induced podosomes (Burgstaller and Gimona, 2005). The data presented in this thesis show that, when A7r5 cells are cultured on cross-linked gelatin, they form F-actin- and cortactin-rich structures, which digest the matrix through metalloproteinase activity and resemble invadopodia. However, these structures display certain differences compared to classical invadopodia. First, they form preferentially at cell periphery (like

podosomes), while invadopodia form in the central region of the cell. Second, they do not appear as finger-like extensions, but rather as columns of actin and cortactin, occupying the space where gelatin is digested, and this is more similar to podosome morphology. This second difference is probably due to two factors: 1) cell type-specific response to local ECM environment, and 2) differences in the techniques used for the preparation of coverslips for the assay. A7r5 cells display ventral actin stress fibres that are immerged deep into the matrix, and this is probably linked with the circumstance that vascular smooth muscle cells in vivo are encapsulated by a basal membrane; thus, the thickness of a single layer of gelatin would not be enough to see invadopodia as finger-like extensions. In fact in the study on primary smooth muscle cells, these were cultured on a double-layered matrix consisting of labeled fibronectin on top of cross-linked gelatin (Furmaniak-Kazmierczak *et al.*, 2007), whereas in this thesis cells were cultured on a single layer of cross-linked gelatin. Furthermore, in both studies mentioned above cells were in contact with fibronectin (Burgstaller and Gimona, 2005; Furmaniak-Kazmierczak *et al.*, 2007). This could explain in part why the authors could not see unstimulated A7r5 cells digesting the matrix; it is possible that cross-linked gelatin triggers a signalling cascade, leading to invadopodia formation, that fibronectin is unable to induce. Such considerations clearly argue for mechanosensation and mechanotransduction events being involved in podosome and invadopodia formation. Notably, podosomes have recently been defined as mechanosensory cellular structures (Collin *et al.*, 2008), lending support to this theory. As a future perspective it will thus be important to further characterize the molecular components of A7r5 cell invadopodia and to investigate the signalling cascade(s) responsible for their formation. Although these data are preliminary, I report in this thesis for the first time the existence of a specific cell type that is capable of

forming both invadopodia and podosomes in different conditions. This unique phenomenon could help to shed light on the relationship between these two structures.

4.5 Conclusions

Taken together, the results presented in this thesis show that Tks5 specifically recruits AFAP-110, p190RhoGAP, and cortactin via its fifth SH3 domain, and that this recruitment is necessary for podosome formation. Based on these results I propose a model in which, upon PDBu-stimulation, the PX domain of Tks5 interacts with the products of PKC-activated PI3K, resulting in the recruitment of AFAP-110, p190RhoGAP, and cortactin by Tks5, and in their positioning in close proximity to the sites of podosome formation, where PKC activates AFAP-110, which subsequently activates Src. Src-dependent phosphorylation of p190RhoGAP and cortactin (and likely of other substrates), results in the local down-regulation of RhoA activity with consequent dissolution of focal adhesions, and Arp2/3-dependent de-novo actin polymerization, leading to the formation of the podosome core and the subsequent assembly of adhesion components in the podosome ring (Figure 4.1).

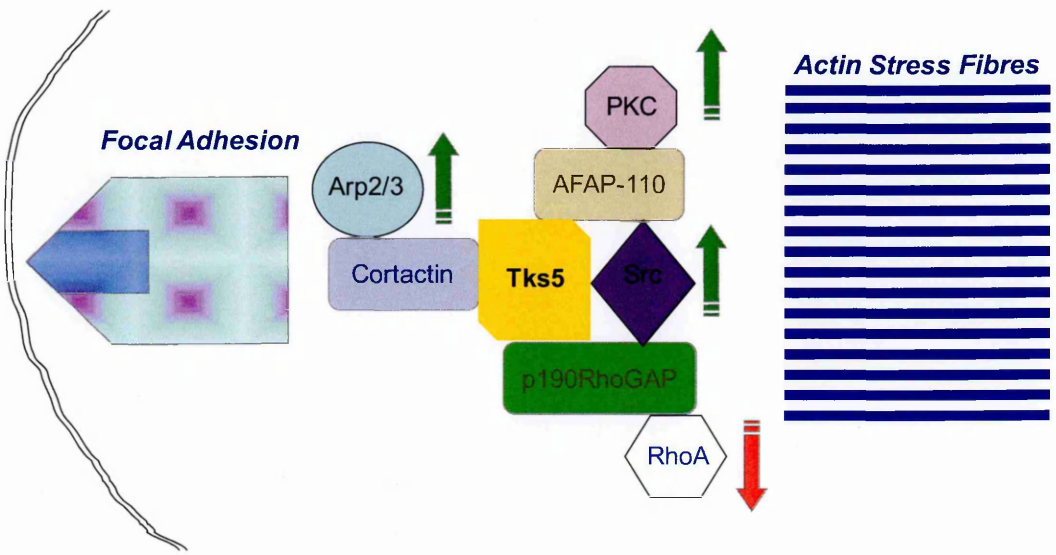

Figure 4.1 – Model of podosome components recruitment by Tks5 during podosome formation. This cartoon depicts a model of Tks5 in recruiting and coordinating AFAP-110, p190RhoGAP, and cortactin during podosome formation. The green arrows indicate up-regulation of activity, while the red arrow indicates down-regulation of activity.

Acknowledgements

I would like to thank my director of studies Dr. Mario Gimona for his mentorship and support during the course of my PhD studies.

I wish to thank my supervisor Prof. Steve Winder for helpful suggestions and discussions.

Thanks to Dr. Roberto Buccione for helpful discussions.

I am grateful to Giada Giacchetti and Giusi Caldieri for their friendly and technical help with the ECM degradation assay.

I would like to thank Dr. Gerard Dougherty and the PhD students of the Department of Cell Biology and Oncology for their friendship.

Thanks to Dr. Alberto Luini for his help with the final phase of my PhD studies.

A special thank to my family, whose support has been very important.

Finally, support from the European Union (Marie Curie Excellence grant MEXT-CT-2003-002573, to Dr. Mario Gimona) is gratefully acknowledged.

References

Abercrombie, M., Heaysman, J.E., and Pegrum, S.M. (1971). The locomotion of fibroblasts in culture. IV. Electron microscopy of the leading lamella. Exp Cell Res *67*, 359-367.

Abram, C.L., Seals, D.F., Pass, I., Salinsky, D., Maurer, L., Roth, T.M., and Courtneidge, S.A. (2003). The adaptor protein fish associates with members of the ADAMs family and localizes to podosomes of Src-transformed cells. J Biol Chem *278*, 16844-16851.

Akisaka, T., Yoshida, H., Inoue, S., and Shimizu, K. (2001). Organization of cytoskeletal F-actin, G-actin, and gelsolin in the adhesion structures in cultured osteoclast. J Bone Miner Res *16*, 1248-1255.

Anesti, V., and Scorrano, L. (2006). The relationship between mitochondrial shape and function and the cytoskeleton. Biochim Biophys Acta *1757*, 692-699.

Arber, S., Barbayannis, F.A., Hanser, H., Schneider, C., Stanyon, C.A., Bernard, O., and Caroni, P. (1998). Regulation of actin dynamics through phosphorylation of cofilin by LIM-kinase. Nature *393*, 805-809.

Arcaro, A. (1998). The small GTP-binding protein Rac promotes the dissociation of gelsolin from actin filaments in neutrophils. J Biol Chem *273*, 805-813.

Artym, V.V., Zhang, Y., Seillier-Moiseiwitsch, F., Yamada, K.M., and Mueller, S.C. (2006). Dynamic interactions of cortactin and membrane type 1 matrix

metalloproteinase at invadopodia: defining the stages of invadopodia formation and function. Cancer Res *66*, 3034-3043.

Ayala, I., Baldassarre, M., Giacchetti, G., Caldieri, G., Tete, S., Luini, A., and Buccione, R. (2008). Multiple regulatory inputs converge on cortactin to control invadopodia biogenesis and extracellular matrix degradation. J Cell Sci *121*, 369-378.

Badolato, R., Sozzani, S., Malacarne, F., Bresciani, S., Fiorini, M., Borsatti, A., Albertini, A., Mantovani, A., Ugazio, A.G., and Notarangelo, L.D. (1998). Monocytes from Wiskott-Aldrich patients display reduced chemotaxis and lack of cell polarization in response to monocyte chemoattractant protein-1 and formyl-methionyl-leucyl-phenylalanine. J Immunol *161*, 1026-1033.

Badowski, C., Pawlak, G., Grichine, A., Chabadel, A., Oddou, C., Jurdic, P., Pfaff, M., Albiges-Rizo, C., and Block, M.R. (2008). Paxillin Phosphorylation Controls Invadopodia/Podosomes Spatiotemporal Organization. Mol Biol Cell *19*, 633-645.

Baldassarre, M., Pompeo, A., Beznoussenko, G., Castaldi, C., Cortellino, S., McNiven, M.A., Luini, A., and Buccione, R. (2003). Dynamin participates in focal extracellular matrix degradation by invasive cells. Mol Biol Cell *14*, 1074-1084.

Barberis, D., Casazza, A., Sordella, R., Corso, S., Artigiani, S., Settleman, J., Comoglio, P.M., and Tamagnone, L. (2005). p190 Rho-GTPase activating protein associates with plexins and it is required for semaphorin signalling. J Cell Sci *118*, 4689-4700.

Bearer, E.L. (1991). Direct observation of actin filament severing by gelsolin and binding by gCap39 and CapZ. J Cell Biol *115*, 1629-1638.

Berdeaux, R.L., Diaz, B., Kim, L., and Martin, G.S. (2004). Active Rho is localized to podosomes induced by oncogenic Src and is required for their assembly and function. J Cell Biol *166*, 317-323.

Binks, M., Jones, G.E., Brickell, P.M., Kinnon, C., Katz, D.R., and Thrasher, A.J. (1998). Intrinsic dendritic cell abnormalities in Wiskott-Aldrich syndrome. Eur J Immunol *28*, 3259-3267.

Blouw, B., Seals, D.F., Pass, I., Diaz, B., and Courtneidge, S.A. (2008). A role for the podosome/invadopodia scaffold protein Tks5 in tumor growth in vivo. Eur J Cell Biol *87*, 555-567.

Boldogh, I.R., and Pon, L.A. (2007). Mitochondria on the move. Trends Cell Biol *17*, 502-510.

Bowden, E.T., Barth, M., Thomas, D., Glazer, R.I., and Mueller, S.C. (1999). An invasion-related complex of cortactin, paxillin and PKCmu associates with invadopodia at sites of extracellular matrix degradation. Oncogene *18*, 4440-4449.

Bowden, E.T., Onikoyi, E., Slack, R., Myoui, A., Yoneda, T., Yamada, K.M., and Mueller, S.C. (2006). Co-localization of cortactin and phosphotyrosine identifies active invadopodia in human breast cancer cells. Exp Cell Res *312*, 1240-1253.

Bradley, W.D., Hernandez, S.E., Settleman, J., and Koleske, A.J. (2006). Integrin signaling through Arg activates p190RhoGAP by promoting its binding to p120RasGAP and recruitment to the membrane. Mol Biol Cell *17*, 4827-4836.

Brandt, D., Gimona, M., Hillmann, M., Haller, H., and Mischak, H. (2002). Protein kinase C induces actin reorganization via a Src- and Rho-dependent pathway. J Biol Chem *277*, 20903-20910.

Bubeck, P., Pistor, S., Wehland, J., and Jockusch, B.M. (1997). Ligand recruitment by vinculin domains in transfected cells. J Cell Sci *110 (Pt 12)*, 1361-1371.

Buccione, R., Orth, J.D., and McNiven, M.A. (2004). Foot and mouth: podosomes, invadopodia and circular dorsal ruffles. Nat Rev Mol Cell Biol *5*, 647-657.

Buchsbaum, R.J. (2007). Rho activation at a glance. J Cell Sci *120*, 1149-1152.

Burgstaller, G., and Gimona, M. (2004). Actin cytoskeleton remodelling via local inhibition of contractility at discrete microdomains. J Cell Sci *117*, 223-231.

Burgstaller, G., and Gimona, M. (2005). Podosome-mediated matrix resorption and cell motility in vascular smooth muscle cells. Am J Physiol Heart Circ Physiol *288*, H3001-3005.

Burns, S., Thrasher, A.J., Blundell, M.P., Machesky, L., and Jones, G.E. (2001). Configuration of human dendritic cell cytoskeleton by Rho GTPases, the WAS protein, and differentiation. Blood *98*, 1142-1149.

Burns, S., Hardy, S.J., Buddle, J., Yong, K.L., Jones, G.E., and Thrasher, A.J. (2004). Maturation of DC is associated with changes in motile characteristics and adherence. Cell Motil Cytoskeleton *57*, 118-132.

Calle, Y., Jones, G.E., Jagger, C., Fuller, K., Blundell, M.P., Chow, J., Chambers, T., and Thrasher, A.J. (2004). WASp deficiency in mice results in failure to form osteoclast sealing zones and defects in bone resorption. Blood *103*, 3552-3561.

Carballido-Lopez, R. (2006). The bacterial actin-like cytoskeleton. Microbiol Mol Biol Rev *70*, 888-909.

Carlier, M.F., Laurent, V., Santolini, J., Melki, R., Didry, D., Xia, G.X., Hong, Y., Chua, N.H., and Pantaloni, D. (1997). Actin depolymerizing factor (ADF/cofilin) enhances the rate of filament turnover: implication in actin-based motility. J Cell Biol *136*, 1307-1322.

Ceccarelli, S., Cardinali, G., Aspite, N., Picardo, M., Marchese, C., Torrisi, M.R., and Mancini, P. (2007). Cortactin involvement in the keratinocyte growth factor and fibroblast growth factor 10 promotion of migration and cortical actin assembly in human keratinocytes. Exp Cell Res *313*, 1758-1777.

Chabadel, A., Banon-Rodriguez, I., Cluet, D., Rudkin, B.B., Wehrle-Haller, B., Genot, E., Jurdic, P., Anton, I.M., and Saltel, F. (2007). CD44 and beta3 integrin organize two functionally distinct actin-based domains in osteoclasts. Mol Biol Cell *18*, 4899-4910.

Chang, J.H., Gill, S., Settleman, J., and Parsons, S.J. (1995). c-Src regulates the simultaneous rearrangement of actin cytoskeleton, p190RhoGAP, and p120RasGAP following epidermal growth factor stimulation. J Cell Biol *130*, 355-368.

Charrier, S., Stockholm, D., Seye, K., Opolon, P., Taveau, M., Gross, D.A., Bucher-Laurent, S., Delenda, C., Vainchenker, W., Danos, O., and Galy, A. (2005). A lentiviral vector encoding the human Wiskott-Aldrich syndrome protein corrects immune and cytoskeletal defects in WASP knockout mice. Gene Ther *12*, 597-606.

Chellaiah, M.A., Soga, N., Swanson, S., McAllister, S., Alvarez, U., Wang, D., Dowdy, S.F., and Hruska, K.A. (2000). Rho-A is critical for osteoclast podosome organization, motility, and bone resorption. J Biol Chem *275*, 11993-12002.

Chen, W.T. (1989). Proteolytic activity of specialized surface protrusions formed at rosette contact sites of transformed cells. J Exp Zool *251*, 167-185.

Chong, L.D., Traynor-Kaplan, A., Bokoch, G.M., and Schwartz, M.A. (1994). The small GTP-binding protein Rho regulates a phosphatidylinositol 4-phosphate 5-kinase in mammalian cells. Cell *79*, 507-513.

Chou, H.C., Anton, I.M., Holt, M.R., Curcio, C., Lanzardo, S., Worth, A., Burns, S., Thrasher, A.J., Jones, G.E., and Calle, Y. (2006). WIP regulates the stability and localization of WASP to podosomes in migrating dendritic cells. Curr Biol *16*, 2337-2344.

Collin, O., Na, S., Chowdhury, F., Hong, M., Shin, M.E., Wang, F., and Wang, N. (2008). Self-organized podosomes are dynamic mechanosensors. Curr Biol *18*, 1288-1294.

Colonna, C., and Podesta, E.J. (2005). ACTH-induced caveolin-1 tyrosine phosphorylation is related to podosome assembly in Y1 adrenal cells. Exp Cell Res *304*, 432-442.

Colucci, S., Grano, M., Argentino, L., Zambonin Zallone, A., and Teti, A. (1990). The role of protein kinase C in the osteoclast activity. Boll Soc Ital Biol Sper *66*, 1059-1064.

Cooper, J.A. (1987). Effects of cytochalasin and phalloidin on actin. J Cell Biol *105*, 1473-1478.

Cosen-Binker, L.I., and Kapus, A. (2006). Cortactin: the gray eminence of the cytoskeleton. Physiology (Bethesda) *21*, 352-361.

Coue, M., Brenner, S.L., Spector, I., and Korn, E.D. (1987). Inhibition of actin polymerization by latrunculin A. FEBS Lett *213*, 316-318.

DeNofrio, D., Hoock, T.C., and Herman, I.M. (1989). Functional sorting of actin isoforms in microvascular pericytes. J Cell Biol *109*, 191-202.

Desai, A., and Mitchison, T.J. (1997). Microtubule polymerization dynamics. Annu Rev Cell Dev Biol *13*, 83-117.

Destaing, O., Saltel, F., Geminard, J.C., Jurdic, P., and Bard, F. (2003). Podosomes display actin turnover and dynamic self-organization in osteoclasts expressing actin-green fluorescent protein. Mol Biol Cell *14*, 407-416.

Dib, K., Melander, F., and Andersson, T. (2001). Role of p190RhoGAP in beta 2 integrin regulation of RhoA in human neutrophils. J Immunol *166*, 6311-6322.

Drees, B., Friederich, E., Fradelizi, J., Louvard, D., Beckerle, M.C., and Golsteyn, R.M. (2000). Characterization of the interaction between zyxin and members of the Ena/vasodilator-stimulated phosphoprotein family of proteins. J Biol Chem *275*, 22503-22511.

Duong, L.T., Lakkakorpi, P.T., Nakamura, I., Machwate, M., Nagy, R.M., and Rodan, G.A. (1998). PYK2 in osteoclasts is an adhesion kinase, localized in the sealing zone, activated by ligation of alpha(v)beta3 integrin, and phosphorylated by src kinase. J Clin Invest *102*, 881-892.

Duong, L.T., and Rodan, G.A. (2000). PYK2 is an adhesion kinase in macrophages, localized in podosomes and activated by beta(2)-integrin ligation. Cell Motil Cytoskeleton *47*, 174-188.

Engel, J., Fasold, H., Hulla, F.W., Waechter, F., and Wegner, A. (1977). The polymerization reaction of muscle actin. Mol Cell Biochem *18*, 3-13.

Fincham, V.J., Chudleigh, A., and Frame, M.C. (1999). Regulation of p190 Rho-GAP by v-Src is linked to cytoskeletal disruption during transformation. J Cell Sci *112 (Pt 6)*, 947-956.

Flynn, D.C., Leu, T.H., Reynolds, A.B., and Parsons, J.T. (1993). Identification and sequence analysis of cDNAs encoding a 110-kilodalton actin filament-associated pp60src substrate. Mol Cell Biol *13*, 7892-7900.

Fradelizi, J., Noireaux, V., Plastino, J., Menichi, B., Louvard, D., Sykes, C., Golsteyn, R.M., and Friederich, E. (2001). ActA and human zyxin harbour Arp2/3-independent actin-polymerization activity. Nat Cell Biol *3*, 699-707.

Frazier, J.A., and Field, C.M. (1997). Actin cytoskeleton: are FH proteins local organizers? Curr Biol *7*, R414-417.

Frederick, R.L., and Shaw, J.M. (2007). Moving mitochondria: establishing distribution of an essential organelle. Traffic *8*, 1668-1675.

Fultz, M.E., Li, C., Geng, W., and Wright, G.L. (2000). Remodeling of the actin cytoskeleton in the contracting A7r5 smooth muscle cell. J Muscle Res Cell Motil *21*, 775-787.

Furmaniak-Kazmierczak, E., Crawley, S.W., Carter, R.L., Maurice, D.H., and Cote, G.P. (2007). Formation of extracellular matrix-digesting invadopodia by primary aortic smooth muscle cells. Circ Res *100*, 1328-1336.

Gallwitz, D., and Sures, I. (1980). Structure of a split yeast gene: complete nucleotide sequence of the actin gene in Saccharomyces cerevisiae. Proc Natl Acad Sci U S A *77*, 2546-2550.

Gatesman, A., Walker, V.G., Baisden, J.M., Weed, S.A., and Flynn, D.C. (2004). Protein kinase Calpha activates c-Src and induces podosome formation via AFAP-110. Mol Cell Biol *24*, 7578-7597.

Gawler, D.J., Zhang, L.J., and Moran, M.F. (1995a). Mutation-deletion analysis of a Ca(2+)-dependent phospholipid binding (CaLB) domain within p120 GAP, a GTPase-activating protein for p21 ras. Biochem J *307 (Pt 2)*, 487-491.

Gawler, D.J., Zhang, L.J., Reedijk, M., Tung, P.S., and Moran, M.F. (1995b). CaLB: a 43 amino acid calcium-dependent membrane/phospholipid binding domain in p120 Ras GTPase-activating protein. Oncogene *10*, 817-825.

Geiger, B., and Bershadsky, A. (2001). Assembly and mechanosensory function of focal contacts. Curr Opin Cell Biol *13*, 584-592.

Geiger, B., Bershadsky, A., Pankov, R., and Yamada, K.M. (2001). Transmembrane crosstalk between the extracellular matrix--cytoskeleton crosstalk. Nat Rev Mol Cell Biol *2*, 793-805.

Ghersi, G., Dong, H., Goldstein, L.A., Yeh, Y., Hakkinen, L., Larjava, H.S., and Chen, W.T. (2002). Regulation of fibroblast migration on collagenous matrix by a cell surface peptidase complex. J Biol Chem *277*, 29231-29241.

Ghersi, G., Zhao, Q., Salamone, M., Yeh, Y., Zucker, S., and Chen, W.T. (2006). The protease complex consisting of dipeptidyl peptidase IV and seprase plays a

role in the migration and invasion of human endothelial cells in collagenous matrices. Cancer Res *66*, 4652-4661.

Gimona, M., and Buccione, R. (2006). Adhesions that mediate invasion. Int J Biochem Cell Biol *38*, 1875-1892.

Gimona, M., Buccione, R., Courtneidge, S.A., and Linder, S. (2008). Assembly and biological role of podosomes and invadopodia. Curr Opin Cell Biol *20*, 235-241.

Goldman, R.D., Grin, B., Mendez, M.G., and Kuczmarski, E.R. (2008). Intermediate filaments: versatile building blocks of cell structure. Curr Opin Cell Biol *20*, 28-34.

Goley, E.D., and Welch, M.D. (2006). The ARP2/3 complex: an actin nucleator comes of age. Nat Rev Mol Cell Biol *7*, 713-726.

Goode, B.L., Drubin, D.G., and Lappalainen, P. (1998). Regulation of the cortical actin cytoskeleton in budding yeast by twinfilin, a ubiquitous actin monomer-sequestering protein. J Cell Biol *142*, 723-733.

Gringel, A., Walz, D., Rosenberger, G., Minden, A., Kutsche, K., Kopp, P., and Linder, S. (2006). PAK4 and alphaPIX determine podosome size and number in macrophages through localized actin regulation. J Cell Physiol *209*, 568-579.

Grubinger, M., and Gimona, M. (2004). CRP2 is an autonomous actin-binding protein. FEBS Lett *557*, 88-92.

Guegan, F., Tatin, F., Leste-Lasserre, T., Drutel, G., Genot, E., and Moreau, V. (2008). p190B RhoGAP regulates endothelial-cell-associated proteolysis through MT1-MMP and MMP2. J Cell Sci *121*, 2054-2061.

Hai, C.M., Hahne, P., Harrington, E.O., and Gimona, M. (2002). Conventional protein kinase C mediates phorbol-dibutyrate-induced cytoskeletal remodeling in a7r5 smooth muscle cells. Exp Cell Res *280*, 64-74.

Hall, A., and Nobes, C.D. (2000). Rho GTPases: molecular switches that control the organization and dynamics of the actin cytoskeleton. Philos Trans R Soc Lond B Biol Sci *355*, 965-970.

Helfrich, M.H., Nesbitt, S.A., Lakkakorpi, P.T., Barnes, M.J., Bodary, S.C., Shankar, G., Mason, W.T., Mendrick, D.L., Vaananen, H.K., and Horton, M.A. (1996). Beta 1 integrins and osteoclast function: involvement in collagen recognition and bone resorption. Bone *19*, 317-328.

Hennessey, E.S., Drummond, D.R., and Sparrow, J.C. (1993). Molecular genetics of actin function. Biochem J *291 (Pt 3)*, 657-671.

Higgs, H.N., and Pollard, T.D. (1999). Regulation of actin polymerization by Arp2/3 complex and WASp/Scar proteins. J Biol Chem *274*, 32531-32534.

Hotchin, N.A., and Hall, A. (1995). The assembly of integrin adhesion complexes requires both extracellular matrix and intracellular rho/rac GTPases. J Cell Biol *131*, 1857-1865.

Hu, K.Q., and Settleman, J. (1997). Tandem SH2 binding sites mediate the RasGAP-RhoGAP interaction: a conformational mechanism for SH3 domain regulation. Embo J *16*, 473-483.

Hurst, I.R., Zuo, J., Jiang, J., and Holliday, L.S. (2004). Actin-related protein 2/3 complex is required for actin ring formation. J Bone Miner Res *19*, 499-506.

Indolfi, C., Mongiardo, A., Curcio, A., and Torella, D. (2003). Molecular mechanisms of in-stent restenosis and approach to therapy with eluting stents. Trends Cardiovasc Med *13*, 142-148.

Izzard, C.S., and Lochner, L.R. (1980). Formation of cell-to-substrate contacts during fibroblast motility: an interference-reflexion study. J Cell Sci *42*, 81-116.

Janmey, P.A., Iida, K., Yin, H.L., and Stossel, T.P. (1987). Polyphosphoinositide micelles and polyphosphoinositide-containing vesicles dissociate endogenous gelsolin-actin complexes and promote actin assembly from the fast-growing end of actin filaments blocked by gelsolin. J Biol Chem *262*, 12228-12236.

Johansson, M.W., Lye, M.H., Barthel, S.R., Duffy, A.K., Annis, D.S., and Mosher, D.F. (2004). Eosinophils adhere to vascular cell adhesion molecule-1 via podosomes. Am J Respir Cell Mol Biol *31*, 413-422.

Jones, G.E., Zicha, D., Dunn, G.A., Blundell, M., and Thrasher, A. (2002). Restoration of podosomes and chemotaxis in Wiskott-Aldrich syndrome macrophages following induced expression of WASp. Int J Biochem Cell Biol *34*, 806-815.

Kasai, M., Asakura, S., and Oosawa, F. (1962a). The cooperative nature of G-F transformation of actin. Biochim Biophys Acta *57*, 22-31.

Kasai, M., Asakura, S., and Oosawa, F. (1962b). The G-F equilibrium in actin solutions under various conditions. Biochim Biophys Acta *57*, 13-21.

Kaverina, I., Stradal, T.E., and Gimona, M. (2003). Podosome formation in cultured A7r5 vascular smooth muscle cells requires Arp2/3-dependent de-novo actin polymerization at discrete microdomains. J Cell Sci *116*, 4915-4924.

Kelly, T., Mueller, S.C., Yeh, Y., and Chen, W.T. (1994). Invadopodia promote proteolysis of a wide variety of extracellular matrix proteins. J Cell Physiol *158*, 299-308.

Kinosian, H.J., Selden, L.A., Estes, J.E., and Gershman, L.C. (1993). Nucleotide binding to actin. Cation dependence of nucleotide dissociation and exchange rates. J Biol Chem *268*, 8683-8691.

Kozma, R., Ahmed, S., Best, A., and Lim, L. (1995). The Ras-related protein Cdc42Hs and bradykinin promote formation of peripheral actin microspikes and filopodia in Swiss 3T3 fibroblasts. Mol Cell Biol *15*, 1942-1952.

Krause, M., Wild, M., Rosenzweig, B., and Hirsh, D. (1989). Wild-type and mutant actin genes in Caenorhabditis elegans. J Mol Biol *208*, 381-392.

Kureishy, N., Sapountzi, V., Prag, S., Anilkumar, N., and Adams, J.C. (2002). Fascins, and their roles in cell structure and function. Bioessays *24*, 350-361.

Lakkakorpi, P.T., and Vaananen, H.K. (1991). Kinetics of the osteoclast cytoskeleton during the resorption cycle in vitro. J Bone Miner Res *6*, 817-826.

Lakkakorpi, P.T., Bett, A.J., Lipfert, L., Rodan, G.A., and Duong le, T. (2003). PYK2 autophosphorylation, but not kinase activity, is necessary for adhesion-induced association with c-Src, osteoclast spreading, and bone resorption. J Biol Chem *278*, 11502-11512.

Lassing, I., and Lindberg, U. (1985). Specific interaction between phosphatidylinositol 4,5-bisphosphate and profilactin. Nature *314*, 472-474.

Lassing, I., and Lindberg, U. (1988). Specificity of the interaction between phosphatidylinositol 4,5-bisphosphate and the profilin:actin complex. J Cell Biochem *37*, 255-267.

Lener, T., Burgstaller, G., Crimaldi, L., Lach, S., and Gimona, M. (2006). Matrix-degrading podosomes in smooth muscle cells. Eur J Cell Biol *85*, 183-189.

Lengsfeld, A.M., Low, I., Wieland, T., Dancker, P., and Hasselbach, W. (1974). Interaction of phalloidin with actin. Proc Natl Acad Sci U S A *71*, 2803-2807.

Linder, S., Nelson, D., Weiss, M., and Aepfelbacher, M. (1999). Wiskott-Aldrich syndrome protein regulates podosomes in primary human macrophages. Proc Natl Acad Sci U S A *96*, 9648-9653.

Linder, S., Higgs, H., Hufner, K., Schwarz, K., Pannicke, U., and Aepfelbacher, M. (2000a). The polarization defect of Wiskott-Aldrich syndrome macrophages is linked to dislocalization of the Arp2/3 complex. J Immunol *165*, 221-225.

Linder, S., Hufner, K., Wintergerst, U., and Aepfelbacher, M. (2000b). Microtubule-dependent formation of podosomal adhesion structures in primary human macrophages. J Cell Sci *113 Pt 23*, 4165-4176.

Linder, S., and Kopp, P. (2005). Podosomes at a glance. J Cell Sci *118*, 2079-2082.

Linder, S. (2007). The matrix corroded: podosomes and invadopodia in extracellular matrix degradation. Trends Cell Biol *17*, 107-117.

Lock, P., Abram, C.L., Gibson, T., and Courtneidge, S.A. (1998). A new method for isolating tyrosine kinase substrates used to identify fish, an SH3 and PX domain-containing protein, and Src substrate. Embo J *17*, 4346-4357.

Luxenburg, C., Addadi, L., and Geiger, B. (2006a). The molecular dynamics of osteoclast adhesions. Eur J Cell Biol *85*, 203-211.

Luxenburg, C., Parsons, J.T., Addadi, L., and Geiger, B. (2006b). Involvement of the Src-cortactin pathway in podosome formation and turnover during polarization of cultured osteoclasts. J Cell Sci *119*, 4878-4888.

Luxenburg, C., Geblinger, D., Klein, E., Anderson, K., Hanein, D., Geiger, B., and Addadi, L. (2007). The architecture of the adhesive apparatus of cultured osteoclasts: from podosome formation to sealing zone assembly. PLoS ONE *2*, e179.

Machesky, L.M., Mullins, R.D., Higgs, H.N., Kaiser, D.A., Blanchoin, L., May, R.C., Hall, M.E., and Pollard, T.D. (1999). Scar, a WASp-related protein, activates nucleation of actin filaments by the Arp2/3 complex. Proc Natl Acad Sci U S A *96*, 3739-3744.

Maekawa, M., Ishizaki, T., Boku, S., Watanabe, N., Fujita, A., Iwamatsu, A., Obinata, T., Ohashi, K., Mizuno, K., and Narumiya, S. (1999). Signaling from Rho to the actin cytoskeleton through protein kinases ROCK and LIM-kinase. Science *285*, 895-898.

Mandal, S., Johnson, K.R., and Wheelock, M.J. (2008). TGF-beta induces formation of F-actin cores and matrix degradation in human breast cancer cells via distinct signaling pathways. Exp Cell Res *314*, 3478-3493.

Mannherz, H.G., Kabsch, W., and Leverman, R. (1977). Crystals of skeletal muscle actin: pancreatic DNAase I complex. FEBS Lett *73*, 141-143.

Marchisio, P.C., D'Urso, N., Comoglio, P.M., Giancotti, F.G., and Tarone, G. (1988). Vanadate-treated baby hamster kidney fibroblasts show cytoskeleton and adhesion patterns similar to their Rous sarcoma virus-transformed counterparts. J Cell Biochem *37*, 151-159.

McGlade, J., Brunkhorst, B., Anderson, D., Mbamalu, G., Settleman, J., Dedhar, S., Rozakis-Adcock, M., Chen, L.B., and Pawson, T. (1993). The N-terminal region of GAP regulates cytoskeletal structure and cell adhesion. Embo J *12*, 3073-3081.

McLean, B.G., Huang, S.R., McKinney, E.C., and Meagher, R.B. (1990). Plants contain highly divergent actin isovariants. Cell Motil Cytoskeleton *17*, 276-290.

Miki, H., Miura, K., and Takenawa, T. (1996). N-WASP, a novel actin-depolymerizing protein, regulates the cortical cytoskeletal rearrangement in a PIP2-dependent manner downstream of tyrosine kinases. Embo J *15*, 5326-5335.

Miki, H., Sasaki, T., Takai, Y., and Takenawa, T. (1998a). Induction of filopodium formation by a WASP-related actin-depolymerizing protein N-WASP. Nature *391*, 93-96.

Miki, H., Suetsugu, S., and Takenawa, T. (1998b). WAVE, a novel WASP-family protein involved in actin reorganization induced by Rac. Embo J *17*, 6932-6941.

Mizutani, K., Miki, H., He, H., Maruta, H., and Takenawa, T. (2002). Essential role of neural Wiskott-Aldrich syndrome protein in podosome formation and degradation of extracellular matrix in src-transformed fibroblasts. Cancer Res *62*, 669-674.

Monsky, W.L., Kelly, T., Lin, C.Y., Yeh, Y., Stetler-Stevenson, W.G., Mueller, S.C., and Chen, W.T. (1993). Binding and localization of M(r) 72,000 matrix metalloproteinase at cell surface invadopodia. Cancer Res *53*, 3159-3164.

Moreau, V., Tatin, F., Varon, C., and Genot, E. (2003). Actin can reorganize into podosomes in aortic endothelial cells, a process controlled by Cdc42 and RhoA. Mol Cell Biol *23*, 6809-6822.

Moritz, M., Braunfeld, M.B., Sedat, J.W., Alberts, B., and Agard, D.A. (1995). Microtubule nucleation by gamma-tubulin-containing rings in the centrosome. Nature *378*, 638-640.

Mueller, S.C., and Chen, W.T. (1991). Cellular invasion into matrix beads: localization of beta 1 integrins and fibronectin to the invadopodia. J Cell Sci *99 (Pt 2)*, 213-225.

Mueller, S.C., Ghersi, G., Akiyama, S.K., Sang, Q.X., Howard, L., Pineiro-Sanchez, M., Nakahara, H., Yeh, Y., and Chen, W.T. (1999). A novel protease-docking function of integrin at invadopodia. J Biol Chem *274*, 24947-24952.

Nakahara, H., Nomizu, M., Akiyama, S.K., Yamada, Y., Yeh, Y., and Chen, W.T. (1996). A mechanism for regulation of melanoma invasion. Ligation of alpha6beta1 integrin by laminin G peptides. J Biol Chem *271*, 27221-27224.

Nakahara, H., Howard, L., Thompson, E.W., Sato, H., Seiki, M., Yeh, Y., and Chen, W.T. (1997). Transmembrane/cytoplasmic domain-mediated membrane type 1-matrix metalloprotease docking to invadopodia is required for cell invasion. Proc Natl Acad Sci U S A *94*, 7959-7964.

Nakahara, H., Mueller, S.C., Nomizu, M., Yamada, Y., Yeh, Y., and Chen, W.T. (1998). Activation of beta1 integrin signaling stimulates tyrosine phosphorylation of p190RhoGAP and membrane-protrusive activities at invadopodia. J Biol Chem *273*, 9-12.

Nakamura, I., Pilkington, M.F., Lakkakorpi, P.T., Lipfert, L., Sims, S.M., Dixon, S.J., Rodan, G.A., and Duong, L.T. (1999). Role of alpha(v)beta(3) integrin in osteoclast migration and formation of the sealing zone. J Cell Sci *112 (Pt 22)*, 3985-3993.

Narumiya, S., Ishizaki, T., and Watanabe, N. (1997). Rho effectors and reorganization of actin cytoskeleton. FEBS Lett *410*, 68-72.

Naumanen, P., Lappalainen, P., and Hotulainen, P. (2008). Mechanisms of actin stress fibre assembly. J Microsc *231*, 446-454.

Nermut, M.V., Eason, P., Hirst, E.M., and Kellie, S. (1991). Cell/substratum adhesions in RSV-transformed rat fibroblasts. Exp Cell Res *193*, 382-397.

Nobes, C.D., and Hall, A. (1995). Rho, rac, and cdc42 GTPases regulate the assembly of multimolecular focal complexes associated with actin stress fibers, lamellipodia, and filopodia. Cell *81*, 53-62.

Ochoa, G.C., Slepnev, V.I., Neff, L., Ringstad, N., Takei, K., Daniell, L., Kim, W., Cao, H., McNiven, M., Baron, R., and De Camilli, P. (2000). A functional link between dynamin and the actin cytoskeleton at podosomes. J Cell Biol *150*, 377-389.

Ochs, H.D., Slichter, S.J., Harker, L.A., Von Behrens, W.E., Clark, R.A., and Wedgwood, R.J. (1980). The Wiskott-Aldrich syndrome: studies of lymphocytes, granulocytes, and platelets. Blood *55*, 243-252.

Oda, T., Makino, K., Yamashita, I., Namba, K., and Maeda, Y. (2001). The helical parameters of F-actin precisely determined from X-ray fiber diffraction of well-oriented sols. Results Probl Cell Differ *32*, 43-58.

Oikawa, T., Itoh, T., and Takenawa, T. (2008). Sequential signals toward podosome formation in NIH-src cells. J Cell Biol *182*, 157-169.

Olivier, A., Jeanson-Leh, L., Bouma, G., Compagno, D., Blondeau, J., Seye, K., Charrier, S., Burns, S., Thrasher, A.J., Danos, O., Vainchenker, W., and Galy, A. (2006). A partial down-regulation of WASP is sufficient to inhibit podosome formation in dendritic cells. Mol Ther *13*, 729-737.

Oreffo, R.O., Teti, A., Triffitt, J.T., Francis, M.J., Carano, A., and Zallone, A.Z. (1988). Effect of vitamin A on bone resorption: evidence for direct stimulation of isolated chicken osteoclasts by retinol and retinoic acid. J Bone Miner Res *3*, 203-210.

Osiak, A.E., Zenner, G., and Linder, S. (2005). Subconfluent endothelial cells form podosomes downstream of cytokine and RhoGTPase signaling. Exp Cell Res *307*, 342-353.

Otey, C.A., Kalnoski, M.H., and Bulinski, J.C. (1988). Immunolocalization of muscle and nonmuscle isoforms of actin in myogenic cells and adult skeletal muscle. Cell Motil Cytoskeleton *9*, 337-348.

Otterbein, L.R., Graceffa, P., and Dominguez, R. (2001). The crystal structure of uncomplexed actin in the ADP state. Science *293*, 708-711.

Owens, G.K., Kumar, M.S., and Wamhoff, B.R. (2004). Molecular regulation of vascular smooth muscle cell differentiation in development and disease. Physiol Rev *84*, 767-801.

Palmgren, S., Vartiainen, M., and Lappalainen, P. (2002). Twinfilin, a molecular mailman for actin monomers. J Cell Sci *115*, 881-886.

Pantaloni, D., and Carlier, M.F. (1993). How profilin promotes actin filament assembly in the presence of thymosin beta 4. Cell *75*, 1007-1014.

Papakonstanti, E.A., Ridley, A.J., and Vanhaesebroeck, B. (2007). The p110delta isoform of PI 3-kinase negatively controls RhoA and PTEN. Embo J *26*, 3050-3061.

Paunola, E., Mattila, P.K., and Lappalainen, P. (2002). WH2 domain: a small, versatile adapter for actin monomers. FEBS Lett *513*, 92-97.

Pellegrin, S., and Mellor, H. (2007). Actin stress fibres. J Cell Sci *120*, 3491-3499.

Peterson, L.J., Rajfur, Z., Maddox, A.S., Freel, C.D., Chen, Y., Edlund, M., Otey, C., and Burridge, K. (2004). Simultaneous stretching and contraction of stress fibers in vivo. Mol Biol Cell *15*, 3497-3508.

Pfaff, M., and Jurdic, P. (2001). Podosomes in osteoclast-like cells: structural analysis and cooperative roles of paxillin, proline-rich tyrosine kinase 2 (Pyk2) and integrin alphaVbeta3. J Cell Sci *114*, 2775-2786.

Pistor, S., Chakraborty, T., Niebuhr, K., Domann, E., and Wehland, J. (1994). The ActA protein of Listeria monocytogenes acts as a nucleator inducing reorganization of the actin cytoskeleton. Embo J *13*, 758-763.

Pixley, F.J., Xiong, Y., Yu, R.Y., Sahai, E.A., Stanley, E.R., and Ye, B.H. (2005). BCL6 suppresses RhoA activity to alter macrophage morphology and motility. J Cell Sci *118*, 1873-1883.

Pollard, T.D., Blanchoin, L., and Mullins, R.D. (2000). Molecular mechanisms controlling actin filament dynamics in nonmuscle cells. Annu Rev Biophys Biomol Struct *29*, 545-576.

Pollard, T.D. (2007). Regulation of actin filament assembly by Arp2/3 complex and formins. Annu Rev Biophys Biomol Struct *36*, 451-477.

Popp, D., Lednev, V.V., and Jahn, W. (1987). Methods of preparing well-orientated sols of f-actin containing filaments suitable for X-ray diffraction. J Mol Biol *197*, 679-684.

Qian, Y., Baisden, J.M., Westin, E.H., Guappone, A.C., Koay, T.C., and Flynn, D.C. (1998). Src can regulate carboxy terminal interactions with AFAP-110, which influence self-association, cell localization and actin filament integrity. Oncogene *16*, 2185-2195.

Redondo-Munoz, J., Escobar-Diaz, E., Samaniego, R., Terol, M.J., Garcia-Marco, J.A., and Garcia-Pardo, A. (2006). MMP-9 in B-cell chronic lymphocytic leukemia is up-regulated by alpha4beta1 integrin or CXCR4 engagement via distinct signaling pathways, localizes to podosomes, and is involved in cell invasion and migration. Blood *108*, 3143-3151.

Ridley, A.J., and Hall, A. (1992). The small GTP-binding protein rho regulates the assembly of focal adhesions and actin stress fibers in response to growth factors. Cell *70*, 389-399.

Ridley, A.J., Paterson, H.F., Johnston, C.L., Diekmann, D., and Hall, A. (1992). The small GTP-binding protein rac regulates growth factor-induced membrane ruffling. Cell *70*, 401-410.

Rohatgi, R., Ma, L., Miki, H., Lopez, M., Kirchhausen, T., Takenawa, T., and Kirschner, M.W. (1999). The interaction between N-WASP and the Arp2/3 complex links Cdc42-dependent signals to actin assembly. Cell *97*, 221-231.

Rohatgi, R., Ho, H.Y., and Kirschner, M.W. (2000). Mechanism of N-WASP activation by CDC42 and phosphatidylinositol 4, 5-bisphosphate. J Cell Biol *150*, 1299-1310.

Romer, L.H., Birukov, K.G., and Garcia, J.G. (2006). Focal adhesions: paradigm for a signaling nexus. Circ Res *98*, 606-616.

Saltel, F., Destaing, O., Bard, F., Eichert, D., and Jurdic, P. (2004). Apatite-mediated actin dynamics in resorbing osteoclasts. Mol Biol Cell *15*, 5231-5241.

Sato, T., del Carmen Ovejero, M., Hou, P., Heegaard, A.M., Kumegawa, M., Foged, N.T., and Delaisse, J.M. (1997). Identification of the membrane-type matrix metalloproteinase MT1-MMP in osteoclasts. J Cell Sci *110 (Pt 5)*, 589-596.

Sato, T.K., Overduin, M., and Emr, S.D. (2001). Location, location, location: membrane targeting directed by PX domains. Science *294*, 1881-1885.

Schramp, M., Ying, O., Kim, T.Y., and Martin, G.S. (2008). ERK5 promotes Src-induced podosome formation by limiting Rho activation. J Cell Biol *181*, 1195-1210.

Schwartz, S.M. (1997). Smooth muscle migration in atherosclerosis and restenosis. J Clin Invest *100*, S87-89.

Seals, D.F., and Courtneidge, S.A. (2003). The ADAMs family of metalloproteases: multidomain proteins with multiple functions. Genes Dev *17*, 7-30.

Seals, D.F., Azucena, E.F., Jr., Pass, I., Tesfay, L., Gordon, R., Woodrow, M., Resau, J.H., and Courtneidge, S.A. (2005). The adaptor protein Tks5/Fish is required for podosome formation and function, and for the protease-driven invasion of cancer cells. Cancer Cell *7*, 155-165.

Settleman, J., Albright, C.F., Foster, L.C., and Weinberg, R.A. (1992). Association between GTPase activators for Rho and Ras families. Nature *359*, 153-154.

Spinardi, L., Rietdorf, J., Nitsch, L., Bono, M., Tacchetti, C., Way, M., and Marchisio, P.C. (2004). A dynamic podosome-like structure of epithelial cells. Exp Cell Res *295*, 360-374.

Sumi, T., Matsumoto, K., Takai, Y., and Nakamura, T. (1999). Cofilin phosphorylation and actin cytoskeletal dynamics regulated by rho- and Cdc42-activated LIM-kinase 2. J Cell Biol *147*, 1519-1532.

Sun, H.Q., Yamamoto, M., Mejillano, M., and Yin, H.L. (1999). Gelsolin, a multifunctional actin regulatory protein. J Biol Chem *274*, 33179-33182.

Symons, M., Derry, J.M., Karlak, B., Jiang, S., Lemahieu, V., McCormick, F., Francke, U., and Abo, A. (1996). Wiskott-Aldrich syndrome protein, a novel effector for the GTPase CDC42Hs, is implicated in actin polymerization. Cell *84*, 723-734.

Tarone, G., Cirillo, D., Giancotti, F.G., Comoglio, P.M., and Marchisio, P.C. (1985). Rous sarcoma virus-transformed fibroblasts adhere primarily at discrete protrusions of the ventral membrane called podosomes. Exp Cell Res *159*, 141-157.

Tatin, F., Varon, C., Genot, E., and Moreau, V. (2006). A signalling cascade involving PKC, Src and Cdc42 regulates podosome assembly in cultured endothelial cells in response to phorbol ester. J Cell Sci *119*, 769-781.

Tatsis, N., Lannigan, D.A., and Macara, I.G. (1998). The function of the p190 Rho GTPase-activating protein is controlled by its N-terminal GTP binding domain. J Biol Chem *273*, 34631-34638.

Tehrani, S., Faccio, R., Chandrasekar, I., Ross, F.P., and Cooper, J.A. (2006). Cortactin has an essential and specific role in osteoclast actin assembly. Mol Biol Cell *17*, 2882-2895.

Teti, A., Marchisio, P.C., and Zallone, A.Z. (1991). Clear zone in osteoclast function: role of podosomes in regulation of bone-resorbing activity. Am J Physiol *261*, C1-7.

Thompson, O., Kleino, I., Crimaldi, L., Gimona, M., Saksela, K., and Winder, S.J. (2008). Dystroglycan, Tks5 and Src mediated assembly of podosomes in myoblasts. PLoS ONE *3*, e3638.

Tilney, L.G., Bonder, E.M., Coluccio, L.M., and Mooseker, M.S. (1983). Actin from Thyone sperm assembles on only one end of an actin filament: a behavior regulated by profilin. J Cell Biol *97*, 112-124.

Tolias, K.F., Cantley, L.C., and Carpenter, C.L. (1995). Rho family GTPases bind to phosphoinositide kinases. J Biol Chem *270*, 17656-17659.

Tu, C., Ortega-Cava, C.F., Chen, G., Fernandes, N.D., Cavallo-Medved, D., Sloane, B.F., Band, V., and Band, H. (2008). Lysosomal cathepsin B participates in the podosome-mediated extracellular matrix degradation and invasion via secreted lysosomes in v-Src fibroblasts. Cancer Res *68*, 9147-9156.

Uruno, T., Liu, J., Zhang, P., Fan, Y., Egile, C., Li, R., Mueller, S.C., and Zhan, X. (2001). Activation of Arp2/3 complex-mediated actin polymerization by cortactin. Nat Cell Biol *3*, 259-266.

Vandekerckhove, J., and Weber, K. (1978). At least six different actins are expressed in a higher mammal: an analysis based on the amino acid sequence of the amino-terminal tryptic peptide. J Mol Biol *126*, 783-802.

Varon, C., Tatin, F., Moreau, V., Van Obberghen-Schilling, E., Fernandez-Sauze, S., Reuzeau, E., Kramer, I., and Genot, E. (2006). Transforming growth factor beta induces rosettes of podosomes in primary aortic endothelial cells. Mol Cell Biol *26*, 3582-3594.

Walker, V.G., Ammer, A., Cao, Z., Clump, A.C., Jiang, B.H., Kelley, L.C., Weed, S.A., Zot, H., and Flynn, D.C. (2007). PI3K activation is required for PMA-directed activation of cSrc by AFAP-110. Am J Physiol Cell Physiol *293*, C119-132.

Watanabe, N., Madaule, P., Reid, T., Ishizaki, T., Watanabe, G., Kakizuka, A., Saito, Y., Nakao, K., Jockusch, B.M., and Narumiya, S. (1997). p140mDia, a mammalian homolog of Drosophila diaphanous, is a target protein for Rho small GTPase and is a ligand for profilin. Embo J *16*, 3044-3056.

Weaver, A.M., Karginov, A.V., Kinley, A.W., Weed, S.A., Li, Y., Parsons, J.T., and Cooper, J.A. (2001). Cortactin promotes and stabilizes Arp2/3-induced actin filament network formation. Curr Biol *11*, 370-374.

Weaver, A.M., Young, M.E., Lee, W.L., and Cooper, J.A. (2003). Integration of signals to the Arp2/3 complex. Curr Opin Cell Biol *15*, 23-30.

Weaver, A.M. (2008). Cortactin in tumor invasiveness. Cancer Lett *265*, 157-166.

Webb, B.A., Eves, R., Crawley, S.W., Zhou, S., Cote, G.P., and Mak, A.S. (2005). PAK1 induces podosome formation in A7r5 vascular smooth muscle cells in a

PAK-interacting exchange factor-dependent manner. Am J Physiol Cell Physiol *289*, C898-907.

Webb, B.A., Eves, R., and Mak, A.S. (2006). Cortactin regulates podosome formation: roles of the protein interaction domains. Exp Cell Res *312*, 760-769.

Wegner, A. (1976). Head to tail polymerization of actin. J Mol Biol *108*, 139-150.

Welch, M.D., Iwamatsu, A., and Mitchison, T.J. (1997). Actin polymerization is induced by Arp2/3 protein complex at the surface of Listeria monocytogenes. Nature *385*, 265-269.

Wheeler, A.P., Smith, S.D., and Ridley, A.J. (2006a). CSF-1 and PI 3-kinase regulate podosome distribution and assembly in macrophages. Cell Motil Cytoskeleton *63*, 132-140.

Wheeler, A.P., Wells, C.M., Smith, S.D., Vega, F.M., Henderson, R.B., Tybulewicz, V.L., and Ridley, A.J. (2006b). Rac1 and Rac2 regulate macrophage morphology but are not essential for migration. J Cell Sci *119*, 2749-2757.

Xiao, H., Eves, R., Yeh, C., Kan, W., Xu, F., Mak, A.S., and Liu, M. (2009). Phorbol ester-induced podosomes in normal human bronchial epithelial cells. J Cell Physiol *218*, 366-375.

Yamaguchi, H., Lorenz, M., Kempiak, S., Sarmiento, C., Coniglio, S., Symons, M., Segall, J., Eddy, R., Miki, H., Takenawa, T., and Condeelis, J. (2005). Molecular mechanisms of invadopodium formation: the role of the N-WASP-Arp2/3 complex pathway and cofilin. J Cell Biol *168*, 441-452.

Yamaguchi, H., Pixley, F., and Condeelis, J. (2006). Invadopodia and podosomes in tumor invasion. Eur J Cell Biol *85*, 213-218.

Yonezawa, N., Nishida, E., Iida, K., Yahara, I., and Sakai, H. (1990). Inhibition of the interactions of cofilin, destrin, and deoxyribonuclease I with actin by phosphoinositides. J Biol Chem *265*, 8382-8386.

Zaidel-Bar, R., Cohen, M., Addadi, L., and Geiger, B. (2004). Hierarchical assembly of cell-matrix adhesion complexes. Biochem Soc Trans *32*, 416-420.

Zaidel-Bar, R., Itzkovitz, S., Ma'ayan, A., Iyengar, R., and Geiger, B. (2007). Functional atlas of the integrin adhesome. Nat Cell Biol *9*, 858-867.

Zambonin-Zallone, A., Teti, A., Carano, A., and Marchisio, P.C. (1988). The distribution of podosomes in osteoclasts cultured on bone laminae: effect of retinol. J Bone Miner Res *3*, 517-523.

Zambonin-Zallone, A., Teti, A., Grano, M., Rubinacci, A., Abbadini, M., Gaboli, M., and Marchisio, P.C. (1989). Immunocytochemical distribution of extracellular matrix receptors in human osteoclasts: a beta 3 integrin is colocalized with vinculin and talin in the podosomes of osteoclastoma giant cells. Exp Cell Res *182*, 645-652.

Zamir, E., Katz, M., Posen, Y., Erez, N., Yamada, K.M., Katz, B.Z., Lin, S., Lin, D.C., Bershadsky, A., Kam, Z., and Geiger, B. (2000). Dynamics and segregation of cell-matrix adhesions in cultured fibroblasts. Nat Cell Biol *2*, 191-196.

Zhou, S., Webb, B.A., Eves, R., and Mak, A.S. (2006). Effects of tyrosine phosphorylation of cortactin on podosome formation in A7r5 vascular smooth muscle cells. Am J Physiol Cell Physiol *290*, C463-471.

Zicha, D., Allen, W.E., Brickell, P.M., Kinnon, C., Dunn, G.A., Jones, G.E., and Thrasher, A.J. (1998). Chemotaxis of macrophages is abolished in the Wiskott-Aldrich syndrome. Br J Haematol *101*, 659-665.